Development and regulation of synaptic divergence in the mammalian retina

Clare R. Gamlin

A dissertation

submitted in partial fulfillment of the

requirements for the degree of

Doctor of Philosophy

University of Washington

2019

Reading Committee:

Rachel O. Wong, Chair

Frederick Rieke

Thomas Reh

Program Authorized to Offer Degree:

Neuroscience

University of Washington

Abstract

Development and regulation of synaptic divergence in the mammalian retina

Clare R. Gamlin

Chair of the Supervisory Committee:

Professor Rachel O. Wong

Department of Biological Structure

During neural development, neurons must not only contact the appropriate postsynaptic partners, but also form precise stereotypic patterns of connectivity, the characteristic number and distribution of synapses onto partners. These stereotypic patterns determine how and where information is processed within a circuit, and thus their proper development is critical to normal circuit function. While progress has been made in understanding the cellular and molecular mechanisms that match neurons with their synaptic partners and even to subcellular locations on these partners, it is not yet well understood how most neurons achieve their synaptic distribution patterns. Both cell-autonomous and non-cell autonomous mechanisms have been found to regulate the development of synapses from multiple distinct presynaptic cell types onto a common postsynaptic partner (convergence). However, it remains unknown how an individual neuron establishes synapses with multiple distinct cell types (divergence), especially when the distribution of synapses is unequal across partners. Therefore, the goal of my thesis was to determine the cellular strategies and mechanisms that underlie the development of synaptic divergence in a central nervous system (CNS) circuit. The retina is an excellent model system for studying the development of synaptic patterns because the compact and laminar organization of the cells and their connections makes all components of the circuit accessible for visualization

and manipulation. Thus, I focused on the development of a retinal inhibitory circuit in which an interneuron (amacrine cell) connects to distinct postsynaptic cell types. In Chapter 1, I review what is known about the mechanisms underlying the development of synaptic patterns and inhibitory circuits in the CNS. I also briefly review the development of the vertebrate retina, the model system for my studies. In Chapter 2, I investigate the cellular strategies that shape the development of amacrine cell synaptic output patterning. In Chapter 3, I examine potential mechanisms that underlie the development of AII AC presynaptic structures and synaptic patterning described in Chapter 2. In Chapter 4, I summarize my findings and discuss future directions based on my findings thus far.

TABLE OF CONTENTS

LIST OF FIGURES

LIST OF TABLES

ACKNOWLEDGEMENTS

This thesis was made possible by the love and support of many, many people.

First, I would like to thank my graduate committee, Tom, Fred, Andres, and Marti, for all of your advice and support.

I would also like to thank my graduate program- the current directors, Paul and Horacio, and former directors David and Jane. Thank you to Lucia and Kyle for always making sure I registered on time and filled out paperwork correctly. Thank you also to Margie and Ann.

Thank you to my home department- the Department of Biological Structure - for being a wonderful place to do science and a very supportive environment for grad students. I would like to thank Jon from the PBIO office and Shellee from the Rieke lab for helping me organize events on numerous occasions. As well as thank you to Ed and Dale for all of their technical support with the EM blocks. I have also been fortunate enough to be supported by two different training grants, the DBTG and VTG, during my time as a graduate student.

Of course, thank you to my advisor, Rachel, for all of your advice and support over the years. I have learned so much from you. First and foremost, you have taught me how to keep the big picture in mind without sacrificing attention to detail- and on top of that, how to take nice images. You have also been generous in sharing your love of food. Thank you.

A huge thank you to everyone I have had the honor to work alongside in the Wong Lab. You have made the lab a lovely place to do science every day. Special thanks to fellow grad students, Phil and Florie for letting me be an unofficial member of the fish group.

I also owe many thanks to Dr. Mrinalini Hoon for being such a wonderful role model and friend. You have helped me become a better scientist.

To my many wonderful friends, thank you for all of the laughs and adventures over the years. They have meant so much to me. In particular, I'd like to thank Una and Edie, who have been there for me from the very beginning. Thanks to my cohort, who were always happy to have another journal club meeting. I'd also like to thank my un-official cohort and grad student family, Hannah, Benja, Kiri, Jason, Devon, Karl, Will and Jason.

I would like to thank my family and the Siegel-Browning family for their unwavering support throughout this journey. In particular, I'd like to thank my parents, Paul and Julie, for initially fostering my love of science and for always believing in me. I love you, Mom and Dad.

Lastly, thank you to Yoni. Even when I feel as though I'm moving slowly uphill, you are always there next to me, cheering me on. I could not have done this without you. I love you.

Chapter 1. Introduction

Circuit development is a highly complex process that requires the coordination of cells across both space and time. Neurons must migrate to the correct brain region and lamina, contact appropriate partners, and establish the proper pattern of synapses onto those partners. The stereotypic distribution of synapses between neurons determines where and how information is processed within a circuit. Thus, the establishment of these synaptic patterns is critical for the normal function of the circuit. While much work has been done to understand the mechanisms underlying partner matching and subcellular targeting, less is known regarding the mechanisms that underlie the establishment and maintenance of synaptic patterns.

1.1 Types of synaptic patterning and their role in information processing

Three distinct synaptic pattern motifs are found throughout the nervous system (Figure 1.1A). The first motif is a one-to-one connection, whereby a single neuron synapses onto a single postsynaptic partner. Examples of this pattern are seen from the auditory brainstem (calyx of held to MNTB) to cerebellum (climbing fiber onto purkinje cell) to the peripheral nervous system (neuromuscular junction) (Hoffpauir 2006; Watanabe & Kano 2011; Sanes & Lichtman 1999). In many circuits, the one-to-one connection arises once connections from other presynaptic cells are eliminated and continued poly-innervation can disrupt the function of these circuits (Kakizawa et al. 2000).

More commonly, multiple pre- and postsynaptic neurons are interconnected leading to convergence and divergence, which often occur in the same circuits (Figure 1.1A). In convergence, multiple presynaptic neurons impinge onto the same postsynaptic partner.

Convergence is observed in diverse neural structures including sensory circuits (e.g. retina, olfactory system) and the cerebellum (Hoon et al. 2014; Mombaerts 2006; Huang et al. 2013). Synaptic convergence allows for the integration of information within a circuit and underlie functions such as coincidence detection and noise reduction (Jeanne & Wilson 2015).

Divergence occurs when a single presynaptic neuron synapses onto multiple postsynaptic partners. Divergence is observed across neural circuits including sensory and motor circuits. For example, in the retina individual photoreceptors provide input onto multiple postsynaptic bipolar cells (Cohen & Sterling 1990; Wässle, Puller, et al. 2009; Dunn & Wong 2012). Additionally, individual sensory-motor neurons synapse onto distinct motor neuron pools (Mendelsohn et al. 2015). This connectivity motif allows for the diversification and amplification of signals if synapses are formed onto distinct or similar targets, respectively (Asari & Meister 2012). Divergence also allows information to be sent across 'parallel channels' within a circuit, which could speed the rate of information transfer (Stein 1967).

While much is known regarding the cellular and molecular mechanisms that guide neurons to a specific postsynaptic partner, and the subcellular location onto that partner (Reviewed by Sanes & Yamagata 2009; Gamlin et al. 2018), it remains incompletely understood how neurons establish and regulate stereotypic patterns of synapses across partners. Understanding how neurons achieve their synaptic distribution patterns is critical for understanding circuit development.

1.2 Cellular strategies and mechanisms for achieving stereotypic synaptic patterns

During development, neurons often undergo changes in connectivity to achieve their final, mature synaptic patterns. Three distinct cellular strategies have been found to underlie the development of stereotypic patterns: Preferential synaptogenesis, synaptic pruning, and maintenance (Figure 1.1B).

Preferential synaptogenesis occurs when a cell preferentially receives or forms synapses with one partner versus the other(s). Preferential synaptogenesis has been described in the development of both convergent and divergent connectivity patterns (Figure 1.2). In the zebrafish retina, one cell type, H3 Horizontal Cell (H3 HC) contacts presynaptic blue and ultraviolet (UV) cones in a 1:5 ratio, favoring UV cones. H3 HCs initially contact blue and UV cones, but preferentially reach out and synapse with UV cones during maturation. When UV cones are silenced, H3 HCs add contacts with blue cones, but maintain the same number of connections with UV cones; however, silencing blue cones had no effect on H3 HC cone contacts (Figure 1.2 A) (Yoshimatsu et al. 2014). Therefore, the activity of a major presynaptic partner can selectively regulate connectivity with a minor presynaptic partner, but not necessarily vice versa. In the mouse retina, retinal ganglion cells (RGC) receive input from multiple presynaptic bipolar cells, and these bipolar cells can differentially reach their final number of synapses onto their RGC targets. For example, for one type of RGC, the ON-alpha, each presynaptic bipolar cell type reaches its final connectivity with the ON-alpha differently. Specifically, the Type 6 bipolar cells (T6), increase connectivity with the ON-alpha with maturation. Type 7 bipolar cells (T7) maintain the same number of synapses with their ON-alpha partner, and the rod bipolar cells (RBC), eliminate synapses with the ON-alpha RGC. Neurotransmission bi-directionally drives synaptogenesis of T6 cells on the RGCs (increased T6 activity drives formation of synapses onto the RGC, loss of

drive results in fewer output synapses onto the RGC) in a cell-autonomous manner and has no effect on maintenance or removal of synapses from the other two presynaptic partners onto the ON-alpha RGC (Morgan et al. 2011; Soto et al. 2012; Okawa et al. 2014). On the other hand, loss of the T6 cells results in the RGC contacting novel presynaptic partners (Okawa et al. 2014). Thus, the physical presence of a major presynaptic partner can prevent a neuron from connecting with incorrect presynaptic targets. These findings show that activity-dependent and cell contact-mediated mechanisms can differentially and independently regulate synaptic connectivity from converging inputs onto a shared partner. Preferential synaptogenesis can also occur in a divergent circuit (Figure 1.2B). In primary somatosensory cortex, experience-mediated activity drives increased synaptogenesis from thalamocortical axons onto layer 4, but not layer 6 neurons, resulting in a bias for layer 4 targets (Crocker-Buque et al. 2015). Interestingly, whisker-trimming, which leads to sensory-deprivation, prevents the preferential synaptogenesis onto layer 4 neurons, but does not alter thalamocortical synapses onto layer 6 neurons. Thus, activity-dependent mechanisms can independently regulate connectivity with a major versus minor postsynaptic partner.

Often, neurons form more synapses during development than they will maintain at maturity, requiring pruning of excess synapses (Figure 1.1B). Pruning can occur in circuits with all three synaptic pattern motifs described in section 1.1 (one-to-one, convergence, divergence). At both the neuromuscular junction and climbing fiber-Purkinje cell synapses in the cerebellum, multiple axons initially innervate the postsynaptic cell, but synapse elimination reduces connectivity to one or a few axons via activity-dependent competition (Reviewed Sanes & Lichtman 1999; Hashimoto & Kano 2013). Excess synapses must also be pruned in converging circuits. For example, in the auditory brainstem, axons projecting from the medial nucleus of the trapezoid

body (MNTB) form excess synapses onto targets in both the lateral (LSO) and medial superior olive (MSO) nuclei. Interestingly spontaneous excitatory activity is required for the removal of excess synapses onto LSO neurons, whereas binaurally-driven inhibitory activity is required for pruning of synapses onto MSO neurons. Thus, while activity-dependent mechanisms can underlie synaptic pruning, either excitatory or inhibitory neurotransmitters may be involved (Reviewed by Gamlin et al. 2018). Synapse elimination can also occur within a divergent circuit to yield a biased connectivity with one partner versus the other(s) (Figure 1.1B). For example, sensory-motor neurons provide input to two distinct classes of motor neurons: homonymous and heteronymous. "Homonymous" motor neuron pools contain motor neurons that synapse onto the same muscles from which a sensory-motor neuron receives input. On the other hand, a motor neuron pool is "heteronymous" if the motor neurons synapse onto muscles that the given sensory-motor neuron does not. When silenced, sensory-motor neurons form excess synapses onto heteronymous targets, revealing a role for activity in restricting the number of synapses formed onto this partner (Figure 1.2 C) (Mendelsohn et al. 2015). Interestingly, the number of synapses that sensory-motor neurons formed onto homonymous targets does not change. Therefore, across convergent and divergent neural circuits, activity can independently regulate connectivity with one partner to create biased connectivity within the circuit. Surprisingly, activity does not always regulate connectivity with the preferred partner (e.g. H3 HCs, homonymous motor neurons).

Maintenance describes the retention of a proportion of synapses that have already been formed onto specific partners. Studies in the cerebellum have revealed that Purkinje cells rely on input-specific transsynaptic organizing proteins for the formation, maintenance and function of synapses, and that synapses from distinct input-partners can be independently regulated (Zhang

et al. 2015). Both molecular and activity-dependent mechanisms can regulate synapse maintenance. Recent work has shown that presynaptic neurons use distinct synapse organizing proteins, such as Neurexin (Nrx-1), to form and maintain synapses with one target versus another (Philbrook et al. 2018). Thus, distinct molecular mechanisms can regulate the formation and maintenance of connectivity in a partner-specific manner in both convergent and divergent circuits. Maintenance can also include preventing excess synaptogenesis or synapse removal. For example, in the retina, T7 bipolar cells are normally a minor presynaptic partner of ON alpha retinal ganglion cells. When the major bipolar cell partner (T6) population is ablated, but not when it is silenced, T7 bipolar cells expand their axon territories and increase the number and density of synapses formed onto ON-alpha RGCs (Okawa et al. 2014). This study illustrates a non-cell autonomous, activity-independent mechanism that restricts the axon terminal and thus the connectivity of a minor presynaptic partner. Furthermore, as described above, T6 connectivity with ON-alpha RGCs is regulated by activity; therefore, multiple, distinct mechanisms can regulate the connectivity in a partner-specific manner in a single circuit. Activity can also play a role in the maintenance of synapses. For example, in the retina, loss of inhibitory synaptic transmission prevents the accumulation of GABAergic but not glycinergic synapses onto bipolar cell axons (Hoon et al. 2015). On the other hand, loss of transmission in the spinal cord prevents the maturation of glycinergic, but not GABAergic synapses (Kirsch & Betz 1998). Thus, the role of activity in maintaining synapses may be circuit specific.

In sum, there are diverse cellular strategies that shape connectivity between individual neurons, and these strategies can act in a partner-specific and independent manner. Furthermore, both activity-dependent and independent mechanisms can regulate connectivity with distinct

postsynaptic partners in a divergent circuit, but it remains unknown whether these mechanisms are regulated by independent mechanisms within a single circuit.

1.3 Role of inhibition within neural circuits

Inhibition plays an important role in neural function by providing a necessary check on excitatory activity within the nervous system. Disruptions in inhibition can lead to neural disorders characterized by hyperexcitability, such as hyperekplexia and epilepsy (Bode & Lynch 2014; Tai et al. 2014). Beyond reducing the level of activity in the brain, inhibition can shape and control the timing of neural signals as they move through a circuit. Inhibitory circuits are found throughout the CNS and are diverse in their functions. There are the two major inhibitory neurotransmitters in the nervous system (GABA and glycine), and at least one of these neurotransmitters is present in every brain region. In some areas, such as the spinal cord and retina, both GABA and glycine are present, and can act on the same the same circuit, and in at least one circuit are released from the same synapse (reviewed Gamlin et al. 2018). Diversity in inhibitory circuit function also arises from the distinct composition of receptors found at the postsynapse. Inhibitory receptors are heteropentameric ligand-gated chloride channels and can vary greatly in subunit composition. GABA receptors are typically comprised of two α(1-6), two β(1-4), and one γ subunit (Sieghart et al. 1999). Glycine receptors are typically comprised of α (1-4) and β(1) subunits, but studies have yet to distinguish between a 2:3 and 3:2 stoichiometry (reviewed Dutertre et al. 2012; Patrizio et al. 2017). Importantly, subunit composition can determine receptor kinetics (Takahashi et al. 1992). Inhibitory receptors vary in subunit composition both within and across brain regions, and even across cell compartments of an

individual neuron (Hoon et al. 2015), leading to a diversity of postsynaptic responses to a single neurotransmitter.

Inhibition expands the neural computations possible within a circuit and can have distinct effects when applied at the pre- versus postsynapse (Figure 1.3A). For example, presynaptic inhibition can extend the dynamic range across which a neuron can signal (Sagdullaev et al. 2006). Furthermore, presynaptic inhibition can diversify signals by allowing a single neuron to provide distinct signals to different postsynaptic partners (Asari & Meister 2012). On the other hand, postsynaptic inhibition can control the timing of signaling within a circuit and even underlie feature selectivity (Taylor et al. 2000). Thus, the role of an inhibitory neurotransmitter must be evaluated with respect to specific circuit function and even synaptic location.

1.4 Development of inhibitory circuits

As in excitatory circuits, the first step in inhibitory circuit development is the proper targeting of synaptic partners. In highly laminated neural structures, such as the retina, partners must send processes to the same layer in order to contact each other. Thus, cues that direct processes to specific lamina contribute to partner matching. Cell adhesion molecules have been shown to restrict the processes of inhibitory retinal interneurons, amacrine cells, to specific lamina. For example, cell adhesion molecules, DSCAM/DSCAM-L and sidekicks (Sdk1 and Sdk2), direct the development of amacrine cell neurites in the chick retina, and mis-expression of one of these molecules can direct neurites to an aberrant layer (Yamagata & Sanes 2008a). In the mouse retina, amacrine cell processes can be directed to specific layers by the repulsive cues of semaphorins, transmembrane cell adhesion molecules (Matsuoka, Nguyen-Ba-Charvet, et al. 2011; Matsuoka, Chivatakarn, et al. 2011). Loss of semaphorin or Plexin, a semaphorin receptor,

expression allows amacrine cells to send neurites to the incorrect lamina. Interestingly, the postsynaptic partners of mis-targeted amacrine cells similarly mis-laminate after semaphorin loss, allowing the partners to still connect. Thus, in the retina, there are likely cues, such as cell-cell recognition molecules, that act independently of lamination cues to ensure proper synaptic targeting.

Cell-cell recognition molecules also underlie local synaptic targeting for inhibitory interneurons in the spinal cord. In the spinal cord sensory-motor circuit, sensory afferents target motor neurons, and distinct populations of inhibitory interneurons target either the sensory afferents or the motor neurons. When sensory afferents are ablated by expression of diphtheria toxin, the inhibitory interneurons that normally contact the sensory afferents continue to extend processes towards, but not form synapses onto, the motor neurons. Instead, the inhibitory neurons eventually retract their processes (Betley et al. 2009). The inhibitory neuron specificity for sensory afferents is due to the specific expression of cell adhesion molecules amongst the two populations. Specifically, the inhibitory axons express two proteins from the immunoglobulin (Ig) superfamily, CHL1 and NrCAM, whereas the sensory afferents express NB2, a protein from the Ig superfamily, and Caspr4, a contactin-associated protein (Ashrafi et al. 2014). Thus, cell adhesion molecule expression determines the high specificity between inhibitory interneurons and their targets in the spinal cord.

In addition to contacting the proper postsynaptic partners, inhibitory neurons must target the correct subcellular location of those synaptic partners. For example, GABAergic basket cells and GABAergic stellate cells rely on distinct cell adhesion molecules to guide them to the axon initial segment and distal dendrites of cerebellar Purkinje cells, respectively (Ango et al. 2004;

Ango et al. 2008). Targeting specificity can also apply to within a single subcellular area. For example, in the retina, each quadrant of an inhibitory starburst amacrine cell (SACs) preferentially synapses onto one of four types of direction-selective ganglion cells (DSGC) that respond to motion in one of the four cardinal directions (dorsal, ventral, nasal, temporal). Importantly, the specific connectivity between SACs and DSGCs underlies direction-selectivity in this circuit. In the absence of the *FRMD7* gene, which encodes a FERM domain protein family member that is enriched in SACs (Moleirinho et al. 2013), 'horizontally tuned' DSGCs receive erroneous connections from other quadrants of the SAC arbor, resulting in a loss of horizontal direction selectivity (Yonehara et al. 2016). Thus, expression of membrane-associated proteins can regulate the pattern of output synapses of an inhibitory neuron.

Once inhibitory neurons contact the proper subcellular locations of their targets, they must form synapses. Synaptogenesis describes the complex process of localizing presynaptic release machinery opposite postsynaptic receptors coordinated by synapse organizing proteins. Neurotransmission is not required for either excitatory or inhibitory synapse formation (reviewed in Gamlin et al. 2018), thus much work has been done to determine the molecular mechanisms that underlie synapse assembly. As at excitatory synapses, transsynaptic proteins, such as presynaptic neurexins and postsynaptic neuroligins, bring the future pre and postsynaptic membranes in close apposition. Distinct isoforms of these proteins can preferentially lead to the formation of excitatory vs inhibitory synapses, and even GABA vs glycinergic synapses. Just as at excitatory postsynapses, inhibitory postsynapses contain synapse organizing proteins and receptor clusters. While most excitatory synapses contain PSD95 (postsynaptic density 95 protein) at the postsynapse, inhibitory synapses typically contain gephyrin.

Inhibitory circuits also undergo changes in signaling and receptor properties with maturation. During early neural development, neurons have a higher intracellular chloride concentration that at maturity. Therefore, activation of GABA or glycine receptors causes an efflux of chloride from the cell and is depolarizing (Ben-Ari 2002). Developmental increases in the expression and activity of the chloride transporter KCC2 reverses the chloride gradient such that GABA and glycine receptor activation 'switches' from depolarizing to hyperpolarizing (Ben-Ari 2002; Rivera et al. 1999). Thus, during initial circuit formation, GABA and glycine release is depolarizing, but becomes hyperpolarizing via a shared KCC2-mediated mechanism. In the mouse retina, GABA and glycine become hyperpolarizing at P6 (Zhang et al. 2006). Other developmental 'switches' are common during inhibitory circuit development including changes in receptor subunit composition. Typically, receptors 'switch' from slower to faster subunits. For example, many GABA and glycine receptors change from containing $\alpha 2$ subunits to $\alpha 1$ subunits which contributes to the faster kinetics of the mature circuit (Okada et al. 2000; Takahashi et al. 1992).

1.5 Organization of the vertebrate retina

The retina is the light-sensitive neural tissue found at the back of the eye, and its proper function is required for normal vision. The retina is organized into distinct layers, each of which is comprised of specific cell populations (Figure 1.4A). Additionally, neurons synapse with specific partners in distinct plexiform layers to form highly conserved circuits. The organization and compact nature of the retina makes it possible to identify cell types and reconstruct entire circuits across developmental time points. Thus, the retina provides a unique opportunity for studying the development of complex neural circuits and the synaptic patterning within those circuits.

The retina is made up of five neural and one glial cell type, which are organized and synapse within distinct layers of the retina (Figure 1.4A). Photoreceptors are the light-sensitive neurons located at the outermost part of the retina, the outer nuclear layer (ONL), and they synapse onto horizontal cell and bipolar cell (BC) dendrites at the outer plexiform layer (OPL). Bipolar cell somas reside in the inner nuclear layer (INL) and send axons to synapse onto the dendrites of retinal ganglion cells forming the inner plexiform layer (IPL). Retinal ganglion cell (RGC) bodies reside in the ganglion cell layer (GCL) and axons from these cells form the optic nerve, which exits the eye and sends visual information to other parts of the central nervous system. Amacrine cells (ACs), which are inhibitory interneurons, are located in either the INL or GCL and form inhibitory synapses onto bipolar cell axons, retinal ganglion cell dendrites, and other amacrine cells.

Photoreceptors are comprised of an opsin-expressing, and therefore light-sensing, outer segment and an inner segment, which contains synaptic release machinery including specialized ribbon synapses. There are two types of photoreceptors, rods and cones, which can be distinguished by their morphology, function, and connectivity. Rods express rhodopsin in their outer segments, which makes them extremely sensitive to light and able to signal the absorption of a single photon (Baylor et al. 1979). Cones are less sensitive to light because they express different wavelength-sensitive opsins. Cones allow animals to see at brighter light levels and have color vision. In the mammalian retina, rods synapse onto rod bipolar cells, whereas cones synapse onto cone bipolar cells. In response to the absorption of photons, all photoreceptors halt their tonic release of glutamate at ribbon synapses onto the dendrites of bipolar cells and horizontal cells. Horizontal cells in turn provide feedback inhibition onto photoreceptor terminals (Drinnenberg et al. 2018; Baylor et al. 1971).

Bipolar cells receive input from photoreceptors and extend axon terminals into one of two distinct plexuses in the IPL of the retina. Bipolar cells that respond to decrements in light stratify deeper in the IPL (closer to the photoreceptor layer) in the "OFF" layer, whereas bipolar cells that respond to increments in light stratify further from the photoreceptor layer, in the "ON" layer of the IPL. All rod bipolar cells stratify in the "ON" layer, whereas cone bipolar cells stratify in either the "OFF" or "ON" layer. To date there are 14 genetically identified cone bipolar cells and one rod bipolar cell. Of the cone bipolar cells, 6 are "OFF" and 8 are "ON" (Shekhar et al. 2016). Each of these bipolar cell subtypes is thought to represent a distinct pathway of information within the retina (Euler et al. 2014), and each subtype contacts specific retinal ganglion cell partners (Dunn & Wong 2014). Bipolar cell axons typically provide graded glutamatergic output at ribbon synapses (Baden et al. 2013) onto the dendrites of retinal ganglion cells, which also stratify in "OFF", "ON", or both IPL layers.

Retinal ganglion cells receive input from bipolar cells corresponding with the IPL layers in which their dendrites stratify. As such, retinal ganglion cells can be classified as "OFF", "ON", or "ON-OFF". To date, there are estimated to be at least 32 distinct retinal ganglion cell subtypes in the mouse retina. Each retinal ganglion cell subtype tiles the retina and is thought to underlie detection of specific visual features (Baden et al. 2016). Retinal ganglion cell axons bundle together to form the optic nerve, which leaves the eye and projects to several distinct downstream visual areas.

Amacrine cells provide GABAergic and glycinergic input onto bipolar cells, retinal ganglion cells, and other amacrine cells. They are the most morphologically diverse class of neurons in the

retina, and most amacrine cells have not been morphologically or synaptically characterized yet (Vaney 1990; Masland 2012; Franke et al. 2017). Due to the high level of morphological diversity, amacrine cells are often defined by the extent to which their neurites extend, and these dimensions vary amongst species. Narrow-field amacrine cells tend to be glycinergic and are thought to mediated local inhibition across retinal layers and along specific parallel channels. Whereas wider-field amacrine cells tend to be GABAergic and are thought to be involved in larger-scale visual processing.

The AII amacrine cell (AII AC), which is the focus of this thesis, is part of the "rod pathway" (Famiglietti & Kolb 1975; Strettoi et al. 1992). As described above, rod photoreceptors provide input to the dendrites of rod bipolar cells. Rod bipolar cells in turn synapse onto two types of amacrine cells: A17 and AII ACs. A17s provide inhibitory GABAergic feedback onto the rod bipolar cell terminal (Nelson & Kolb 1985). AII ACs receive input form rod bipolar cells at their distal dendrites and form glycinergic output synapses onto OFF cone bipolar cells and OFF retinal ganglion cells at specialized presynaptic structures called "lobular appendages" (Famiglietti & Kolb 1975) (Figure 2.1C). All ACs output synapses onto both bipolar cell and retinal ganglion cell partners contain the α1 glycine receptor subunit (Wässle, Heinze, et al. 2009). AII ACs are the main conduit for very dim or scotopic light (Nelson & Kolb 1985; Demb & Singer 2012). The structure and function of rod pathway is highly conserved in mammals, including mice, rats, rabbits, cats, primates and even humans (Tsukamoto & Omi 2017; Wässle et al. 1993; Strettoi et al. 1992; Famiglietti & Kolb 1975; Wässle et al. 1995; Scher et al. 2003) making this circuit a useful model for studying circuit development and for the regulation of synaptic patterning.

1.6 Development of the vertebrate retina

Neurogenesis and stratification

All cells types within the vertebrate retina (5 neural and 1 glial) are generated from a single population of retinal progenitor cells (Turner & Cepko 1987). The cell types undergo a final mitotic division ("born") in a highly stereotyped and overlapping order (Figure 1.4B). Retinal ganglion cells are generated first with amacrine cells and cone photoreceptors following closely afterwards. Rod photoreceptors and horizontal cells are born next. Bipolar cells and Muller glia (MG) are generated last (Cepko et al. 1996; Young 1985). Thus, cells that reside at the inner and outermost layers of the retina are generated first, while cells that span layers (BC) or even the whole retina (MG) are generated later. In mouse development, retinal ganglion cells are born as early as embryonic day 8 (E8) with a peak in cell birth at E12 (Voinescu et al. 2009). Once retinal ganglion cells are born, they must migrate basally. At E13 some RGC somata are already in the appropriate layer and have begun to extend axons towards the future optic nerve (Hinds & Hinds 1974). Retinal ganglion cells must subsequently elaborate dendritic arbors in the appropriate lamina and do so as early as postnatal day 3 (P3) (Stacy & Wong 2003). Ganglion cell dendrites reach their final lamination in a subtype-specific manner with some neurons targeting the correct layer from the outset while other undergo structural refinement (Kim et al. 2010).

Amacrine cells start genesis after retinal ganglion cells. In mice, amacrine cells are first born around embryonic day 8 (E8), and peak at E17, but some amacrine cells are generated as late as P3 (Young 1985; Voinescu et al. 2009). GABAergic and glycinergic amacrine cells are born at distinct but overlapping times, with GABAergic amacrine cells becoming postmitotic a few days

before glycinergic amacrine cells (Voinescu et al. 2009). Peak generation of GABAergic amacrine cells is E14, the peak for glycinergic cells is around P0 (Voinescu et al. 2009). ChAT+ starburst amacrine cells (SACs) are some of the earliest born amacrine cells, detectable as early as E10 (Voinescu et al. 2009). Once amacrine cells are generated they must migrate and extend processes to the correct lamina. SACs are present in the INL by P0 and their processes have stratified into distinct ON and OFF layers by P3, when RGCs have also begun to elaborate dendrites (Stacy & Wong 2003). However, work in both zebrafish and mouse retina reveal that amacrine cell differentiation, migration, and stratification are not dependent on the presence of retinal ganglion cells (Brown et al. 2001; Wang et al. 2001; Kay et al. 2001). Furthermore, in the zebrafish retina, ACs preferentially target neurites to the future ON and OFF layers of the retina (Godinho et al. 2005), indicating they may provide laminar guidance for later born retinal cells. Some amacrine cells follow a different developmental timeline. In the rabbit retina, AII ACs are present at birth, but do not have a mature appearance until the end of the 2nd postnatal week. Processes are first visible extending toward the ganglion cell layer, likely putative distal dendrites, and later processes are visible extending more horizontally, likely putative lobular appendages (Casini et al. 1998). Murine AII ACs follow a similar morphological developmental profile with putative distal dendrites appearing prior to lobular appendages (Rice & Curran 2000). Thus, morphological differentiation can be distinct for different amacrine cell types but may also be stereotyped for a given amacrine cell type.

Bipolar cells are one of the last cell types generated in the retina. In the mouse, bipolar cells are first born starting around E18, peaking between P1-3 (Voinescu et al. 2009). They must migrate past the already present outer retinal layers and extend axons towards their laminating targets, amacrine cells and retinal ganglion cells. At P3, ON bipolar cell somas are present in the inner

nuclear layer (Figure 1.4A), and extended processes to the outer and inner limiting membranes (Morgan et al. 2006). At this stage, short neurites extended from the basal process at many depths of the retina but extend preferentially in the IPL. By P5, most axonal extensions are present at the correct layer of the IPL (ON vs OFF), but some processes are present in other layers of the IPL and in the ganglion cell layers. At P5, ON BCs are also extending proto-dendritic processes from the apical neuroepithelia process (Morgan et al. 2006). By P9, most apical and basal processes have retracted, as BCs take on a more bipolar morphology. While BCs are the last neural cell types to develop, they can develop and stratify normally in the absence of retinal ganglion cells (Günhan-Agar et al. 2000), but mislaminate when amacrine cell lamination is disrupted (Rice et al. 2001; Kay et al. 2004; Matsuoka, Chivatakarn, et al. 2011). These findings suggest that amacrine cells may serve as a guide for bipolar cell development. However, not all amacrine cells contribute to bipolar cell lamination. For example, SACs are not required for proper bipolar cell ON/OFF segregation (Gunhan et al. 2002; Williams et al. 2001). Thus, it remains to be determined whether specific AC populations guide BC stratification or whether these cell types rely on a shared cue.

Synaptogenesis

In the developing mouse retina, conventional synapses (presumed amacrine cell) are observed first (P3-10), whereas ribbon synapses (excitatory) are observed later (P11-15) (Fisher 1979). Spontaneous excitatory postsynaptic currents (EPSCs) are observed in RGCs at P7, prior to the appearance of ribbons, indicating excitatory synapses can be functional prior to the development of these specialized structures (Johnson et al. 2003; Morgan et al. 2008). During early synaptogenesis, GABA and glycine mediated transmission is depolarizing, but at P6, GABA and glycine transmission become hyperpolarizing (Zhang et al. 2006). Thus, when many inhibitory

synapses are formed (prior to P6), GABA and/or glycine release will depolarize the postsynaptic cell. At P8, glycinergic inhibitory currents are recorded in OFF bipolar cells, and some of those currents likely originate from AII ACs (Schubert et al. 2008). Around this time in retinal development, rod bipolar cells begin to provide glutamatergic input to AII ACs (Schubert et al. 2008). Thus, the AII AC circuit comes "online" around P8.

Cell Death

As we will be studying changes in synaptic patterning that occur with maturation, it is important to know how the cellular composition of circuits may be altered by apoptosis. In the retina, as in other neural structures, more cells are generated than will be incorporated into mature circuits, and thus some neurons will undergo apoptosis during retinal development. Apoptosis of each retinal cell type generally follows the same developmental sequence as cell genesis (Figure 1.4B). In mouse retina, RGC death largely occurs between P2-4 (Farah & Easter 2005; Young 1985). Amacrine cell death is estimated to occur between P3-7, and bipolar cell death occurs between P7-11 (Farah & Easter 2005; Young 1985). Of note, the number of cells that undergoes apoptosis can occur in a subtype specific manner. For example, when apoptosis is blocked in a Bax KO mouse, the Type 2 bipolar cell population increases by 64%, whereas the Type 3b bipolar cell population increases by 50%, but Type 4 bipolar cells only increase by 15% (Keeley et al. 2014). Thus, by the time of eye-opening (~P14) the cellular composition of the retina should not change much as most cell types have undergone apoptosis.

1.7 Role of inhibition in the retina

As described earlier, like elsewhere in the CNS, inhibition in the retina plays an important role in moderating excitation and extending the computations that can be performed by a circuit. The retina is exposed to visual stimuli that can differ by a factor of over one billion in light level (Shapely 1984). In order to remain responsive to high light levels that would otherwise quickly overwhelm highly sensitive circuits, retinal circuits must adapt. Such adaptation has been shown to occur in response to the absorption of a single photon of light (Dunn & Rieke 2008). At the rod bipolar cell axon terminal, reciprocal inhibition from GABAergic A17 amacrine cells 'feeds back' onto the rod bipolar cell axon (Nelson & Kolb 1985). This feedback inhibition has been found to modulate the speed of rod signals within the retina (Dong & Hare 2003). Other inhibitory 'motifs' are seen in neural circuits: feedforward and crossover inhibition (Figure 1.3B). Feedforward inhibition occurs when excitation precedes inhibition within a circuit. Feedforward inhibition typically occurs when a single presynaptic input drives excitation of both a primary neuron and an inhibitory interneuron, and the inhibitory interneuron inhibits the primary neuron. Such feedforward inhibition has been shown to tightly control the timing of retinal ganglion cell firing (Cafaro & Rieke 2010). Cross-over inhibition occurs when excitation and inhibition are negatively correlated in a circuit. For example, activity of a single presynaptic input excites a primary neuron and an inhibitory interneuron. The inhibitory interneuron in turn inhibits a second primary neuron, causing the two primary neurons to be driven in opposite directions. The AII AC drives such crossover inhibition by inhibiting 'OFF' retinal ganglion cells when 'ON' retinal ganglion cells are being excited (Pang et al. 2003; Manookin et al. 2008). Cross-over inhibition is thought to contribute to spatial selectivity and edge detection in the retina (Cafaro & Rieke 2013; Werblin 2010). Inhibition in the retina also underlies direction selectivity. As described earlier in section 1.4, direction selectivity arises from the specific

wiring of starburst amacrine cell (SAC) quadrants with direction-selective retinal ganglion cell dendritic arbors. This circuitry has been described in both mouse and rabbit (Wei et al. 2011; Ghosh et al. 1990). Thus, many of the specific computations performed in the retina rely on inhibition, yet much remains unknown regarding the development of the retina's key inhibitory circuits.

1.8 Thesis Overview

In my thesis, I examined how an individual neuron establishes its stereotypic pattern of synaptic divergence and explored potential cellular mechanisms that underlie this process. I focused on the development of the AII amacrine cell (AII AC), because it has a biased divergent synaptic pattern and all of its postsynaptic partners are confined to the retina. First, I used confocal microscopy and immunohistochemistry to label and reconstruct the morphological development of the AII AC. Next, I used serial blockface electron microscopy (SBFEM) to map the output synapses and postsynaptic partners of individual AII ACs at postnatal day 24 (P24). I confirmed earlier studies that showed that both bipolar cells and retinal ganglion cells are the major and minor postsynaptic partners of the AII AC, respectively. Having determined the mature connectivity map of the AII AC for comparison, I then examined the connectivity map of AII ACs at P11 to determine whether the major postsynaptic partner is established prior to eye-opening (~P14) and whether there are changes in the AII AC synapse distribution pattern with maturation. I found that bipolar cells receive more synapses than other partner cell types (RGCs and ACs) prior to eye-opening, and that this bias increases with maturation. I also found that individual presynaptic neurons can undergo partner-specific changes in connectivity. Additionally, I attempted to gain insight to the mechanisms underlying the development and maintenance of AII AC output structures and synapses using a combination of transgenic mouse

lines and optic nerve sectioning. The preliminary results from these experiments suggest that rod pathway activity is not required for AII AC development, output structure growth, or synaptogenesis with the major postsynaptic partner. AII ACs cannot fully compensate for the loss of synaptic partners by increasing synapses onto surviving partners. Furthermore, loss of a minor postsynaptic partner in the mature circuit does not induce changes in synaptic connectivity with the major postsynaptic partner, suggesting that synapses onto distinct partners may be regulated independently.

1.9 Figures

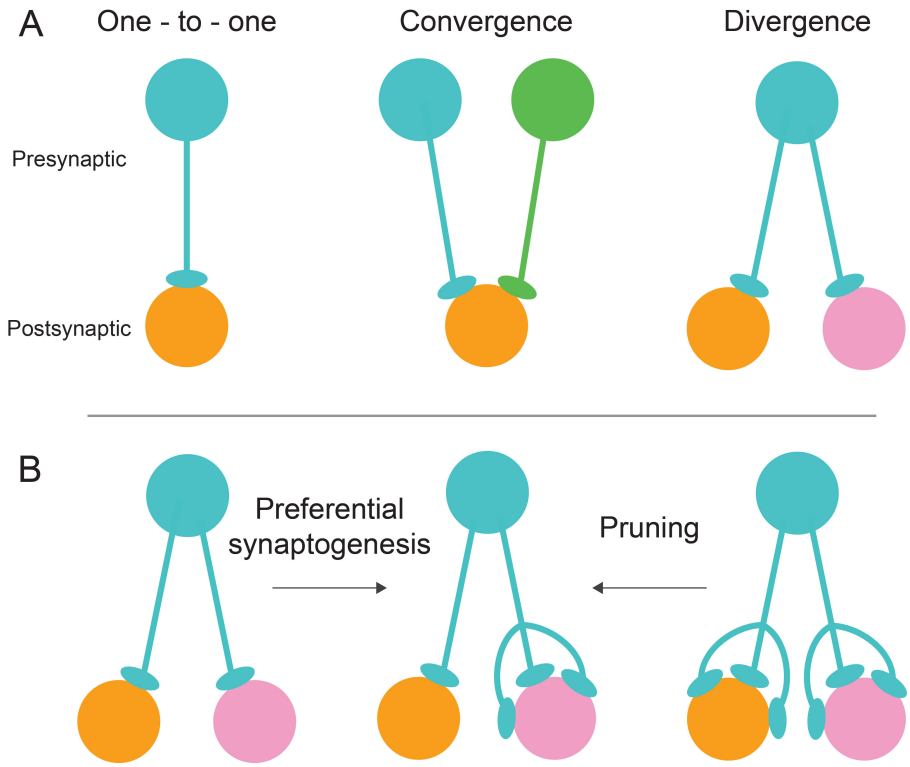

Figure 1.1 Circuit motifs and cellular strategies for achieving biased synaptic divergence.

A. Circuit connectivity motifs. **B.** Preferential synaptogenesis occurs when synapses are added onto one partner over others. Pruning occurs when synapses are eliminated onto a partner.

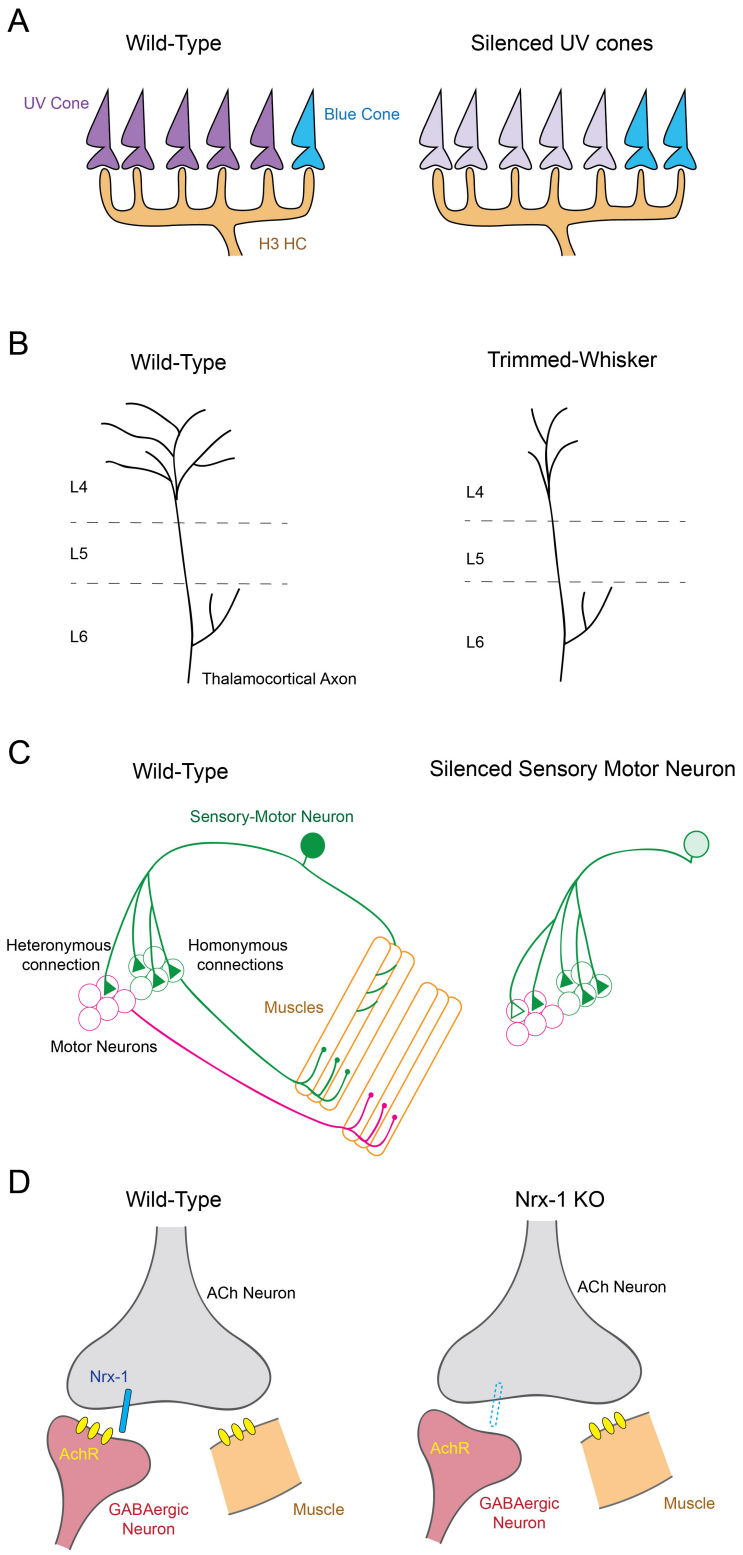

Figure 1.2 Molecular mechanisms underlying the establishment of biased connectivity. **A.** In wildtype zebrafish retina, H3 horizontal cells (H3 HC) preferentially contact UV cones over blue cones in a 5:1 ratio. Loss of transmission from UV cones (faded) leads H3 HC to contact more blue cones, but loss of transmission from blue cones does not alter H3 HC

connectivity with UV cones (Yoshimatsu et al. 2014). **B.** During normal development, thalamocortical axons preferentially expand axon territories and synapses to layer 4 versus layer 6 of the somatosensory cortex. Trimming the whiskers of young postnatal mice leads to sensory deprivation of the barrel cortex (whisker-representation in somatosensory cortex). Whisker-trimming results in a failure of thalamocortical axons to expand in layer 4, but does not affect connectivity in layer 6 (Crocker-Buque et al. 2015). **C.** In wildtype animals, sensory-motor neurons synapse onto pools of motor neurons that feedback onto the same muscle (homonymous) or other muscle (heteronymous) from which the sensory-motor neuron receives input. Typically, sensory-motor neurons form more synapses onto homonymous than heteronymous motor pools. When the sensory-motor neurons are silenced with tetanus toxin (fade), they form more synapses onto heteronymous motor pools. **D.** In *c. elegans*, cholinergic neurons (grey) form synapses onto GABAergic motor neurons (red) and muscles (orange). Cholinergic neurons express Neurexin (Nrx-1) specifically at synapses with GABAergic neurons, and loss of Nrx-1 results in loss of synapses onto GABAergic but not muscle partners (Philbrook et al. 2018).

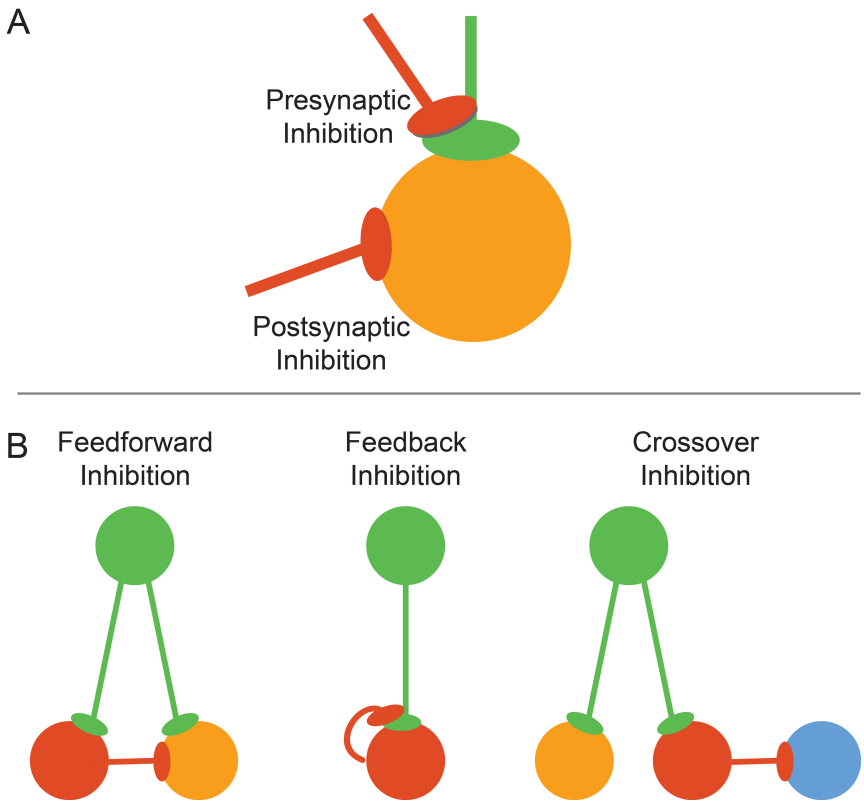

Figure 1.3 Motifs of synaptic and circuit inhibition.

A. Forms of synaptic inhibition. Presynaptic inhibition occurs when inhibition is applied at the presynaptic side (green) of a synapse. Postsynaptic inhibition occurs when inhibition is applied onto the postsynaptic cell (orange). **B.** Motifs of circuit inhibition. Feedforward inhibition occurs when a single presynaptic cell (green) drives both excitation and inhibition onto the same partner (orange) via direct excitation and excitation of an intermediate inhibitory interneuron (red). Feedback inhibition occurs when a neuron (red) inhibits the neuron that drives it (green). Crossover inhibition occurs when the activity of one presynaptic neuron (green) drives both excitation and inhibition of distinct pathways (orange vs. blue).

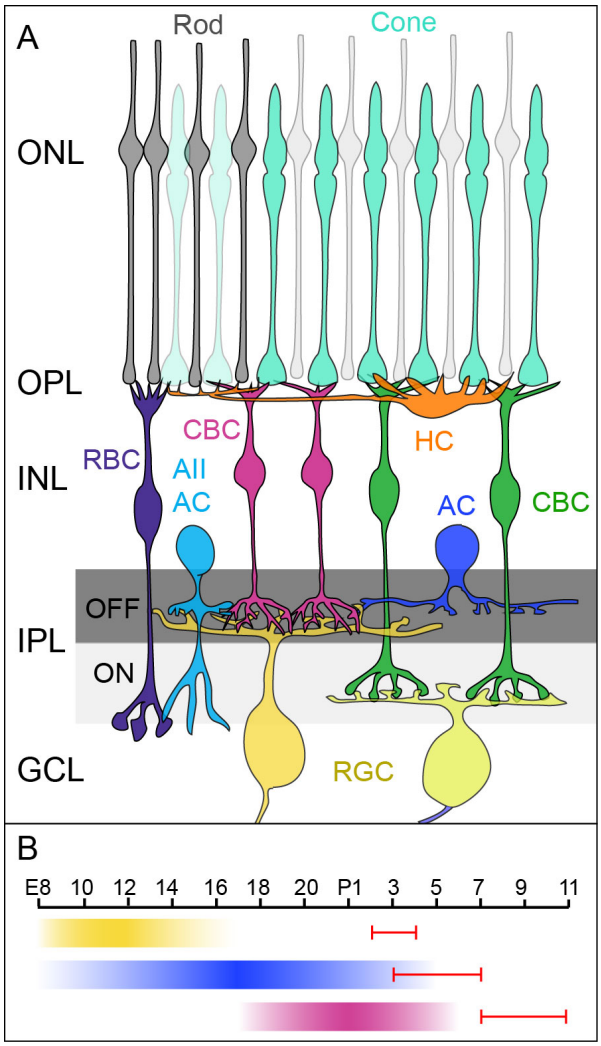

Figure 1.4 Organization and developmental timeline of the vertebrate retina.

A. Schematic of the vertebrate retina. Photoreceptors (rod and cones) are light sensitive neurons that synapse onto bipolar cells (BCs) at the outer plexiform layer (OPL). BCs in turn synapse onto retinal ganglion cells (RGCs), the sole output neuron of the retina, at the inner plexiform layer (IPL). The IPL can be subdivided into OFF and ON layers, where BCs and RGCs that preferentially respond to decrements and increments of light stratify, respectively. Horizontal cells (HC) provide inhibition at the photoreceptor to bipolar cell synapse in the OPL. Amacrine cells (ACs) provide GABA and glycinergic inhibition onto BCs and RGCs in the INL. ONL: Outer nuclear layer, somas of photoreceptors. OPL: Outer plexiform layer, synapses between photoreceptors and BCs. INL: Inner nuclear layer, somas of BCs and ACs. IPL: Inner plexiform layer, synapses between BCs, ACs, and RGCs. GCL: Ganglion cell layer, somas of RGCs. Figure adapted from (D'Orazi et al. 2014) **B.** Developmental timelines for retinal ganglion cells (yellow), amacrine cells (blue), and bipolar cells (magenta). Colorful plots show timing of cell genesis by cell type. Red bars indicate periods of apoptosis for each cell type during development.

CHAPTER 2: Determining the cellular strategies underlying the development of biased synaptic divergence.

2.1 Introduction

During development, neurons must not only target the correct postsynaptic partners, but also establish their stereotypic patterns of synaptic connections with those partners. Establishing the appropriate circuit patterns is necessary because connectivity errors lead to circuit dysfunction. There are two broad circuit patterns that are adopted by the majority of neurons in the nervous system: Synaptic convergence and divergence. Synaptic convergence involves multiple neurons and neuronal cell types providing input that is integrated by a common postsynaptic partner. Synaptic divergence entails an individual presynaptic neuron synapsing onto multiple, and often distinct postsynaptic partner types. Synaptic divergence is important for parallel processing of information and noise reduction within a circuit (Asari & Meister 2012; Kazama & Wilson 2009; Jeanne & Wilson 2015; Pelkey et al. 2006; Toth et al. 2000).

Much is now known concerning the developmental mechanisms that regulate synaptic convergence (Kerschensteiner et al. 2009; Morgan et al. 2011; Okawa et al. 2014), but despite synaptic divergence being a common circuit feature, much remains unknown regarding the mechanisms that underlie the development of stereotypic patterns of synaptic divergence. This is especially the case when the presynaptic cell is inhibitory and when postsynaptic partners receive unequal numbers of synapses from the presynaptic cell. Filling this gap in knowledge has not been straightforward, largely because reconstructing and quantifying the number of synapses distributed across postsynaptic partners from an individual axonal terminal is difficult for long-range projecting neurons. We thus sought a

compact circuit which demonstrates biased connectivity in favor of one postsynaptic partner type over others and used both light microscopy and serial block-face scanning electron microscopy (SBFSEM) to reconstruct connectivity across ages. We investigated whether biased synaptic divergence is established from the outset of circuit formation, or whether the initial circuitry undergoes changes over the course of development, and how the final circuitry is established.

The circuit we focused on is part of the rod pathway of the vertebrate retina that mediates scotopic, or night-time vision (Völgyi et al. 2004; Nelson & Kolb 1985), and is highly conserved across mammals (Famiglietti & Kolb 1975; Vaney 1985; Chun et al. 1993; Wässle et al. 1993; Wässle et al. 1995; Massey & Mills 1999). Rod photoreceptors input onto rod bipolar cells (BCs), which in turn provide excitatory drive onto the distal dendrites of AII amacrine cells (AII ACs), a narrow-field glycinergic interneuron. AII ACs form output synapses at lobular appendages located at the proximal end of the cell onto distinct classes of retinal neurons (Fig 2.1A). Inhibition from the AII AC occurs at synapses on the dendrites of retinal ganglion cells (RGCs), which hyperpolarize to increasing illumination (OFF RGCs), and at the axon terminals of OFF bipolar cells (BCs), regulating glutamate release from the BCs onto the RGCs. Previous electron microscopy reconstructions from rabbit and mouse retina revealed that an individual AII AC forms a greater number of synapses onto BC partners than onto retinal ganglion cells (RGCs) (Jeon et al. 1998; Marc et al. 2014; Tsukamoto & Omi 2017; Graydon et al. 2018).

The developmental strategies that regulate how the AII AC achieves its biased connectivity are unknown. Further, the two cell classes contacted by AII ACs, the BC and RGCs, are

born and differentiate at different times (Young 1985). By birth, ganglion cells including OFF type GCs, have already elaborated dendrites in the inner plexiform layer (IPL) of the retina, at a level where the AII AC extends its primary stalk. At postnatal day 5 (P5), BC axon terminals are just beginning to elaborate within the IPL and continue to grow in size over the subsequent weeks (Morgan et al. 2006). Thus, because AII ACs are born just prior to birth (Voinescu et al. 2009), they initially develop in a landscape where only the 'minor' GC postsynaptic partners are present. This raises the intriguing question of how late-arriving postsynaptic targets attain the majority of synapses from a presynaptic cell. We thus followed the morphological development and connectivity of the AII AC at early postnatal ages and determined the strategies by which this interneuron achieves its synaptic divergence pattern, considering the potential roles of preferential and differential timing of synaptogenesis, as well as synapse elimination.

2.2 Experimental Procedures

Transgenic Mice

All procedures were conducted in accordance with University of Washington Institutional Animal Care and Use Committee guidelines. CDH1-GFP mice were used in this study (Firl et al. 2015).

Immunohistochemistry

Mice were deeply anesthetized with Isoflurane, cervically dislocated or decapitated, and enucleated. Retinas were dissected in oxygenated mouse artificial cerebral spinal fluid (mACSF, pH 7.4) and flat mounted on filter paper (Millipore, HABP013). Once mounted

retinas were fixed for 15 minutes in 4% paraformaldehyde. Retinas were then rinsed with PBS in 3, 10 minute washes and incubated in blocking solution containing 5% normal donkey serum and 0.5% Triton X-100 overnight at 4° C. Retinas were then incubated with primary antibodies in blocking solution for approximately 72 hours at 4° C. Retinas were rinsed 3-10 minute washes of PBS and then incubated with secondary antibodies in PBS solution overnight at 4° C. Retinas were washed 3, 10 minutes with PBS then mounting on slides with Vectashield anti-fade mounting medium (Vector Labs). Slides were subsequently imaged.

Antibodies

Table 2.1 – Primary Antibodies

Antibody	**Host species**	**Working Concentration**	**Source**
anti-GFP	Chicken, polyclonal	1:1000	Abcam
anti- GlyRα1	Mouse, polyclonal	1:1000	Synaptic Systems
anti-Synaptotagmin-2	Mouse, polyclonal	1:1000	Znp-1, Zebrafish International Resource Center

Table 2.2 – Secondary Antibodies

Secondary	**Host species**	**Working Concentration**	**Source**
anti-chicken Dylight 488	Donkey	1:1000	Jackson Immunoresearch
anti-mouse IgG1 568	Goat	1:1000	Synaptic Systems

anti-mouse IgG2a 647	Donkey or Goat	1:1000	Jackson Immunoresearch

Confocal Image Acquisition

Image stacks were acquired on an Olympus FV1000 microscope using a 60x oil-immersion objective with 1.35 NA. Images were acquired at 0.051 x 0.051 x 0.3 um per pixel x-y-z resolution.

Image Analysis

Image stacked were median filtered in FIJI (NIH). Maximum intensity images were visualized in Amira (FEI). To quantify lobular appendage volume, processes of individual AII ACs were traced in 3D using the labelfield function in Amira. Lobules were traced from individual AII AC somas, but somas and central shafts were excluded for final masks. These binary masks were exported to Matlab and custom scripts were used for quantification of volume. To determine the total number of output synapses, entire AII AC somas and lobular appendages were masked in Amira using the labelfield function. This binary mask was multiplied by the thresholded receptor signal using the Arithmetic function in Amira. The threshold for the receptor signal was determined by the image statistics of the channel as measured by FIJI. Thresholds were 6 standard deviations above the mode pixel intensity, which is an approximation of "noise" within the channel. To determine which puncta were apposed to Type 2 BCs, the thresholded receptor label within the AII AC mask, was multiplied by the binary mask for the Type 2 BC signal (Hoon et al. 2017). All AC puncta were visually confirmed to be between both cells before they were quantified.

Serial Blockface Tissue Preparation

Retinas were dissected as described above, but were then fixed with 4% gluteraldehyde in 0.1 M sodium calcodylate buffer, pH 7.4 at room temperature.

Statistical Analyses

Values were averaged and presented as ± standard error of the mean (SEM). Comparisons between averages were made using the Wilcoxon Rank Sum Test. Comparisons of distributions was made using Kolmogorov-Smirnov tests.

2.3 Results

AII AC output structures develop after their input structures are formed.

Previous studies in rabbit retina reported the appearance of parvalbumin positive processes in the inner part of the IPL prior to the emergence of such processes in the outer IPL (Casini et al. 1998) and in mouse retina, the appearance of individual Dab1 positive processes extending towards the IPL (Rice & Curran 2000). These observations suggest that AII amacrine cells establish their distal dendrites before elaborating their output structures, the lobular appendages. To determine whether mouse AII ACs adopt a similar developmental sequence, we followed the morphological changes of mouse retinal AII ACs across postnatal development. We used CDH1-GFP transgenic mice (Figure 2.1B,C,D), in which the majority of AII ACs express GFP, to visualize these amacrine cells from postnatal day 4 (P4) to adulthood. Because lobular appendages of neighboring AII ACs do not overlap, we were able to digitally isolate these structures for individual cells across ages [see methods] (Figure 2.1D). Although distal dendrites were present, no clear proto-lobular appendage extensions were seen at P4. Thin and short GFP-positive processes were first visible at P6, but became more evident with age and developed lobular structures (Figure 2.1D). Thus, like the rabbit retina, mouse AII ACs also first form distal dendrites prior to the emergence of lobular appendages. Quantitation of the volume of the lobular appendages [see methods] further demonstrated significant growth of these structures with age, especially from the time of eye-opening i.e. after P14 (Figure 2.1E).

Synaptic divergence occurs before eye opening and is shaped by partner-specific changes in connectivity.

We next sought to determine when synapses from AII ACs onto postsynaptic partners are established. In addition, we mapped the pattern of connectivity between developing AII ACs and each postsynaptic cell class. To do so, we performed serial blockface electron microscopy (SEBFEM) on P11 (before eye-opening) and P24 mouse retinas, at a more mature stage. We identified AII ACs from the characteristic dyad synapse between rod bipolar cells, AII ACs, and A17 amacrine cells (Raviola & Dacheux 1987). From these synaptic sites, we followed AII AC distal dendrites to their somata and traced the lobular appendages emerging from the cell. We then identified and quantified all output synapses of the AII AC (Figure 2.2A,B), noting their location on the cell (Figure 2.2A). We then reconstructed the processes of postsynaptic partner types within the imaged volume (Figure 2.2 C). Postsynaptic partner types were identified by their morphology and synapse specializations [see Methods, Supplementary Figure S2.1].

Individual AII ACs showed a significant increase in their total number of output synapses from P11 to P24 (43.3 ± 2.8 SEM to 66 ± 4.1 SEM, $p = 0.029$, $n = 4,4$). At P11, the AII ACs had already formed synapses with bipolar cells, retinal ganglion cells, and amacrine cells. Comparison of synapse numbers that individual AII ACs formed onto each partner class at both P11(n=4) and P24 (n=4) revealed cell class-specific changes in connectivity. The number of synapses formed onto retinal ganglion cells did not change between these two ages (10.8 ±1.9 SEM to 8.0 ± 0.7 SEM, $p = 0.314$); however, the number of synapses onto bipolar cells increased almost three-fold (21.3 ± 1.5 SEM to 57 ± 4.6 SEM, $p = 0.029$, $n = 4,4$). In contrast, the number of synapses onto amacrine cells decreased significantly (10.8 ±

1.7 SEM to 1.00 ± 0.7 SEM, p = 0.029, n = 4,4) (Figure 2.2B). These disparate changes in synapse number with each cell class results in a disproportionate increase in connectivity with bipolar cells (Figure 2.2B).

To determine whether these synaptic changes reflect alterations in the number of postsynaptic partners within each class, we quantified the number of each partner type with an individual AII AC at both ages (Figure 2.2D). There is no significant difference in the total number of postsynaptic partners (25 ± 3.1 SEM to 19.8 ± 0.9 SEM, p = 0.3) or the number of retinal ganglion cell partners between P11 and P24 (8 ± 0.7 SEM to 5.5 ± 0.9, p = 0.086). Although not statistically significant, there is a trend towards an increase in the number of bipolar cell partners with age. In contrast, there is a significant decrease in the number of amacrine cell partners with maturation (9.5 ± 1.9 SEM to 1.00 ± 0.7 SEM, p = 0.029). Overall, the proportion of partners that are bipolar cells increases with maturation (30.1% ± 1.8 SEM to 66.7% ± 6.2 SEM, p = 0.029). Together these results suggest that changes in the number of postsynaptic partners contribute to the alterations in synapse number with each cell class.

Collectively, these findings demonstrate that synaptic divergence from AII ACs onto distinct postsynaptic partner classes is present before eye-opening but continues to refine in a partner class-specific manner with maturation.

Synaptogenesis onto bipolar cells increases non-uniformly across partners.

Although AII ACs increase the number of synapses formed onto bipolar cells with maturation, there is no corresponding increase in the number of bipolar cell partners (Figure

2.2B,D). Thus, we determined whether an AII AC increases synaptic contact across all bipolar cell partners uniformly, or whether synaptogenesis occurs preferentially with a subset of partners. If synaptogenesis occurs uniformly across all bipolar cell partners, there would be an increase in the average number of synapses between all AII-BC pairs, which we did not find (P11: 2.8 ± 0.4 SEM; P24: 4.3 ± 0.7 SEM, p = 0.39, n = 4,4). However, with maturation a subset of bipolar cells received many more synapses than the majority of the partners (Figure 2.3A,B), thus, the maximum number of synapses that an AII AC formed onto an individual BC increased between P11 and P24 (6 ± 1.2 SEM to 20.5 ± 2.9 SEM, p = 0.03 Ranksum test, n = 4,4). These findings show that during maturation, AII ACs increase the number of synapses onto a few, but not all BC partners. One reason that only some bipolar cell partners receive many more synapses from an AII AC could be because their axons are in closer proximity and overlap more with the AII AC lobular appendages (Peter's rule-like) (Rees et al. 2017). We thus traced the appositions of all bipolar cell partners with their AII AC partners at P24 and generated a measure of overlap (see methods). We found that the number of synapses a BC receives is positively correlated with the amount of overlap of the BC axon terminal and the AII AC (R^2 = 0.9, Linear Fit: y = 1.7e-07*x – 0.088), supporting Peter's rule (Rees et al. 2017) (Figure 2.3C, S2.1). When we look at the morphology of the most highly connected bipolar cell partner for three neighboring AII ACs, we find that the bipolar cells show similar axon morphology (branching near the AII AC soma and extending processes downwards into the IPL) and that their axons do not overlap (Figure 2.3D). These anatomical features suggest that these cells are the same type of bipolar cell; however, as we cannot reconstruct the dendritic arbors of the bipolar cells due to the physical limits of the EM block, we cannot definitely classify each bipolar cell by type.

Previous EM reconstructions reveal that mature AII ACs provide the majority of their synapses onto Type 2 BCs (Tsukamoto & Omi 2017). Because our reconstructed volume could not extend beyond the INL, we used immunocytochemistry to identify Type 2 BCs under light microscopy. We used this approach and immunolabeling for the glycine receptor subunit alpha1 in the CDH1-GFP line (Figure 2.4A) to determine whether AII ACs preferentially synapse with Type 2 BCs during development. Light microscopy also enabled us to sample many more ages across development compared to serial blockface EM. We validated our light microscopy data by comparing the total number of output synapses formed by individual AII ACs numbers we obtained from SBFSEM and found them to be comparable (Supplementary Figure S2.1C).

We next compared the number of synapses an AII AC forms onto the Type 2 BCs with the total number of synapses onto bipolar cells from our EM reconstructions (Figure 2.4B). At P24, our EM reconstructions suggest that an AII AC forms on average of about 60 synapses with bipolar cells, however, by extrapolation, only about 27 synapses are formed with Type 2 BCs (Figure 2.4B). This suggests that other bipolar cell types besides the Type 2 are also partners of the AII AC at P24. Interestingly, synaptogenesis with bipolar cells between the first and second postnatal weeks appears to largely be with Type 2 BCs. The P11 EM reconstructions revealed that all bipolar cells receive approximately 21 synapses whereas we estimate that Type 2 BCs receive approximately 14 synapses (or 66% of the BC synapses). Thus, throughout development, AII ACs increase synaptogenesis with bipolar cells, although before eye-opening, synaptogenesis appears biased towards a preferred (T2) bipolar cell type.

Distribution of synapses across AII-RGC pairs is invariant with age.

Despite the lack of changes in the connectivity between an AII AC and the population of retinal ganglion cell partners, it remains possible that with maturation there is re-allocation of the number of synapses amongst individual ganglion cell partners. To determine whether this occurs, we compared the distribution of synapses onto individual retinal ganglion cells in the EM reconstructions (Figure 2.5A). We found that there is no significant difference between the average number of synapses that AII ACs provide onto individual RGC partners between ages (P11: 1.3 ± 0.2 SEM; P24: 1.5 ± 0.2 SEM, $p = 0.33$). The distribution of AII AC synapses across retinal ganglion cells follows a similar distribution at P11 and P24 (KS test could not reject the null hypothesis) (Figure 2.5B).

Our analysis suggests that synaptic connectivity between AII ACs and their RGC partners is established early in development and maintained thereafter without additional refinement.

Synapse elimination refines AII AC connectivity with amacrine cells.

AII ACs initially form many synapses with amacrine cells, but connectivity with amacrine cells decreases with maturation (Figure 2.2B). At P11, the neurites of most amacrine cells postsynaptic to AII ACs laminated narrowly in the IPL (Figure 2.6A). The processes of these amacrine cells rarely branched (within the reconstructed volume) and resembled those of GABAergic wide-field amacrine cells (Figure 2.6A). Each contacted amacrine cell process received a single synapse from the reconstructed AII AC (Figure 2.6B,C). Furthermore, like another described wide-field amacrine cell (Brüggen et al. 2015), the AC partners of the AII AC form output synapses (Figure 2.6C) along the length of the same process where they receive input with no clear spatial segregation of inputs and outputs

(Figure 2.6D). The morphological similarities and stratification levels of the postsynaptic amacrine cell processes suggest that they likely belong to a single type of amacrine cell. Synapses with such wide-field amacrine cells were observed in all four reconstructed P11 AII ACs. Surprisingly, these wide-field processes were rarely encountered postsynaptic to the P24 AII ACs (Figure 2.6A). In one of four reconstructed P24 AII ACs, the AII AC synapsed with another type of amacrine cell that stratified broadly throughout the IPL. Thus, our results suggest that the developmental loss of synapses from AII ACs onto other amacrine cells is due to the elimination of synapses with wide-field AC partners.

2.4 Discussion

While synaptic divergence is a common circuit motif, the cellular strategies that shape the final synaptic distribution pattern of a single presynaptic cell onto distinct targets remain largely unknown. Our study demonstrates that an individual neuron can employ multiple cellular strategies to reach a biased synaptic connectivity pattern. We determined that AII ACs undergo cell class-specific synaptogenesis and rewiring to achieve their mature synaptic divergence pattern. Furthermore, these strategies do not necessarily apply evenly across a cell class, as synaptogenesis can occur non-uniformly across postsynaptic partners of the same type.

AII output structures elaborate when all postsynaptic partners are present.

AII ACs do not begin to develop lobular appendages until their major postsynaptic partners (bipolar cells) extend axon branches into the IPL. This finding is surprising given that other targets of the AII amacrine cells, the retinal ganglion cells, are present and have elaborated their dendrites in the IPL at least a week before bipolar cells differentiate. Moreover, in other neural circuits, axons can elaborate prior to the availability of their final postsynaptic targets. For example, axons from the entorhinal cortex and contralateral side of the hippocampus enter the hippocampus before their targets, pyramidal cell dendrites, develop (Review Chao et al. 2009). Entorhinal and commissural axons form synapses onto intermediate targets, Cajal-Retzius cells and GABAergic interneurons, respectively. Once the entorhinal and commissural axons form synapses onto pyramidal dendrites, both intermediate target cell populations undergo apoptosis (Supèr et al. 1998). Loss of Cajal-Retzius cells prevents entorhinal axons from entering the hippocampus (Del Río et al. 1997),

revealing the necessity of these targets for proper circuit formation. Intermediate synaptic targets are not unique to the hippocampus, as corticogeniculate axons form synapses onto subplate neurons until layer 4 neurons develop (Ghosh et al. 1990). Thus, axons can elaborate lamina-specific arborizations prior to the development of postsynaptic targets but may require a transient synaptic partner. Axons can also extend beyond the region where they will eventually elaborate. For example, retinal ganglion cell axons project along the length of the superior colliculus, often overshooting their final target regions. With maturation, retinal ganglion cells eliminate 'overshooting' arbors and elaborate processes in the correct target region (Simon et al. 1992). Thus, output structures can develop beyond their final targets and undergo subsequent remodeling. In our study, we describe a cell that does not develop an output structure even when postsynaptic partners are present, but appears to 'wait' until the dominant postsynaptic partner elaborates its processes. The timing of AII AC lobular appendage growth suggests a role for bipolar cells as a potential source of an instructive cue. As bipolar cells are both the major pre- and postsynaptic targets of AII AC, the cue could be mediated by synaptic transmission or be target-derived.

Neurotransmission has been shown to shape the development of both dendritic and axonal structures across neural circuits (reviewed Bleckert & Wong 2011). Glutamatergic, cholinergic, and GABAergic signaling can promote filopodial and dendritic motility (Maletic-Savatic 1999; Wong et al. 2000; Wong & Wong 2001). Glutamatergic signaling can promote spine growth (Engert & Bonhoeffer 1999) and expansion of dendritic arbors (Elias et al. 2018). Axonal growth can also be shaped by circuit activity. For example, activity-dependent competition determines which motor-neuron 'wins' and eventually occupies the entire neuromuscular junction for a given muscle (Sanes & Lichtman 1999).

Activity-dependent competition can also determine the axon territory of neurons along the visual pathway. Monocular deprivation (closing one eye) leads to a loss of axonal territory for neurons carrying information from the deprived eye and an expansion of territory for neurons carrying information from the spared eye at both the a retinorecipient area, lateral geniculate nucleus, and primary visual cortex (Wiesel & Hubel 1963; Hubel et al. 1977; Katz, LC; Shatz 1996). Thus, the activity of the rod pathway as conveyed by rod bipolar cells may instruct the development of AII AC lobular appendages.

Target-derived cues may drive lobular appendage extension. One potential bipolar cell-derived cue could be cadherins. Cadherins can bind homophilically (Takeichi 1995) or heterophilically (Brasch et al. 2018) and have been shown to direct neurite growth to specific retinal layers (Yamagata & Sanes 2008) and are expressed by murine amacrine cells (Honjo et al. 2000). AII ACs form some ectopic processes, although many lobular appendages remain when, Fat3, an atypical cadherin, is genetically ablated from amacrine cells (Deans et al. 2011). Recent transcriptomic profiling of the retina has found that OFF bipolar cells express genes for cadherins and protocadherins (Shekhar et al. 2016). Furthermore, cell adhesion molecules, such as N-CAM, can promote the neurite extension of GABAergic amacrine cells *in vitro* (Kljavin et al. 1994). Thus, cell adhesion molecules may play a role in directing lobular appendage and OFF BC axon growth, but a candidate molecule has yet to be identified. AII ACs express Disabled1 (Dab1) (Rice & Curran 2000), an intracellular signaling molecule that is downstream from Reelin, a secreted glycoprotein which plays a role in cell positioning and dendritogenesis during CNS development (Rice et al. 2001; Nichols & Olson 2010). Mice lacking Reelin or Dab1 have normal retinal lamination, but AII AC lobular appendages are sometimes shifted towards the ON lamina

(Rice et al. 2001). Therefore, AII ACs do not require normal Reelin signaling for lobular appendage outgrowth, but Reelin may influence lobular appendage lamination.

Cellular strategies for achieving biased connectivity

Neurons can achieve biased connectivity with specific postsynaptic partners via several, distinct cellular strategies. Biased connectivity could be set up by preferential synaptogenesis, which occurs when the presynaptic cell continues to add synapses onto one partner. For example, in primary somatosensory cortex, thalamocortical (TC) axons initially form equal numbers of synapses onto layer 4 and layer 6 neurons, but preferentially add synapses onto layer 4 (L4) neurons during development (Figure 1.2 B (Crocker-Buque et al. 2015)). Additionally, neurons may undergo selective pruning to achieve a final biased connectivity pattern. For example, in the spinal cord, individual sensory-motor neurons form equal numbers of synapses onto two motor neuron partners but remove synapses onto the minor partner during development (Figure 1.2 C) (Mendelsohn et al. 2015). Our current study showed that these cellular strategies are not mutually exclusive and that a single presynaptic neuron can differentially regulate connectivity across partners.

Altered activity has been shown to prevent preferential synaptogenesis and pruning in thalamocortical and spinal cord circuits, respectively (Crocker-Buque et al. 2015; Mendelsohn et al. 2015); however, in these circuits, changes in activity did not interfere with the maintenance of synapses onto other targets (Crocker-Buque et al. 2015; Mendelsohn et al. 2015). These results indicate that activity-mediated mechanisms can underlie both preferential synaptogenesis and pruning, and that distinct mechanisms may

work in concert to regulate connectivity across partners. There is evidence to suggest, however, that activity-mediated mechanisms may not underlie AII AC preferential synaptogenesis with bipolar cells. In mice lacking vesicular inhibitory amino acid transporter (VIAAT) in the retina, inhibitory retinal interneurons no longer release neurotransmitter (Wojcik et al. 2006), but Type 2 bipolar cells continue to express normal numbers of α1-subunit containing glycine receptors, which are likely from AII ACs (Hoon et al. 2015). Thus, inhibitory neurotransmission from the AII AC may not be necessary for its synaptogenesis with bipolar cells.

Molecular mechanisms have also been found to regulate synaptic connectivity with distinct postsynaptic partners. For example, cholinergic motor neurons in *C. elegans* express Neurexin, a GABAergic or glutamatergic synapse organizing protein (Graf et al. 2004), at synapses with GABAergic neurons, but not at synapses onto muscles (Philbrook et al. 2018). Thus, individual neurons may independently regulate connectivity with different postsynaptic partners through expression of specific synapse organizing proteins. Therefore, it is possible that both activity-dependent and activity-independent mechanisms can independently regulate connectivity onto distinct postsynaptic partners in a divergent circuit. Which mechanisms are employed by the AII ACs to target bipolar cells and ganglion cells and whether connectivity with specific partners is regulated separately remains unknown.

Although we show that AII ACs preferentially synapse onto bipolar cells, we find that synaptogenesis is not uniform across this partner population. We found that the number of synapses a bipolar cell partner receives from an AII AC correlates with the amount of

surface area overlap between the two cells. Our findings are predicted by a variant of Peter's rule. Classically Peter's Rule refers to the colocalization of neural processes as a predictor of synaptic contact between neuron classes (Peters & Feldman 1976). More recently, neuroscientists have extended this "rule" to predict whether surface overlap correlates with the number of synapses between cell pairs (Rees et al. 2017). We considered a variant of Peter's rule that is applied specifically to bipolar cells that are postsynaptic to AII ACs, as surface overlap was also observed between AII ACs and bipolar cells that did not receive synapses. We found that there is a high correlation between the overlap of an AII amacrine cell and its bipolar cell partner and the number of synapses that bipolar cell receives. The cellular mechanisms that establish the degree of surface overlap between AII ACs and their bipolar cell partners remain unknown.

During circuit development, neurons often form more connections than will persist in maturity, requiring refinement or pruning. Typically, the number of synapses between neurons will be reduced by synapse elimination, but the connection between partner types remains (Reviewed by Sanes & Yamagata 2009; Gamlin et al. 2018); however, the AII AC does not maintain any synapses onto wide-field amacrine cells, losing this cell type as a partner. Neurons sometimes form synapses onto partners that later undergo apoptosis. Connectivity with these "transient" partners plays an important role in both the development and maturation of the circuit. For example, Cajal-Retzius cells and subplate neurons receive synaptic input from neurons whose final postsynaptic partners have not yet developed, thus they serve as an intermediate target until the appropriate targets arrive (Reviewed by Chao et al. 2009). As AII AC lobular appendages do not elaborate until bipolar cells are present, it is unlikely that these wide-field amacrine cells serve as an intermediate target. Furthermore,

wide-field amacrine cells with similar morphology and stratification to those postsynaptic to the AII AC have been observed within the mature mouse retina (Helmstaedter et al. 2013) and most amacrine cells have undergone apoptosis by P7 (Farah & Easter 2005; Young 1985), suggesting that these partners may remain after synaptic pruning. Transient synapses can also be formed between surviving cells (Reviewed by Kerschensteiner 2014). For example, in the retina, starburst amacrine cells initially form both GABAergic and cholinergic synapses onto each other, but cholinergic synapses are eliminated with maturation (Ford & Feller 2012). In the cerebellum, Purkinje cells synapse onto each other during the first postnatal week, and these transient connections propagate waves of spontaneous activity within the circuit (Watt et al. 2009). Spontaneous correlated activity (such as retinal waves) has been shown to influence circuit development (e.g. refining retinotopic maps and segregating inputs from different eyes) in downstream areas (Wong 1999) and thus serves an important developmental role. At P11, when the AII AC is synapsing onto widefield amacrine cells, spontaneous glutamatergic waves are present in the retina. AII ACs are known depolarize during the ON phase of the glutamatergic retinal waves (Akrouh & Kerschensteiner 2013) and provide cross-over inhibition onto OFF RGCs following ON pathway activation (Manookin et al. 2008). Thus, AII ACs may inhibit their widefield ACs partners (serial inhibition) during the ON phase of the glutamatergic wave. Future experiments will be necessary to determine whether AII AC synapses onto widefield amacrine cells play a role in glutamatergic retinal wave generation and propagation.

In summary, we found that AII ACs, a retinal interneuron, develop presynaptic structures and form glycinergic synapses with a ‘delay’ relative to the differentiation of their input structures that are contacted by rod bipolar cells. Furthermore, preferential synaptogenesis

and partner-specific pruning of synapses occurs in parallel to shape the final stereotypic synapse distribution pattern. Lastly, the timing of postsynaptic partner development does not predict whether that partner is ‘preferred’ even at early stages of synaptogenesis. Thus, the development of biased synaptic divergence is a highly complex process that occurs in a time and partner-specific manner.

2.5 Figures:

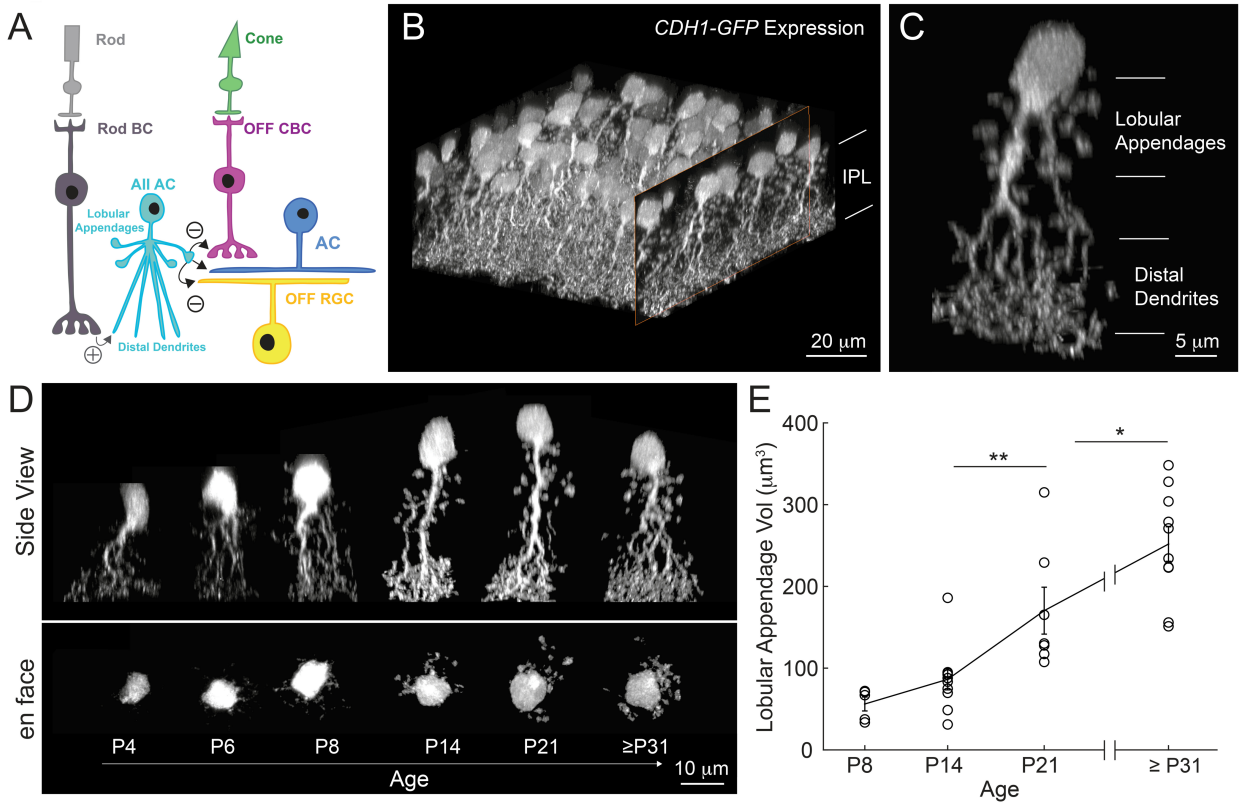

Figure 2.1. Schematic of Rod Pathway and Characterization of AII AC morphology
A. Schematic of the rod pathway in the mammalian retina. Plus signs indicate excitatory input, negative signs indicate inhibitory input. **B.** Rotated confocal volume of maximum intensity projection of AII Amacrine cells in the CDH1-GFP transgenic mouse line retina. The orange plane isolates a single row of AII ACs within the volume. IPL: inner plexiform layer. **C.** Side view of digitally isolated mature AII AC from CDH1-GFP line. **D.** Examples of digitally isolated AII ACs at different developmental time points. The images are maximum intensity projections of the full AII ACs from the side and en face views exclude distal dendrites. **E.** Quantification of the volume of digitally isolated lobular appendages of AII ACs at each time point. Volumes were measured by digitally isolating individual lobular structures using Amira then exporting binary pixel volumes to Matlab for summation ((Hoon et al. 2015, methods). Lobular appendage volume increases significantly with age (One Way Anova). Using the Wilcoxon Rank Sum test, there are significant changes from P14 to P21 and from P21 to ≥P31 (P31 to 3.5 months of age). [One-Way Anova, p = 4.9147e-7,Wilcoxon Rank Sum tests P14-21, p = 0.002, P21- ≥P31 p = 0.0431]

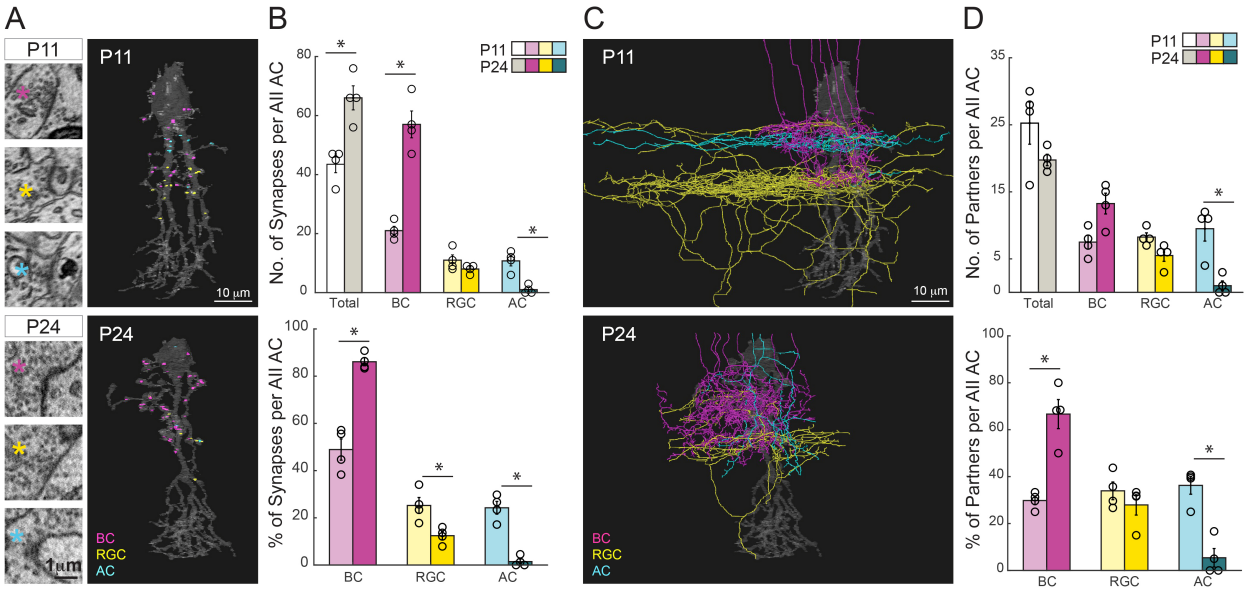

Figure 2.2. EM reconstructions of AII AC at distinct developmental time points
A. Left panel: Examples of synapses with each postsynaptic partner identified from EM. Magenta asterisk indicates a synapse onto a BC partner. Yellow asterisk: a RGC partner. Cyan asterisk: an AC partner. The second panels are EM reconstructions of the volumes of individual AII ACs at P11 and P24. Each output synapse is shown on the AII ACs themselves, color-coded to indicate the identity of the postsynaptic partner at that synapse. **B.** Top: Quantification of the number of total output synapses of four AII ACs at each time point, and the number of output synapses onto each postsynaptic partner cell class. Bottom: Quantification of the percentage of the total output synapses that are formed onto each postsynaptic partner cell class at both P11 and P24. **C.** EM reconstructions of the same AII ACs seen in Fig1A, including traced skeletons of all postsynaptic partners, color-coded by cell class. **D.** Top: Quantification of the number of postsynaptic partners and the number of postsynaptic partners within each cell class at P11 (lighter colors) versus P24 (darker colors). Bottom: Quantification of the percentage of total partners each partner class represents at P11 and P24.

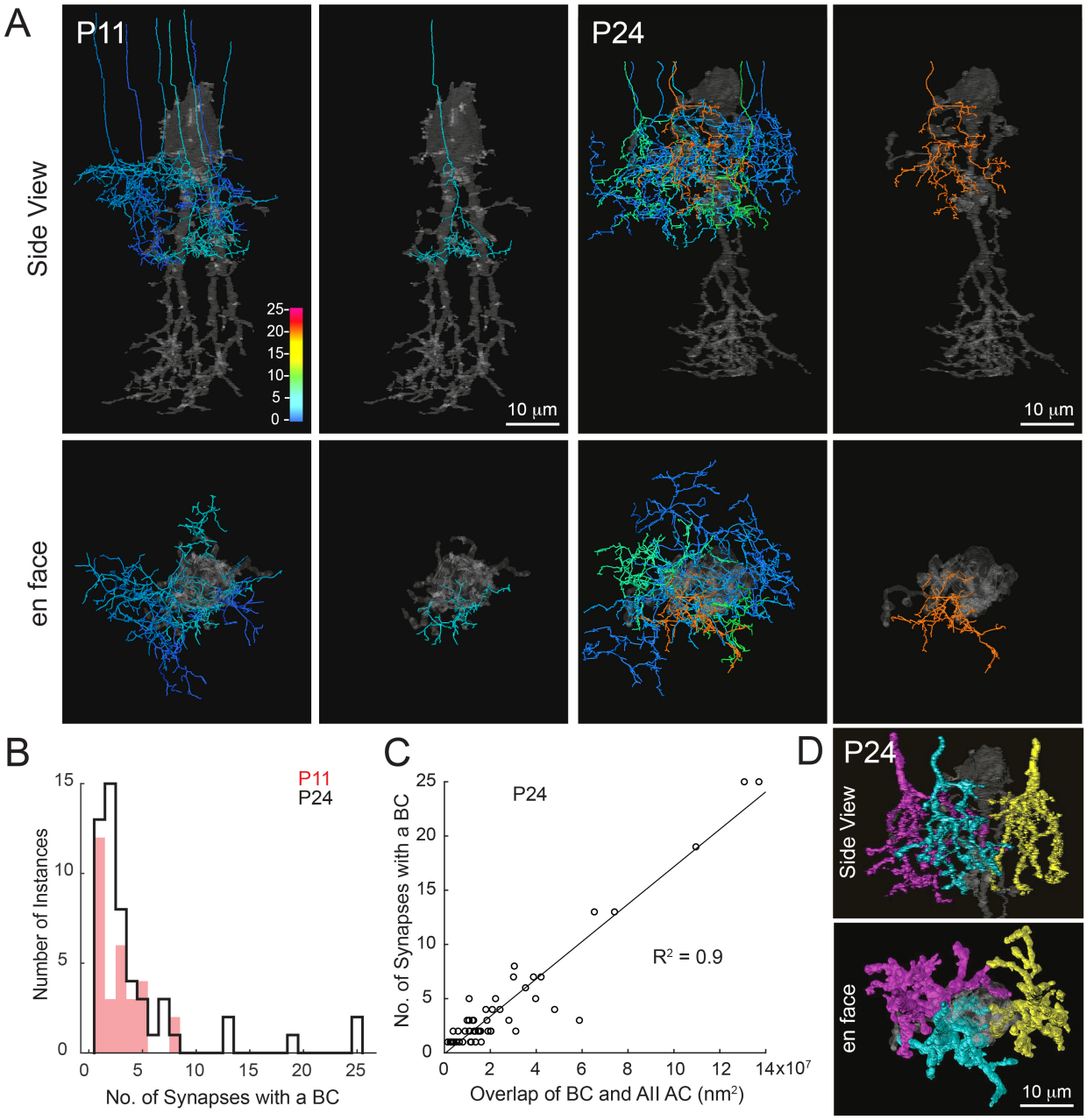

Figure 2.3. EM Reconstruction of bipolar cells postsynaptic to AII ACs
A. EM reconstructions of AII ACs and skeletons of all bipolar cell partners in the leftmost panel. Bipolar cells are color-coded by the number of synapses each receives as indicated by the heatmap. In the right panel, EM reconstructions of the same AII AC with the skeleton of the BC that receives the most synapses from that AII AC. **B.** Histogram of the number of synapses that individual BCs receive at both P11 and P24. **C**. A plot of the overlap of a BC terminal with AII AC lobular appendages and the number of synapses that each BC receives. $R^2 = 0.9$. **D.** Volumes of axon terminals from the most connected BC partner from three neighboring AII ACs. Note their similar branching pattern (top) and non-overlapping processes (bottom).

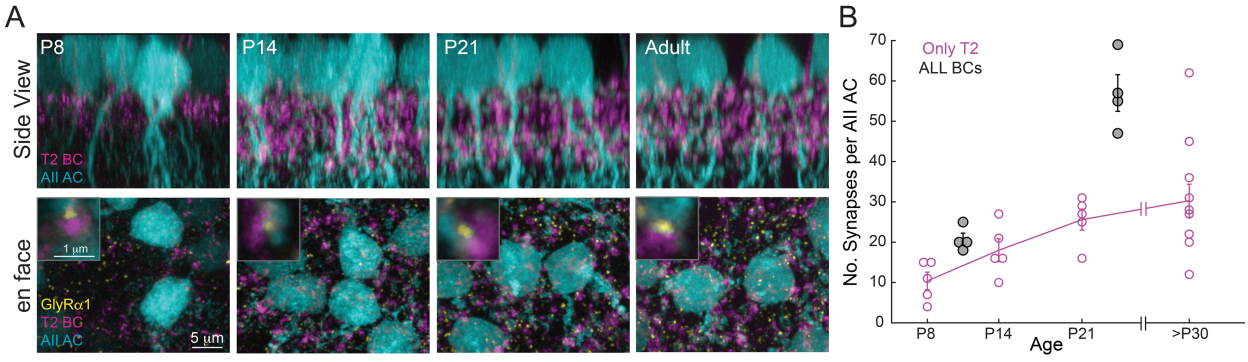

Figure 2.4. AII AC connectivity with Type 2 bipolar cells across development
A. Light microscopy images of immunostaining for AII ACs, Type 2 BCs, and glycine receptor α1 (AII AC output synapses) across ages. **B**. Quantification of the number of synapses that individual AII ACs form in total and onto Type 2 BCs across ages (magenta) and number of synapses formed onto all BCs under EM at P11 and P24 (filled grey).

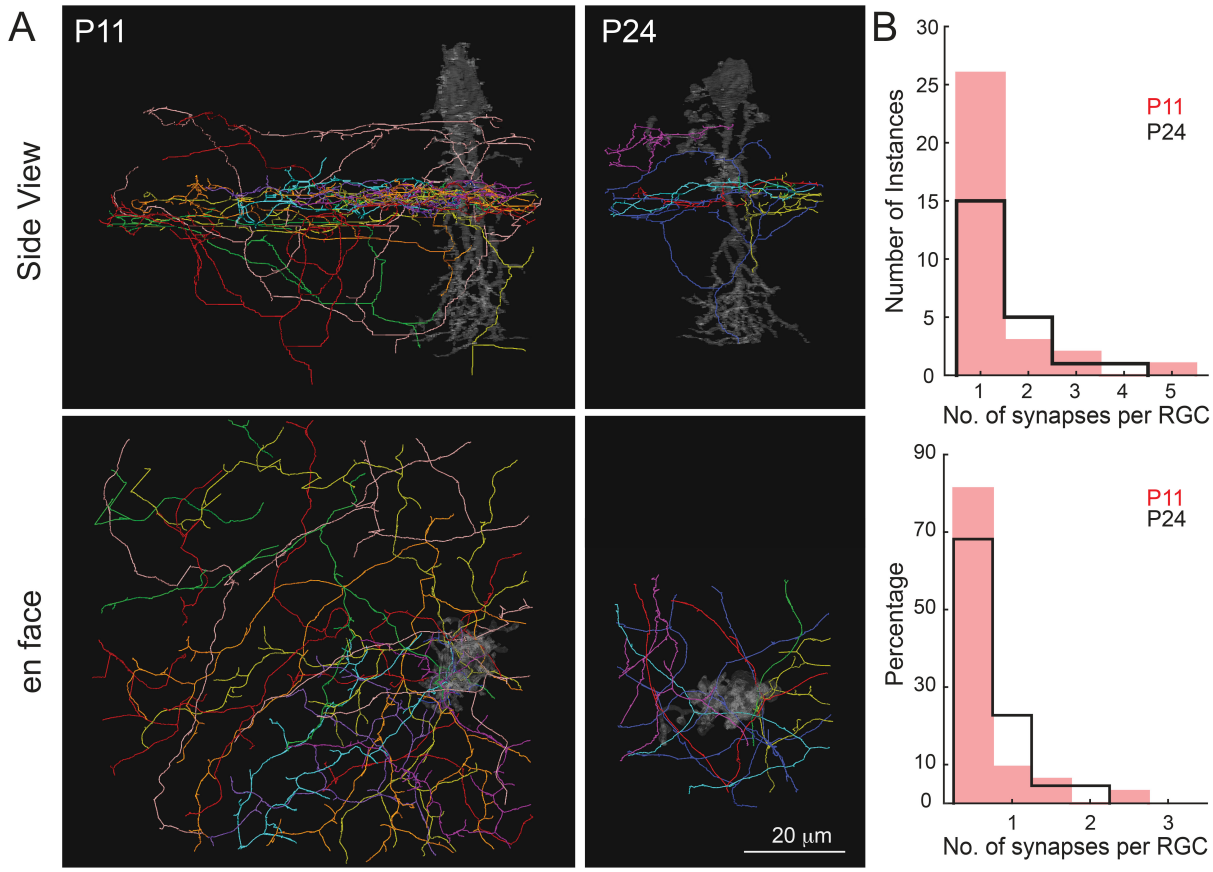

Figure 2.5. EM reconstructions of RGCs postsynaptic to AII ACs
A. EM reconstructions of the skeletons of retinal ganglion cell (RGC) partners of an individual AII AC at P11 and P24. Each RGC partner is traced in a distinct color. **B.** Top: Histogram of the number of synapses formed onto individual RGCs at both P11 and adulthood. Bottom: Normalized histogram showing the frequency with which an AII AC forms a number of synapses onto an individual RGC partner.

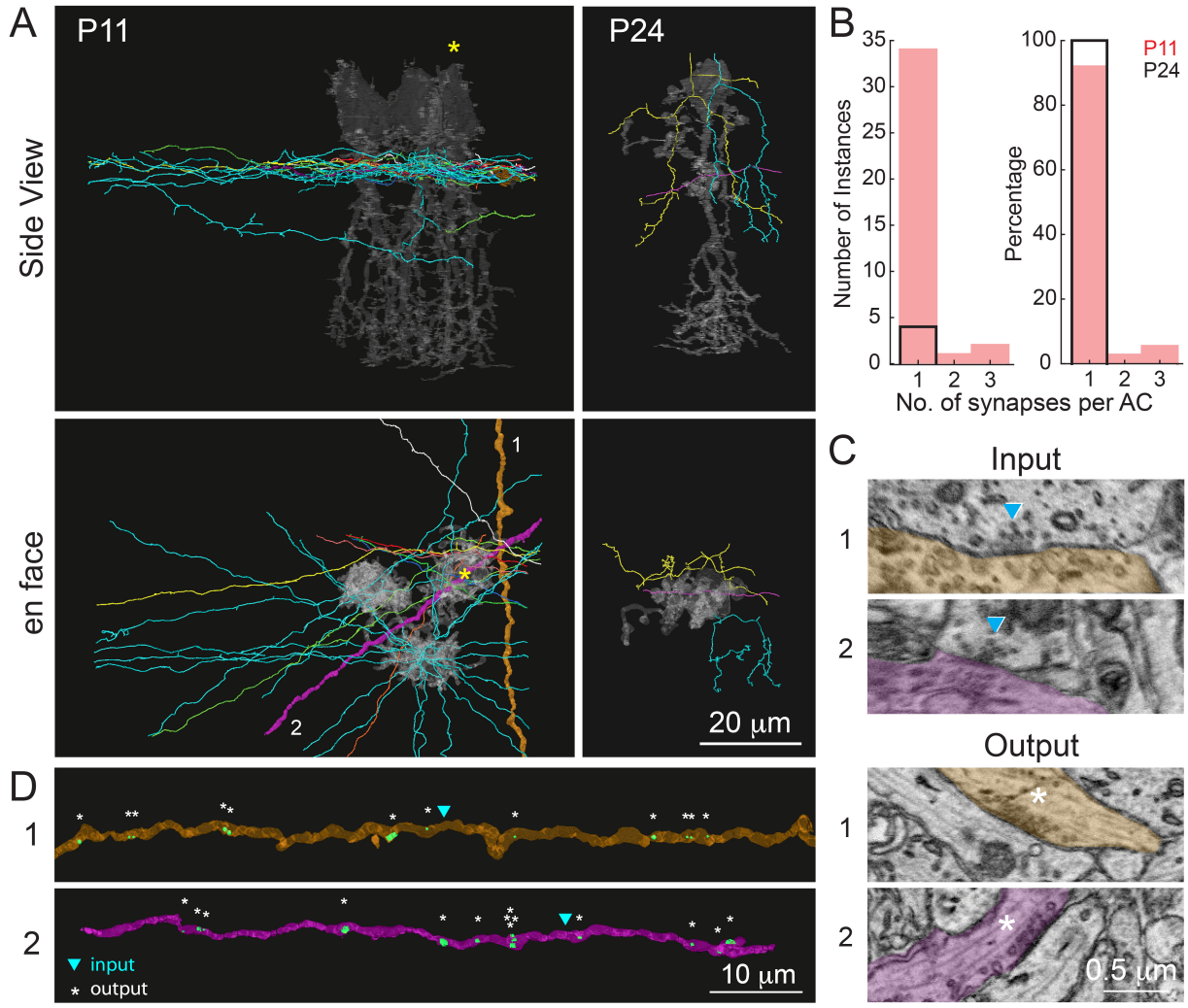

Figure 2.6. EM reconstructions of widefield amacrine cells postsynaptic to AII AC
A. Left: EM reconstructions of the skeletons of wide-field amacrine cell (WF AC) partners of three AII AC at P11. At P11, each AC partner of the AII AC indicated by an asterisk is traced in non-cyan colors. WF AC partners of the other two AII ACs are shown in cyan. Numbers indicate wide-field ACs featured below. Right: EM reconstructions of skeletons of the AC partners of an individual AII AC at P24. **B**. Left: Histogram of the number of synapses formed onto individual ACs at both P11 and adulthood. Right: Normalized histogram showing the frequency with which an AII AC forms a number of synapses onto an individual AC partner. **C.** Top: Input synapses from AII AC onto the WF AC process (colored to match C). Blue arrowhead: AII AC input synapse. Examples of output synapses from the WF ACs pictured left. WF AC processes are colored to match A. **D**. EM reconstruction of volume and output synapses (green) of two wide-field ACs that are postsynaptic to the AII AC indicated by the white asterisk in A. White asterisks indicate output synapses. Cyan arrowhead: location of AII AC input to WF AC.

A

Cell Type	Morphology	Output Synapses	Ribbon Synapses
Bipolar Cell	Single axon descends into IPL, branches into axon terminal.	YES	YES
Ganglion Cell	Large soma in ganglion cell layer, from which, large microtuble-filled dendrites emerge.	NO	N/A
Amacrine Cell	Variable morphology, often contain microtuble -dense processes.	YES	NO

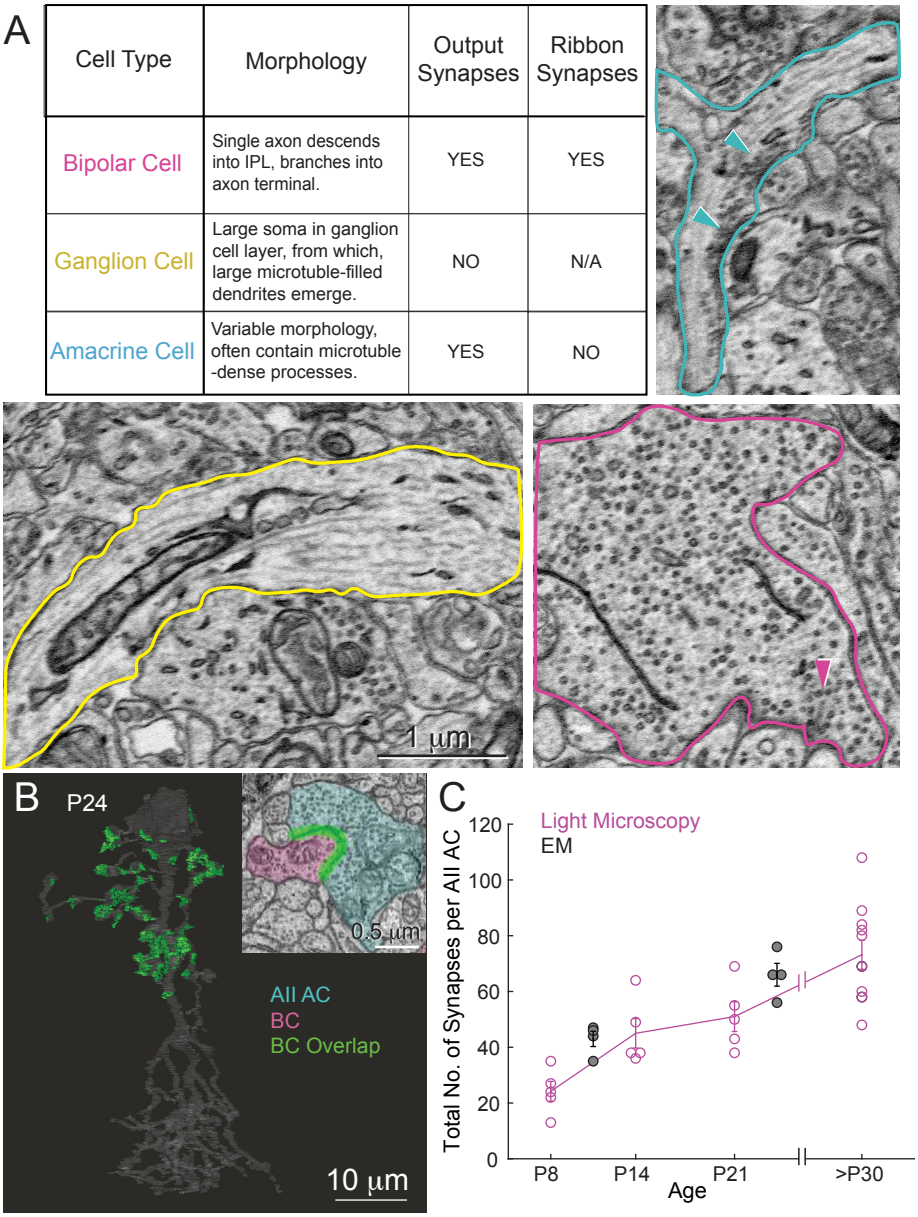

Supplementary Figure 2.1. A. Table detailing the criteria for cell type classification and examples of the raw EM appearance of each cell type. Colored lines trace the outline of each cell. Arrowheads indicate output synapses. **B**. Volume of P24 AII AC showing traced surface overlap with all BC partners (green). Inset: EM image showing example trace of overlap between AII AC and BC in a single plane. **C**. Plot of total output synapses from AII ACs as measured from light microscopy (magenta) and electron microscopy (grey) techniques.

CHAPTER 3: Exploring the role of cellular interactions in establishing the output connectivity of AII amacrine cells.

3.1 Abstract

As discussed in Chapter 2, we found that AII ACs establish biased synaptic divergence by engaging distinct cellular strategies in a partner-specific manner. Specifically, we found that the bias for bipolar cells is established by three mechanisms: 1. preferential synaptogenesis with bipolar cells, 2. no change in synapse formation with retinal ganglion cells, and 3. pruning of synapses onto widefield amacrine cells. We also found that AII ACs elaborate their presynaptic structures and commence synaptogenesis when the dominant postsynaptic partners (bipolar cells) are differentiating, despite the presence of ganglion cell partners earlier in development. Thus, our findings raised two main questions (1) what cellular interactions regulate the elaboration of AII AC presynaptic structures (lobular appendages), and (2) what factors regulate the connectivity of AII ACs with their postsynaptic partner types?

To determine what factors shape AII AC development, we considered the potential cellular interactions between the AII ACs and their presynaptic and postsynaptic partners. First, we examined the pathway that provides input to the AII ACs. We explored whether transmission along the rod-pathway (rods-> rod bipolar cells -> AII ACs) influences the elaboration of AII AC presynaptic structures and their synaptic distribution pattern. We found that AII AC lobular appendages differentiated and were maintained in the absence of photoreceptors, and when rod bipolar cells were silenced or ablated. AII AC synaptic distribution pattern, as measured by the number of output synapses and bias towards Type 2 bipolar cells, was also unaffected in these conditions. Thus, transmission along the rod pathway does not influence the development of AII synaptic divergence.

Next, we examined whether the dominant postsynaptic partners of the AII ACs (Type 2 bipolar cells) are required for the growth or maintenance of lobular appendages, and whether AII ACs reallocate output synapses if the dominant partner is lost. We found that Type 2 bipolar cells were not required for the elaboration or maintenance of lobular appendages. But, AII ACs made significantly fewer output synapses, revealing that they cannot fully compensate for the loss of Type 2 BCs by increasing connectivity with remaining partners. Whether GCs capture more synapses from AII ACs in the absence of T2 bipolar cells remains to be determined.

Lastly, we examined whether loss of retinal ganglion cells in the adult retina, which occurs in some retinal diseases, affects the AII AC synaptic distribution pattern. Ablation of adult ganglion cells did not lead to significant changes in the number of AII output synapses or the number of synapses formed onto Type 2 bipolar cells. Thus, synapses onto distinct partner types may be regulated independently. Together these results reveal that a neuron can establish biased synaptic divergence independently of presynaptic drive, and distribute its synapses in a partner-specific manner.

3.2 Introduction:

In Chapter 2, we described how AII ACs develop a pattern of biased synaptic divergence via several partner-specific cellular strategies. The mechanisms underlying these strategies remain unclear. We also found that the elaboration of AII AC presynaptic structures (lobular appendages) is delayed until their major postsynaptic target, bipolar cells, have differentiated. This ‘delay’ in the differentiation and elaboration of the AII AC presynaptic structures is surprising given that its other synaptic partners (retinal ganglion cells) are present before bipolar

cells differentiate. Our findings thus raise two key questions (1) what are the cellular interactions that regulate lobular appendage elaboration and (2) what factors regulate the development and maintenance of AII AC connectivity with their postsynaptic partners?

The delayed elaboration of AII AC presynaptic structures is surprising given the fact that neurons across circuits develop axons prior to the availability of final postsynaptic targets (Chao et al. 2009), and that retinal ganglion cells, an AII AC postsynaptic partner, are present at an early developmental stage (Stacy & Wong 2003). Since AII ACs extend lobular appendages at the time of bipolar cell differentiation, we hypothesized that bipolar cells may be required for this process. As bipolar cells are the major source of presynaptic input to AII ACs, we sought to determine the role of rod pathway activity in directing the growth of AII AC lobular appendages (Figure 3.1A). Circuit activity can promote and shape axon branching. For example, cortical neurons fail to elaborate axon branches when spontaneous activity or AMPA receptors are blocked (Uesaka et al. 2005). Thalamocortical neurons will branch more or less depending on the level of activity within the neuron and in postsynaptic neurons (Matsumoto et al. 2016; Yamada et al. 2010). Thus, we determined whether AII AC presynaptic structures formed in the absence of rod-mediated transmission in a model of retinitis pigmentosa, in which rod and cone photoreceptors quickly degenerate after birth (Carter-Dawson et al. 1978). We also examined whether lobular appendages formed when rod bipolar cells were silenced by the expression of tetanus toxin, which prevents synaptic release (Schiavo et al. 1992), and when rod bipolar cells are genetically ablated by expression of diphtheria toxin (Figure 3.1B,C). As bipolar cells are also the major postsynaptic target of AII ACs, we determined whether the dominant bipolar cell partners (Type 2 BCs) are necessary for presynaptic structure growth. Loss of postsynaptic

targets has been shown to prevent presynaptic partner axon stabilization and lead to eventual axon retraction (Betley et al. 2009).

In addition to developing presynaptic structures, AII ACs must establish a specific synaptic distribution pattern via several cellular strategies. The cellular interactions underlying these strategies remain unknown. Previous work has shown that some neurons require normal synaptic activity in order to preferentially synapse (Crocker-Buque et al. 2015) or prune synapses (Mendelsohn et al. 2015) onto distinct postsynaptic targets. Synaptic activity can also be required for the maintenance of synapses (Hoon et al. 2015). Thus, we sought to determine whether rod pathway neurotransmission influences the AII AC synaptic distribution pattern. We quantified AII AC output synapses and bias for Type 2 BCs in retinas with altered rod pathway activity (Figure 3.1A,B,C). Connectivity with postsynaptic partners can also be regulated by partner-mediated interactions. For example, some cholinergic neurons in *C. elegans* regulate connectivity with distinct partners (GABAergic versus muscle) by specific expression of synaptic organizing proteins (Philbrook et al. 2018). Thus, we explored whether loss of postsynaptic targets, both during development and at maturity, influenced the AII AC synaptic distribution pattern onto surviving partners. We quantified AII AC output synapses in retinas following genetic ablation of a subset of bipolar cells. We also examined retinas in which retinal ganglion cells were lost from the mature circuit, as can occur in some retinal diseases such as glaucoma (Almasieh et al. 2012) (Figure 3.1D). In one recent study, Pang et al. (2015) found changes at inner retinal synapses within the rod pathway in a mouse model of glaucoma. Thus, we sought to determine whether loss of retinal ganglion cells would induce changes in AII AC morphology or output synapse distribution patterns.

3.3 Methods

Transgenic Mice

All procedures were conducted in accordance with University of Washington Institutional Animal Care and Use Committee guidelines. Several transgenic mouse lines were used in this study. Table of mouse lines and antibodies are shown below.

Table 3.1 – Transgenic mouse lines and manipulations

Mouse Line	**Circuit Effect**	**Manipulation**
CDH1-GFP	AII ACs labeled with GFP	-
RD1	Rapid onset of rod and cone degeneration by missense mutation in pd36 protein in rods.	-
Grm6-TeNT	Silences ON bipolar cells, including rod bipolar cells, by expression of tetanus toxin light chain.	-
Grm6-Cre/Grm6-DTA	Ablation of rod bipolar cells and some Type 2 bipolar cells by expression of Diphtheria toxin alpha subunit (DTA).	-
Pou4f3-DTR	Renders Brn3c+ retinal ganglion cells susceptible to ablation by diphtherial toxin injection by expression of Diphtheria toxin receptor (DTR).	Intramuscular injection of DT
CDH1-GFP (ONS)	Degeneration of all retinal ganglion cells.	Optic nerve transection

Immunohistochemistry

Mice were deeply anesthetized with Isoflurane, cervically dislocated or decapitated, and enucleated. Retinas were dissected in oxygenated mouse artificial cerebral spinal fluid (mACSF, pH 7.4) and flat mounted on filter paper (Millipore, HABP013). Once mounted retinas were fixed for 15 minutes in 4% paraformaldehyde. Retinas were then rinsed with PBS in 3, 10 minute washes and incubated in blocking solution containing 5% normal donkey serum and 0.5% Triton X-100 overnight at 4°C. Retinas were then incubated with primary antibodies in blocking solution for approximately 72 hours at 4°C. Retinas were rinsed 3, 10 minute washes of PBS and then incubated with secondary antibodies in PBS solution overnight at 4°C. Retinas were washed 3-10 minutes with PBS prior to mounting on slides for imaging.

Antibodies

Table 3.2 – Primary Antibodies

Antibody	**Host species**	**Working Concentration**	**Source**
anti-GFP	Chicken, polyclonal	1:1000	Abcam
anti- GlyRα1	Mouse, polyclonal	1:1000	Synaptic Systems
anti-Synaptotagmin-2	Mouse, polyclonal	1:1000	Znp-1, Zebrafish International Resource Center

anti-PKCα	Rabbit	1:2000	Sigma- Aldrich
anti-Dab1	Rabbit	1:500	Gift from Jim Morgan

Table 3.3 – Secondary Antibodies

Secondary	**Host species**	**Working Concentration**	**Source**
anti-chicken Dylight 488	Donkey	1:1000	Jackson Immunoresearch
anti-mouse IgG1 568	Goat	1:1000	Synaptic Systems
anti-mouse IgG2a 647	Donkey or Goat	1:1000	Jackson Immunoresearch

Diphtheria Toxin Injection

Mice were weighed to determine volume of diphtheria toxin (DT) injection. DT was diluted in 0.9% saline solution and kept on ice throughout injections. Mice were briefly anesthetized with Isoflurane and given an intramuscular injection (into thigh muscle) of diphtheria toxin (DT) at a 50 ng/g dose. Diphtheria toxin ablates cells by interfering with protein synthesis (Honjo et al. 1968), and a single molecule of the A-subunit is sufficient lead to cell death (Yamaizumi et al. 1978).

Optic Nerve Section

In collaboration with Jessica Agostinone from the lab of Dr. Adrienne di Polo. Axotomy was performed as described in Agostinone et al. (2018). Mice were deeply anesthetized with Isoflurane. An incision was made into the skin over the superior orbital rim. The dural sheath was exposed and a cut was made transecting the optic nerve 0.5-1 mm from the optic nerve head. Animals were examined that did not have any damage to the retinal blood supply as observed by the health of the retinal fundus. Mice were survived for two weeks following optic nerve sectioning.

3.4 Results

Rod pathway neurotransmission does not influence the development of AII AC morphology and its output connectivity.

We examined AII AC morphology and output synapses onto Type 2 BCs in retinas in which synaptic input to AII ACs is perturbed due to: (i) degeneration of photoreceptors (retinitis pigmentosa), (ii) failure of rod bipolar cells to transmit onto AII ACs, or (iii) ablation of rod bipolar cells (Figure 3.1). Retinitis pigmentosa is a group of retinal diseases characterized by the degeneration of photoreceptors (Hartong et al. 2006). The loss of normal circuit input causes AII ACs to become hyperpolarized and exhibit intrinsic bursting activity (Borowska et al. 2011; Choi et al. 2014; Trenholm & Awatramani 2015) , which can be recorded in ON cone bipolar cells and in retinal ganglion cells (Margolis & Detwiler 2011; Margolis et al. 2014). We used rd1 mice, which have a mutation in phosphodiesterase, a protein in the rod signal transduction cascade (Pittler & Baehr 1991). The mutation in rd1 mice leads to the rapid degeneration of rods by postnatal day 21 (Carter-Dawson et al. 1978).

i) Loss of photoreceptor drive onto rod bipolar cells, presynaptic partners of AII ACs

We found that in the rd1 retina, AII ACs still formed lobular appendages (Figure 3.2). These findings corroborate previous studies that have shown that there is no loss of AII AC presynaptic structures in rd1 animals up to three months old (Strettoi et al. 2002). We also examined the total number of output synapses formed by individual AII ACs in rd1 retinas. We found no significant difference between the total number of synapses between rd1 littermate control (1 animal) (55 ± 7.2 SEM, $p = 0.17$, n = 3 cells) and rd1 retinas (n =1 animal) (58.3 ± 8.4 SEM, n = 3 cells). Thus,

loss of rod photoreceptor-mediated transmission does not prevent the formation of AII AC presynaptic structures or the appropriate number of output synapses.

To determine whether loss of rod-mediated transmission affected the AII AC synaptic distribution pattern, we calculated the percentage of synapses formed onto Type 2 BCs in the rd1 retinas. We found no significant difference between the percentage of synapses formed onto Type 2 BCs in littermate control (52.1% ± 2.0 SEM, n =3 cells) and rd1 retinas (52.3% ± 6.9 SEM, n = 3 cells). These findings suggest that loss of rod-mediated transmission does not affect the AII AC bias for Type 2 BCs.

ii) Silencing rod bipolar cell input to AII ACs

While we found no significant changes in AII AC morphology or formation of output synapses onto Type 2 bipolar cells following photoreceptor degeneration, AII ACs in rd1 retinas show abnormal rhythmic bursting activity (Cembrowski et al. 2012; Choi et al. 2014; Trenholm & Awatramani 2015). Thus, we next sought to determine whether a decrease in synaptic transmission from rod bipolar cell to AII ACs would lead to changes in the formation of synapses with Type 2 bipolar cells. To test this hypothesis, we examined AII ACs in retinas with a subset of rod bipolar cells silenced (Figure 3.3). Rod bipolar cells were silenced by expression of the light chain of tetanus toxin (TeNT) under a bipolar cell specific promoter (Grm6). In the Grm6-TeNT-YFP mice, a subpopulation of ON bipolar cells, including rod bipolar cells express both YFP and TeNT. In these mice, the activity of OFF retinal ganglion cells is normal, whereas ON retinal ganglion cells have significantly fewer and lower amplitude spontaneous excitatory postsynaptic currents (Kerschensteiner et al. 2009). Thus, these retinal ganglion cells do not show the rhythmic ~10 Hz activity seen in the rd1 mice, suggesting AII ACs do not exhibit the

rhythmic bursting behavior characteristic of the retinitis pigmentosa model. We examined lobular appendage morphology and synapses with Type 2 BCs in AII ACs that were postsynaptic to at least one silenced rod bipolar cell (which expresses YFP). There was no difference in the total number of output synapses formed per AII AC in littermate control (50.2 ± 6.9 SEM, n = 2 animals/ 6 cells) or TeNT positive retinas (39.8 ± 6.0 SEM, p = 0.48, n = 3 animals/ 6 cells). Furthermore, there were no significant differences in the percentage of synapses from AII ACs to Type 2 BCs between Grm6-TeNT mice (44.2% ± 5.9 SEM, n = 6) and littermate controls (55.4% ± 3 SEM, n = 6). These results suggest that loss of synaptic input (from silenced rod bipolar cell terminals) does not prevent lobular appendage formation or synaptogenesis with Type 2 bipolar cells.

iii) Ablation of rod bipolar cells

Because not all rod bipolar cells were silenced in the TeNT positive retinas, we examined whether AII ACs continue to elaborate presynaptic structures and output synapses in the absence of rod bipolar cells and some cone bipolar cells (Figure 3.4). In retinas in which rod bipolar cells were genetically ablated by bipolar cell specific expression of the diphtheria toxin A subunit, AII ACs continued to form lobular appendages and maintain synapses onto postsynaptic targets. Our experiments suggest that the formation of lobular appendages and synapses does not require a specific level or pattern of activity within the circuit. Furthermore, rod pathway activity does not influence the AII AC's bias for Type 2 BCs.

Loss of postsynaptic partners during development leads to loss of AII AC output synapses not presynaptic structures.

The observation that AII AC presynaptic structures develop at the same time as bipolar cell axons suggests that bipolar cells are required for lobular appendage elaboration. We found that fortuitously, Type 2 bipolar cells and likely other OFF bipolar cells are ablated by diphtheria toxin in a subset of *Grm6-DTA/Grm6-Cre/CDH1* mice (Figure 3.4). Moreover, in a single field of view, patches of Type 2 bipolar cells were present whereas neighboring regions were depleted of these bipolar cells. This arrangement provided an 'internal' control for assessing the loss of Type 2 BCs. We took advantage of these mice to ask whether AII ACs form lobular appendages in the absence of these major bipolar cell partners. In regions lacking Type 2 bipolar cells, AII ACs still formed lobular appendages (Figure 3.4 B). Thus, we found that AII ACs can develop presynaptic structures in the absence of their dominant postsynaptic bipolar partner. This finding does not rule out a potential role for other bipolar cells, as others likely still remain in regions lacking Type 2 bipolar cells.

We examined whether loss of Type 2 bipolar cells would lead to loss of output synapses and/or rearrangement of synapses onto surviving partners. First, we compared CDH1 retinas to regions of *Grm6-DTA/Grm6-Cre/CDH1(Grm6-DTA)* retinas with some surviving Type 2 bipolar cells. We observed a significant decrease in the number of total output synapses in CDH1 (73.2 ± 5.2 SEM, n = 11 cells) versus *Grm6-DTA* regions with surviving Type 2 BCs (38.3 ± 3.5 SEM, n = 2 animals/11 cells, $p < 0.01$). These results indicated that non-Type 2 BCs were likely ablated in these regions, and that AII ACs did not fully compensate by increasing synapses onto surviving partners. Additionally, we observed a significant loss of synapses formed onto the surviving Type 2 bipolar cells, indicating that AII ACs did not simply reallocate all synapses to surviving

partners of the same type (Grm6-DTA 17.2 ± 2.9 SEM, n = 12 cells versus CDH1 30.3 ± 4.1 SEM, $p < 0.05$, n = 11 cells).

Next, we compared neighboring regions of the Grm6-DTA retinas in which Type 2 bipolar cells are patchy. We found that a significant decrease in the number of output synapses that individual AII ACs form in regions lacking all Type 2 bipolar cells (22.1 ± 2.4 SEM, n = 12 cells) compared to regions with Type 2 BCs ($p < 0.01$). These findings further support the idea that AII ACs did not compensate for the loss of postsynaptic partners by increasing the number of synapses with surviving partners. As no Type 2 BCs are found in these regions, the AII AC forms no synapses onto this population. Taken together, these results reveal that loss of the dominant postsynaptic bipolar cell type is not sufficient to prevent the development of AII AC presynaptic structures. However, AII ACs do not compensate for the loss of synaptic partners by simply reallocating synapses. The further loss of synapses with fewer postsynaptic partners also suggests that synapses onto distinct bipolar cells may be regulated independently.

Loss of a postsynaptic partner in the mature circuit does not induce changes in synapse number with surviving postsynaptic partner.

Changes in rod pathway activity and loss of synaptic partners during development do not prevent AII AC lobular appendage formation or synaptogenesis onto remaining partners. As circuit remodeling is observed in mature retinal circuits following injury or disease (Marc et al. 2003), we sought to determine whether the AII AC can continue to maintain output structures and synapses following the loss of synaptic partners from the mature circuit. To test this hypothesis, we examined AII ACs in retinas in which a subpopulation of retinal ganglion cells are ablated by injection of diphtheria toxin (Figure 3.5A) and in retinas in which many retinal ganglion cells are

lost following the sectioning of the optic nerve (the axons of all retinal ganglion cells) (Figure 3.6A) (Galindo-Romero et al. 2011).

Pou4f3-DTR mice (Golub et al. 2012) were injected with diphtheria toxin to induce ablation of a subset of retinal ganglion cells, specifically those expressing Pou4f3 or Brn3c (Badea & Nathans 2011) (Figure 3.5A). Single intramuscular diphtheria toxin injections of 50 ng/g ablate ~61% of Brn3c+ retinal ganglion cells after at least 4 weeks (Figure 3.5A). Of the AII AC retinal ganglion cell partners, we expect DT injections to ablate OFF-transient alpha retinal ganglion cells as evidenced by the loss of SMI-32 staining (Bleckert et al. 2014) following DT injection (data not shown). We found no significant difference in the number of output synapses individual AII ACs form in CDH1 (73.2 ± 5.2 SEM, n = 11 cells) versus injected retinas (63.6 ± 5.6 SEM, n = 7 cells). We also find no significant difference in the percentage of synapses formed onto the Type 2 BC population in CDH1 (40.3% ± 3.2% SEM) versus Pou4f3-DTR injected retinas (50% ± 2% SEM).

To remove a greater percentage of retinal ganglion cells, we collaborated with Jessica Agostinone (DiPolo lab, University of Montreal, Canada) (Figure 3.6). She performed optic nerve sections on CDH1-GFP mice (n = 2 animals), which survived for 2 weeks. After 2 weeks, we found ~75% of all retinal ganglion cells had degenerated as indicated by RBPMS staining. Despite the loss of retinal ganglion cells, we found no significant difference, but a downward trend in the total number of output synapses from CDH1 (73.2 ± 5.2 SEM, n = 11 cells) versus ONS animals (59 ± 5.1 SEM, n = 8 cells). However, there was a significant difference in the percentage of synapses formed onto Type 2 BCs in CDH1 (40.3% ± 3.2% SEM, n = 11 cells) versus ONS retinas (55% ± 2.2% SEM, p = 0.004, n = 8 cells). However, there was no

significant difference in the number of synapses formed onto Type 2 BCs between CDH1 (30.3 ± 4.1 SEM, n = 11 cells) and ONS retinas (32.6 ± 3.4 SEM, n = 8 cells). The increase in the percentage of synapses with Type 2 BCs likely reflects a loss of synapses onto non-Type 2 partners (most likely the retinal ganglion cells) rather than an increase in connectivity with bipolar cells. Thus, loss of retinal ganglion cells partners does not affect AII AC connectivity with bipolar cells. It remains unknown whether there are changes in the distribution of synapses onto surviving retinal ganglion cells.

In summary, we found that AII AC presynaptic structures and synapse distribution pattern develops independently of rod pathway transmission. We also found that AII ACs does not increase synapses with surviving postsynaptic partners following the loss of some targets, indicating that synapses with distinct partners (both within and across types) may be regulated independently.

3.5 Discussion

While synaptic divergence is commonly found across many neural circuits, the cellular interactions that underlie the establishment of such connectivity patterns remain unknown. In this chapter, we found that presynaptic input onto AII ACs is not required for the development of AII AC presynaptic structures or output synapses. Furthermore, loss of rod pathway activity did not alter the AII AC's bias for Type 2 bipolar cells. We also found that AII ACs lost output synapses onto ablated postsynaptic targets in both the developing or mature retina. As such, AII ACs also failed to increase the number of synapses onto remaining postsynaptic partners indicating that synapses onto distinct partners may be regulated independently.

Potential cues for delayed AII AC presynaptic structure growth.

For many neurons across diverse circuits, neurotransmission shapes the growth of dendritic and axonal structures (Reviewed by Bleckert & Wong 2011); however, we described here a neuron that requires no synaptic input in order to develop its presynaptic structures. Thus, other external or cell intrinsic cues likely signal for the AII AC to extend proto-lobular appendages.

Distinct cues may underlie the 'waiting' period we observed for AII AC lobular appendage growth. These cues could either be repulsive or attractive. If repulsive, the cue likely downregulates or the cell becomes insensitive to the cue at the time of lobular appendage outgrowth. Repulsive cues have been found to delay axon elaboration into a target region. For example, corticothalamic axons arrive at the dorsal lateral geniculate nucleus (dLGN) by postnatal day 4, but do not enter until postnatal day 12 (Seabrook et al. 2013) because the dLGN initially expresses a repulsive proteoglycan (Brooks et al. 2013). Expression of the repulsive cue

is regulated by a different cell population, the retinal ganglion cells, which also project into the dLGN. The proteoglycan is downregulated once retinal ganglion cells have fully innervated the nucleus, leading to sequential innervation of retinal ganglion axons followed by corticogeniculate axons (Brooks et al. 2013; Seabrook et al. 2013). In the retina, Semaphorins, a class of cell adhesion molecules, are known to be a repulsive cue for neurites of some retinal neurons (Matsuoka, Nguyen-Ba-Charvet, et al. 2011). AII ACs are sensitive to Semaphorin-mediated repulsive cues. For example, loss of both Semaphorin 5A/B or the corresponding Plexin receptors (PlexinA1,3) causes AII ACs to aberrantly send neurites towards the inner nuclear layer; however, AII ACs also continue to elaborate lobular appendages in the proper lamina (Matsuoka, Chivatakarn, et al. 2011). Thus, AII ACs respond to repulsive cues, but neurite extension and lamination may be distinctly regulated. Other semaphorins, or similar repulsive cues may mediate lobular appendage outgrowth, but such a cue has yet to be identified.

AII AC lobular appendages may also develop in response to an attractive cue. For example, neurotrophins, such as insulin-like growth factor 1, have been shown to promote amacrine cell neurite outgrowth in culture (Politi et al. 2001), and thus may serve a similar function in *vivo*. Brain derived neurotrophic factor (BDNF) has been shown to regulate the development and elaboration of processes of dopaminergic amacrine cells (Cellerino et al. 1998). It remains unknown, however, whether AII ACs respond to specific neurotrophic factors. Attractive cues can also induce the formation of collaterals from pre-existing axons. For example, in the developing cortex, layer V neurons send axons to the spinal cord and days layer develop collaterals that project to the pons (O'Leary & Terashima 1988). These axon collaterals were found to develop in response to target-derived diffusible, attractive cue (Heffner et al. 1990). Similarly, dorsal root ganglion axons and trigeminal axons develop collaterals in response to

Slit2, a secreted guidance molecule, *in vitro*, and likely *in vivo* (Wang et al. 1999; Ozdinler & Erzurumlu 2002). mRNA expression of Slit2 is upregulated around the time of collateral formation, which occurs after axons have already formed. Thus, time restricted expression of a secreted neurite promoting molecule can underlie the delayed growth of presynaptic structures, but the identity of such a cue directing AII AC lobular appendage differentiation remains elusive.

The timing of AII AC lobular appendage elaboration and OFF cone BCs axon growth suggests that these neurons elaborate pre and postsynaptic processes in a temporal and spatially coordinated manner. The continued growth of AII lobular appendages, despite the loss of Type 2 bipolar cells, does not rule out a role for bipolar cells as the source of a signal because Type 2 bipolar cells are ablated after differentiation. A Type 2 bipolar cell derived cue could be expressed between the time of differentiation and ablation. Cues from other non-Type 2 bipolar cells may be sufficient to promote lobular appendage extension, i.e. that the target-derived cue is common across OFF bipolar cells. As described earlier, recent transcriptomic profiling of bipolar cells has shown that OFF bipolar cells express both cadherins and protocadherins (Shekhar et al. 2016), and candidate proteins are likely expressed across multiple AII AC-bipolar cell targets.

Finally, it is possible that AII ACs develop lobular appendages as the result of cell intrinsic cues. In the absence of other cell types, disassociated parvalbumin-positive amacrine cells (AII AC) do develop neurites and even varicosities in culture (Kunzevitzky et al. 2013); however, the morphologies of these cells differ from those *in vivo*. The discrepancy between the *in vivo* and *in vitro* morphology of these neurons may be in part attributed to culturing in a 2D rather than 3D environment. Further experiments are thus needed to determine if lobular appendages develop independently of extrinsic cues.

Neurotransmission-independent establishment of bias in synaptic divergence.

While neurotransmission is not required for the initial formation of synapses in both excitatory and inhibitory circuits (Reviewed Gamlin et al. 2018), maintenance and sculpting of synaptic distribution patterns often requires synaptic activity (Reviewed Bleckert & Wong 2011; Gamlin et al. 2018). For example, as described in Section 1.2, silencing sensory-motor neurons prevents the preferential synaptogenesis onto others (Mendelsohn et al. 2015). Silencing UV cones does not prevent postsynaptic horizontal cells from preferentially synapsing with UV versus blue cones (Yoshimatsu et al. 2014). As mentioned earlier, in the retina of animals lacking the vesicular inhibitory amino acid transporter (VIAAT), Type 2 bipolar cells continued to receive the proper number of a1-containing glycine receptors across ages (Hoon et al. 2015). This finding indicated that silencing the AII AC does not prevent synaptogenesis or maintenance of synapses onto a major synaptic target. Thus, neurotransmission-independent mechanisms likely underlie the growth and preferential synaptogenesis from AII ACs onto bipolar cells. Studies in the fly olfactory system have revealed a role for transsynaptic proteins (Teneurins) in regulating a neuron's stereotypic synapse number in the CNS. Loss of Ten-a (a presynaptically-expressed teneurin) in null animals and RNAi knockdowns reduced the number of synapses that olfactory receptor neurons form onto their glomerulus by at least 20% (Mosca & Luo 2014). Mosco & Luo speculated that olfactory receptor neuron synapse number was partially regulated by other redundant cues and/or molecules. Thus, a molecule or group of molecules, such as those from the Teneurin family, could be expressed in a subset of AII ACs postsynaptic targets or differentially amongst targets, promoting different number of synapses in an expression-dependent manner. Future studies could explore whether there are differences in the synaptic organizing proteins at

AII AC synapses onto distinct postsynaptic targets even though all target express the same glycine receptor subtype.

In the studies discussed above, activity-dependent mechanisms shaped a neuron's connectivity with one partner, but not with other(s). Thus, it is possible that disruption of rod pathway activity affects maintenance of synapses onto retinal ganglion cells or pruning of synapses onto widefield amacrine cells. Future experiments are required to determine whether all developmental mechanisms shaping AII AC connectivity are neurotransmission-independent.

Partner-independent regulation of output synapse number.

AII ACs continue to form lobular appendages and output synapses following the loss of synaptic partners both during development and at maturity. However, we found that following the loss of postsynaptic partners, AII ACs lose output synapses. The further decrease in synapse number between regions with and without Type 2 bipolar cells reveals that increased partner loss is accompanied by increase synapse loss. Thus, AII ACs do not compensate for the loss of targets by forming more synapses with surviving partners in order to reach the original output number. Synapse number may therefore reflect to some degree the availability of postsynaptic partners, as indicated by the correlation between surface area overlap of AII ACs and bipolar cells and synapse number seen under serial blockface EM (Section 2.3.3). Furthermore, the decrease in the number of synapses formed onto surviving Type 2 bipolar cells indicates that AII ACs do not compensate by increasing synapses even onto the surviving members of preferred postsynaptic type. These results suggest that the AII AC independently regulates the number of synapses formed onto its distinct postsynaptic partners even within a single cell class (bipolar cells) and type (Type 2 BCs).

3.6 Figures:

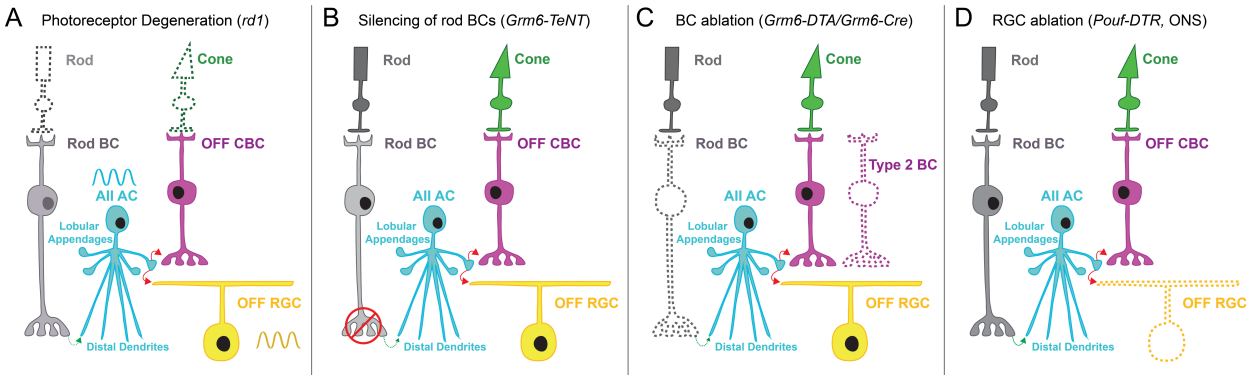

Figure 3.1: Schematics of manipulations within the rod pathway.

A. Loss of photoreceptors due to degeneration in the *rd1* retina. Loss of rod input leads AII ACs to have low resting membrane potential, causing AII ACs to rhythmically burst (sinusoid image). This rhythmic bursting (~10 Hz) can be seen downstream in both ON and OFF retinal ganglion cells. **B.** A subset of rod bipolar cells (and other ON BCs) express the light chain of tetanus toxin (TeNT), which prevents synaptobrevin cleavage (Schiavo et al. 1992) and subsequent fusing of neurotransmitter-containing vesicles, under a bipolar cell specific promoter (Grm6). TeNT-expression prevents action potential-evoked synaptic transmission but does not necessarily prevent spontaneous synaptic release (Williamson et al. 1992). **C.** Genetic ablation of bipolar cells (both ON and OFF) by expression of the A subunit of diphtheria toxin (DTA) under a bipolar cell specific promoter (Grm6). **D.** Ablation of retinal ganglion cells by injection of diphtheria toxin (DT) into mice expressing the diphtheria toxin receptor (DTR) under a retinal ganglion cell specific promoter (Pou4f3 or Brn3c). Retinal ganglion cells were also killed by surgical sectioning of the optic nerve (ONS) (the axons of retinal ganglion cells) (Galindo-Romero et al. 2011).

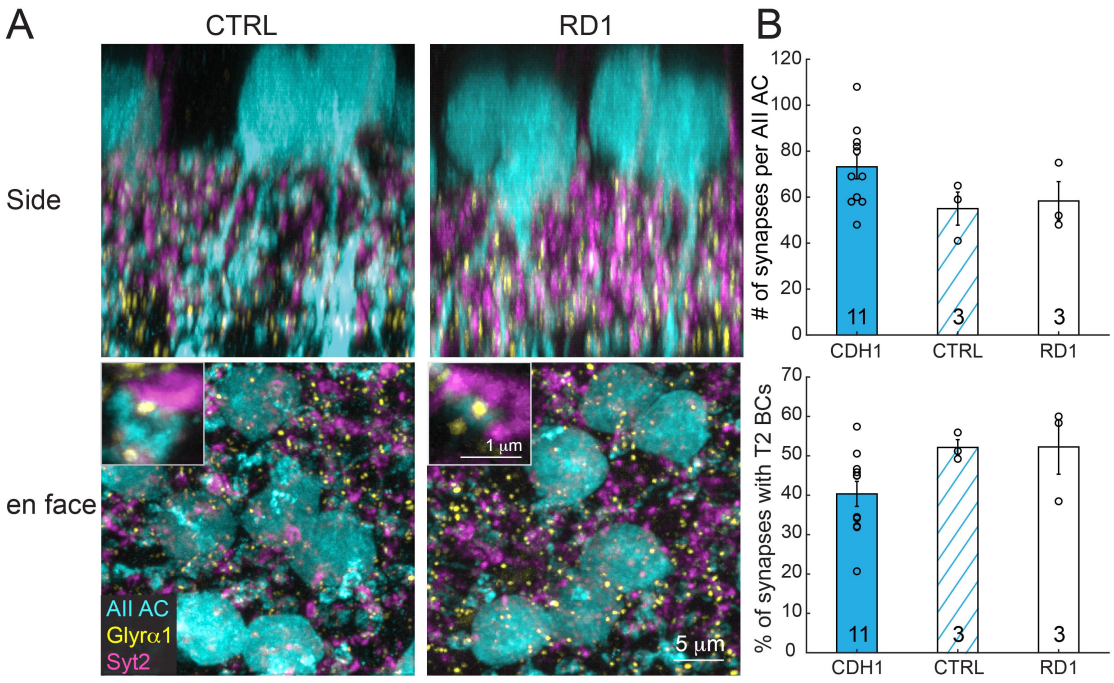

Figure 3.2. Characterization of AII AC connectivity following photoreceptor degeneration.

A. Light microscopy images of immunostaining in a control and RD1 retina. Side and en face views of AII ACs, AII AC output synapses (Glyrα1), and Type 2 BCs (Syt2). Inset: Example synapses between an AII AC and Type 2 BC partner. **B.** Top panel: Quantification of total number of output synapses from individual AII ACs in CDH1, littermate control, and RD1 retina. Bottom panel: Quantification of the percentage of output synapses formed onto Type 2 BCs by AII ACs in CDH1, littermate control, and an RD1 retina. No significant differences were observed between groups as determined by pairwise Wilcoxon-rank sum tests. Numbers in bars indicate number of cells.

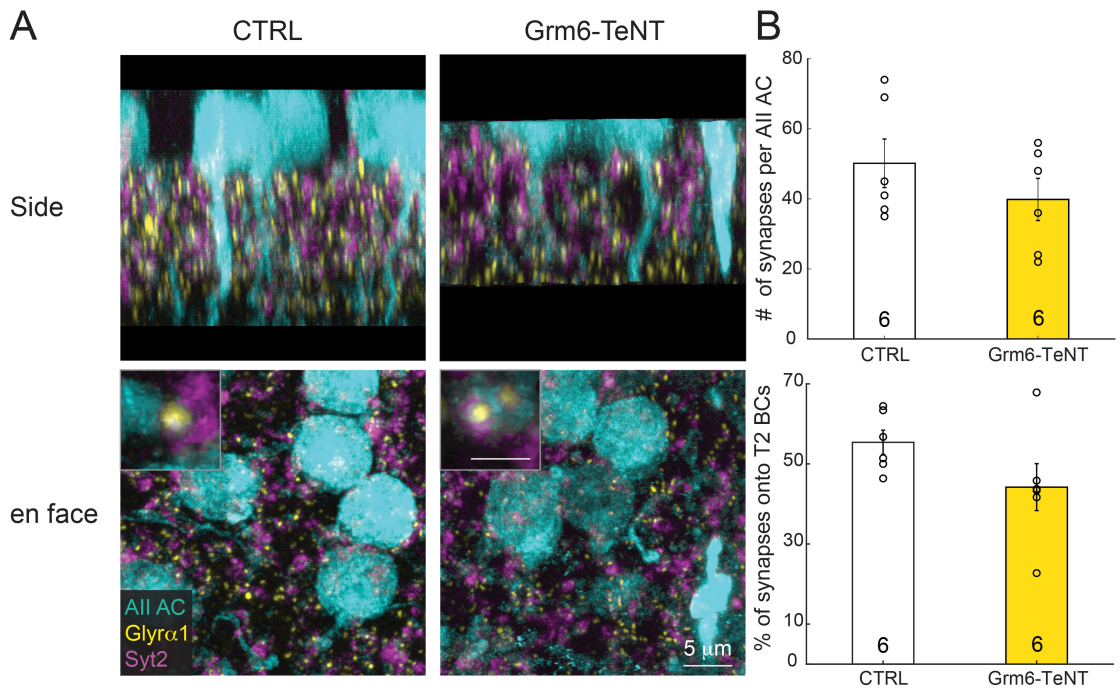

Figure 3.3. Characterization of AII AC connectivity following rod bipolar cell silencing.

A. Light microscopy images of immunostaining in a littermate control and TeNT+ retina. Side and en face views of AII ACs, AII AC output synapses (Glyrα1), and Type 2 BCs (Syt2). Inset: Example synapses between an AII AC and Type 2 BC partner. **B.** Top panel: Quantification of total number of output synapses from individual AII ACs in littermate control and TeNT+ retinas. Bottom panel: Quantification of the percentage of output synapses formed onto Type 2 BCs by AII ACs in littermate control and TeNT+ retinas. No significant differences were observed between groups as determined by Wilcoxon-rank sum tests. Numbers in bars indicate number of cells.

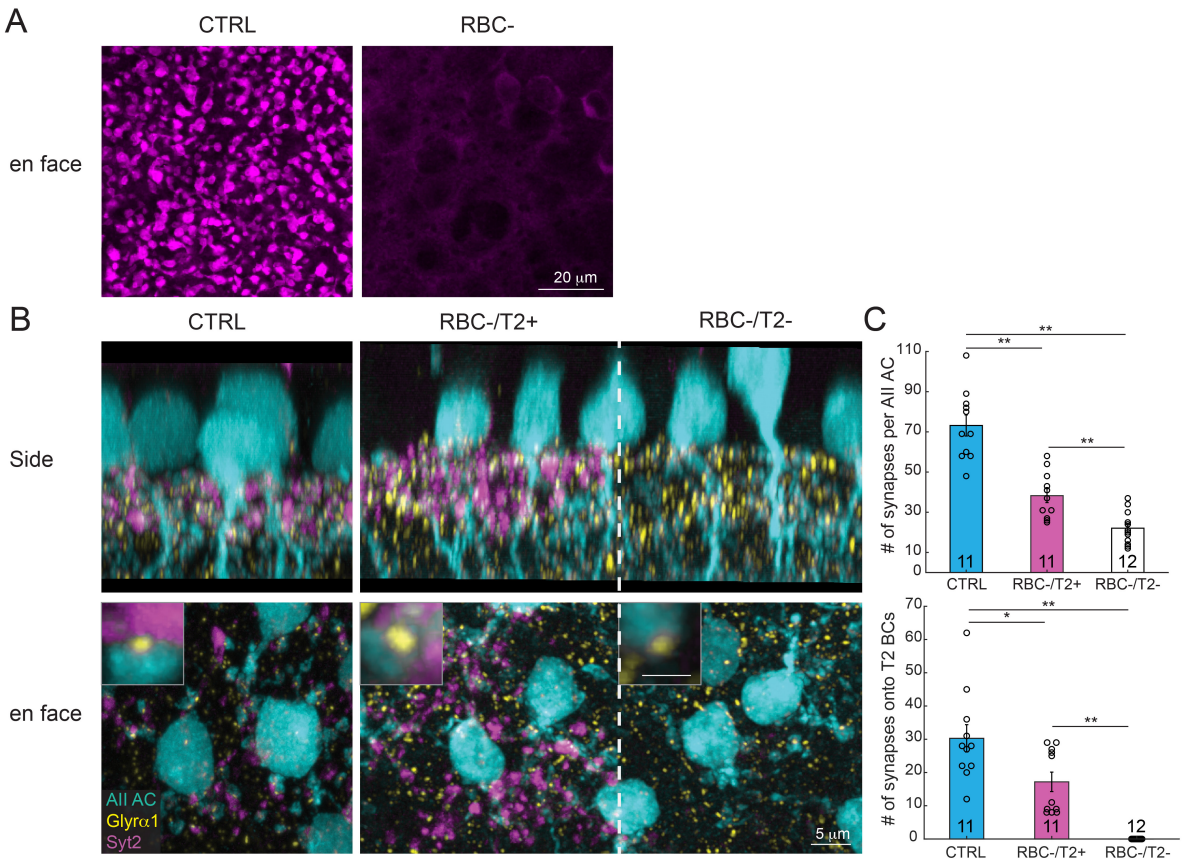

Figure 3.4 Characterization of AII AC connectivity following bipolar cell ablation.
A. Light microscopy images of immunostaining in a CDH1 (not littermate control) and Grm6-Cre/Grm6-DTA/CDH1 retinas in which rod bipolar cells (RBCs) are ablated. Side and en face views of RBCs (PKCα staining). **B.** Light microscopy image of immunostaining in CDH1 and Grm6-Cre/Grm6-DTA/CDH1 retinas in which some Type 2 BCs are ablated. Dotted line divides patches with and without Type 2 BCs in a single area. Side and en face views of AII ACs, AII AC output synapses (Glyrα1), and Type 2 BCs (Syt2). Inset: Example synapses between an AII AC and Type 2 BC (if present). 1 µm scale. **C.** Top panel: Quantification of total number of output synapses from individual AII ACs in CDH1, RBC ablated retinas in regions with surviving Type 2 BCs, and RBC ablated retina in regions without Type 2 BCs. There are significant differences between the number of output synapses formed in CDH1 retinas (73.2 ± 5.2 SEM) as compared to regions with surviving Type 2 BCs (32.3 ± 3.5 SEM, $p < 0.001$) and compared to regions without Type 2 BCs (22.1 ± 2.4 SEM, $p < 0.01$). Furthermore, there is a significant difference between retinas with surviving Type 2 BCs and regions without Type 2 BCs ($p < 0.05$). Bottom panel: Quantification of the number of output synapses formed onto Type 2 BCs by AII ACs in CDH1, regions with surviving Type 2 BCs, and regions absent of Type 2 BCs. There was a significant difference between the number of synapses formed onto Type 2 BCs in the CDH1 (30.3 ± 4.1 SEM) and Type 2 surviving regions (17.2 ± 2.9 SEM, $p < 0.05$). There were also significant differences between the number of synapses formed onto Type

2 BCs in regions without Type 2 BCs (0 ± 0 SEM) as compared to CDH1 retinas ($p < 0.01$) and regions with surviving Type 2 BCs ($p < 0.01$). * $p< 0.05$. ** $p < 0.01$. Numbers in bars indicate number of cells.

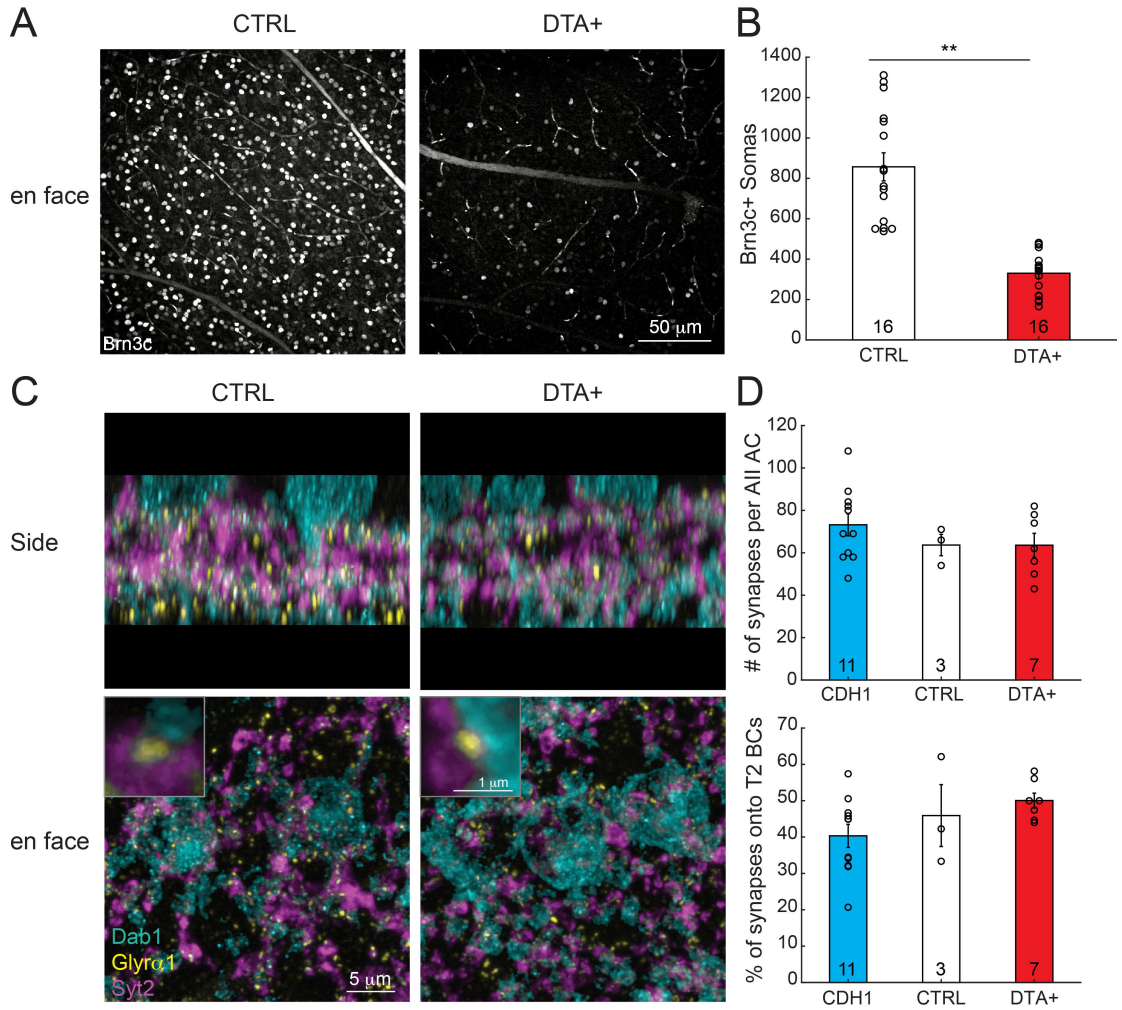

Figure 3.5. Characterization of AII AC connectivity following RGC ablation.

A. Light microscopy images of Brn3c staining to label Brn3c+ retinal ganglion cells in littermate control and diphtheria toxin (DTA) injected animals. **B.** Quantification of the number of Brn3c+ somas in a 45,000 µm^2 region in retinas from control and DT injected animals. There is a significant decrease in the number of Brn3c-positive retinal ganglion cells after DT injection ($p < 0.001$). **C.** Light microscopy images of immunostaining for AII ACs (Dab1), AII AC output synapses (Glyrα1) and Type 2 BCs (Syt2) in side and en face views. Insets: Example synapses from an AII AC onto a Type 2 BC partners. **D.** Top panel: Quantification of total number of output synapses from individual AII ACs in CDH1 (data shown earlier), littermate controls, and DT injected retinas. Bottom panel: Quantification of the percentage of output synapses that individual AII ACs form onto Type 2 BCs in CDH1, littermate controls, and DT injected retinas. There were no significant differences found between groups as calculated by Wilcoxon rank sum test. Numbers in bars indicate number of cells.

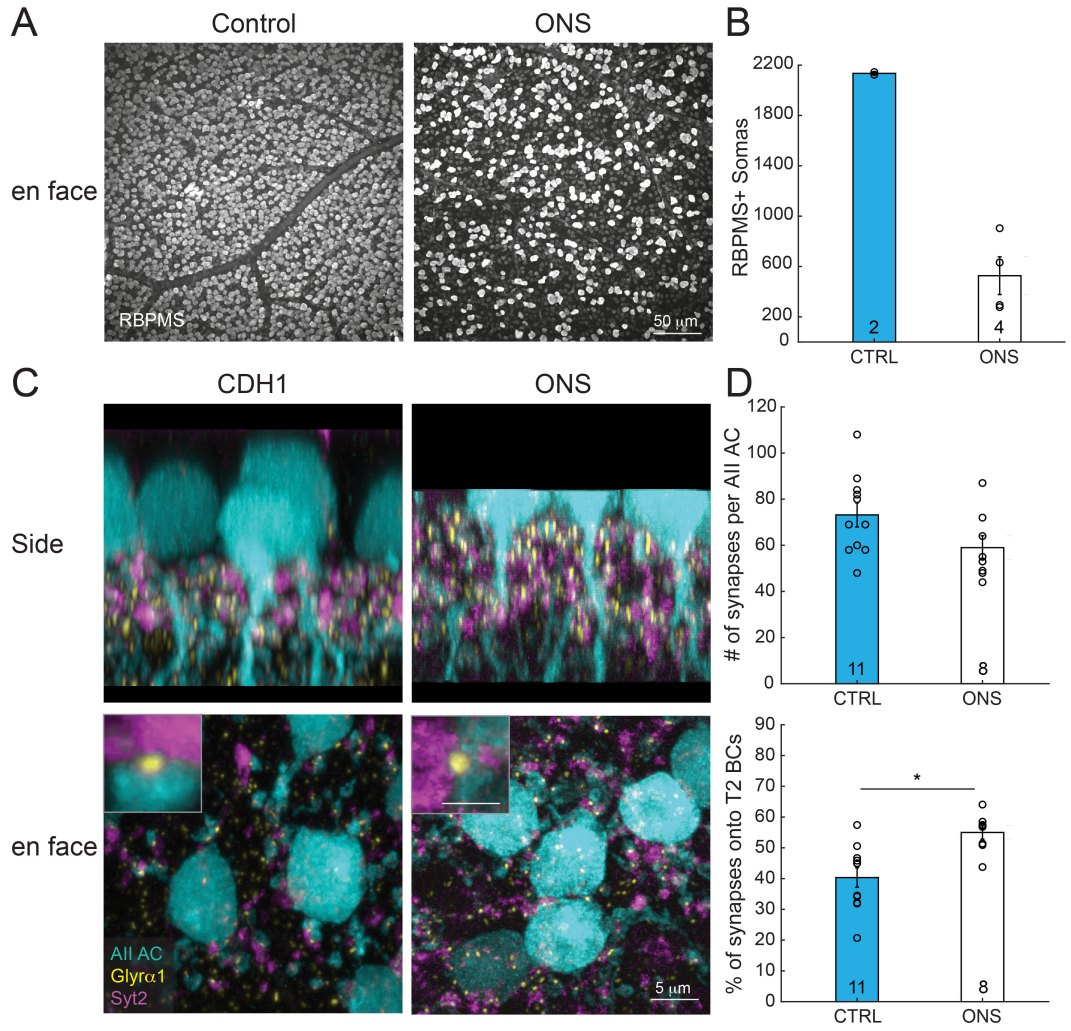

Figure 3.6. Characterization of AII AC connectivity following optic nerve sectioning.
A. Light microscopy images of staining for RBPMS, a pan retinal ganglion cell maker, in retinas from control and animals that have undergone optic nerve section (ONS) two weeks prior. **B.** Quantification of the number of RBPMS somas in control and ONS animals per 104,000 µm^2 region. **C.** Side and en face views of AII ACs, AII AC output synapses (Glyrα1), and Type 2 BCs (Syt2) in CDH1 (data shown earlier) and ONS retinas. Inset: Example synapses between an AII AC and Type 2 BC partner. **D.** Top panel: Quantification of the total number of output synapses formed by individual AII ACs in control (CDH1 data shown earlier) and ONS retinas. There were no significant differences in the total number of output synapses between these conditions, but ONS retinas are trending towards fewer synapses. Bottom panel: Quantification of the percentage of output synapses formed onto Type 2 BCs in CDH1 and ONS retinas. There is a significant increase in the percentage of synapses formed onto Type 2 BCs (* $p < 0.05$); however, there is no significant difference in the total number of synapses formed onto Type 2 BCs between these conditions (data not shown). Thus, the increase in the percentage onto Type 2 BCs is likely a reflection of a loss of synapses onto non-Type 2 partners, likely the degenerating

retinal ganglion cells. * $p < 0.05$. ** $p < 0.01$. Numbers in bars indicate number of regions sampled or cells.

Chapter 4: Conclusions and future directions

Summary

In this thesis, I explored the cellular strategies that underlie the development of biased synaptic divergence from an inhibitory interneuron. I used a combination of confocal light microscopy and serial blockface electron microscopy to map the morphogenesis and synapse development of the AII amacrine cell (AII AC). I found that the AII AC output structures (lobular appendages) grow at a delay relative to the rest of the cell and differentiate at the same time as the AII ACs major postsynaptic partners. Using serial blockface EM, I determined the distribution of AII AC synapses onto its postsynaptic partners after synaptic densities have stabilized in the retina (Tian, 2004). These data confirmed earlier findings that AII ACs form synapses onto both bipolar cells and retinal ganglion cells, with a bias for the former. Furthermore, I found that AII ACs form a large number of synapses onto a small subset of bipolar cell partners, revealing a bias even within a single cell class (bipolar cells). I next reconstructed AII ACs prior to the time of eye-opening (~P14). I found that AII ACs are already biased towards synapsing with bipolar cells before visual experience, but the bias increases with maturation due to (i) preferential synaptogenesis with bipolar cells, (ii) no increase in the number of synapses onto retinal ganglion cells, and (iii) elimination of synapses with a particular amacrine cell type. In the third chapter of my thesis, I explored the cellular mechanisms underlying the development of AII AC lobular appendages and the strategies guiding the development of its synaptic distribution pattern. I found that changes in rod pathway activity did not prevent the differentiation of lobular appendages or synaptic bias for Type 2 bipolar cells. When some postsynaptic partners (both bipolar and retinal ganglion cells) were genetically ablated or killed, AII ACs failed to compensate by increasing synapses onto surviving partners, suggesting that synapses onto distinct partner types are formed and maintained independently. Collectively, these results

suggest that an individual presynaptic neuron can establish and maintain synapses onto distinct partner types in an independent manner.

Several questions remain regarding the mechanisms underlying lobular appendage growth and synaptic distribution patterns. I discuss these questions below and propose experiments to provide greater insight into potential mechanisms.

Cues for lobular appendage elaboration

What cues direct the late differentiation of AII AC lobular appendages? The timing of the presynaptic structure elaboration at the same time as bipolar cells differentiate raises the possibility that bipolar cells may play a role in directing lobular appendage growth. The observation that AII ACs continue to develop lobular appendages even in the absence of Type 2 bipolar cells does not rule out the possibility that non-Type 2 bipolar cell partners of the AII AC may contribute to the elaboration of the AII AC presynaptic structures. A bipolar cell-derived cue may be common to all bipolar cells that are postsynaptic to AII ACs. Furthermore, in the *Grm6-DTA* retinas, bipolar cells are ablated after they differentiate, and therefore, bipolar cells may provide a signal between the time of differentiation and ablation. To determine whether bipolar cells are required for lobular appendage extension, we will need to examine the morphology of AII ACs in retinas in which bipolar cells are never generated. This could be achieved by deleting genes underlying bipolar cell fate. If lobular appendages do not form, bipolar cells are likely the source of an instructive signal. If lobular appendages still form in the absence of bipolar cell genesis, lamina-specific cues such as cell-cell interactions with other amacrine cells (Godinho et al. 2005) or cell intrinsic cues may direct the growth of these structures. To differentiate between these options, AII ACs could be dissociated from retinas and

cultured in a 3D medium (Hertz et al. 2013). If lobular appendages develop in culture, a cell intrinsic mechanism likely drives the process of presynaptic structure elaboration.

Another approach to determine the signal that drives AII AC lobular appendage elaboration is to genetically profile AII ACs before and after lobular appendages elaborate. Sequencing of AII ACs could be achieved by FACs (fluorescent activated cell) sorting (Basu et al. 2010) GFP-positive AII ACs from the *CDH1-GFP* line at two ages, one before (P4) and one after (>P8) lobular appendage growth. Differences in gene expression around the time of presynaptic structure growth may point towards relevant cues.

Mechanisms underlying the preferential synaptogenesis amongst bipolar cells

Our reconstructions of the AII AC output synapses onto bipolar cells at P24 revealed a high correlation between AII AC - bipolar cell surface overlap and the number of synapses that individual bipolar cell received. If the amount of cell surface overlap rather than bipolar cell type (e.g. Type 2 vs 3) dictates the number of synapses a bipolar cell receives, then changing the amount of overlap should change the number of synapses between an AII-BC pair. In the Grm6-Cre/Grm6-DTA/CDH1 mice, some Type 2 (OFF) bipolar cells are ablated, but it is likely that other OFF bipolar cells remain and expand to fill in the new available territory (Okawa et al. 2014). An EM reconstruction of AII ACs in a region devoid of Type 2 bipolar cells would reveal whether other bipolar cells can receive an increased number of synapses with a greater amount of cell surface overlap. If the number of synapses a bipolar cell receives continues to be correlated with the amount of surface overlap between that bipolar cell and the AII AC, then mechanisms that establish the axon stratification of the bipolar cells can largely explain the AII AC output onto its bipolar cell partners. On the other hand, if the AII AC fails to increase the number of

synapses onto bipolar cell partners despite increased cell surface overlap, other Type 2 specific cues may underlie the bias for this bipolar cell type.

Mechanisms underlying the regulation of AII AC output synapses across partners

Following the loss of bipolar cells and retinal ganglion cells, AII ACs fail to increase synapses onto remaining partners. This observation suggests that synapses onto distinct postsynaptic partner types may be regulated independently. One question that arises from this observation is how might a single presynaptic cell independently regulate synapses across multiple partners? A previous study in *C. elegans* has found that an individual presynaptic neuron can use different synapse organizing proteins, such as Neurexin (Nrx-1), to form and maintain synapses with one target but not another (Philbrook et al. 2018). Furthermore, transsynaptic cell adhesion molecules, such as Teneurins and Cadherins, have been shown to control output synapse number between neuron pairs in both flies and mice, respectively (Mosca & Luo 2014; Williams et al. 2011). Cadherins have also been shown to direct the specific wiring of neurons to form direction-selective circuits in the retina. Starburst amacrine cells restrict the lamination and regulate connectivity with distinct populations of direction-selective retinal ganglion cells by the expression of specific combinations of cadherins (Duan et al. 2018). We hypothesize that the AII AC may regulate synapses with specific postsynaptic partners by expressing distinct cell adhesion molecules with each partner class. To determine whether the AII AC expresses molecules or combinations of molecules that are unique to bipolar cells versus ganglion cells, we could carry out genetic profiling of AII ACs to determine their expression of known cell adhesion molecules could be compared with datasets that already exist for bipolar cells (Shekhar et al. 2016). A recent unbiased screen for recognition proteins in the retina found novel receptor-ligand binding pairs (e.g. FLRTs and Uncs) that can direct lamination in a neuronal subtype

specific manner (Visser et al. 2015). Analyses of such datasets might provide other candidates that regulate AII AC connectivity.

One candidate transsynaptic protein that may differentially regulate AII AC connectivity with bipolar cells versus retinal ganglion cells is Neuroligin-4. Hoon et al. (2011) showed that there is a decrease but not complete loss of Glyrα1 staining in retinas that are null for Neuroligin-4 (NL4). One could examine the number of output synapses and the number of synapses AII ACs form onto Type 2 BCs in NL4 knock out retinas. If there is a decrease in total synapse number, but no loss of synapses with Type 2 BCs, this would motivate performing serial blockface EM on NL4 null retinas to reveal whether specific synaptic partner types lost synapses.

Determining whether rod pathway activity underlies pruning of transient synapses

While we did not find a role for rod pathway activity in AII AC preferential synaptogenesis onto bipolar cells, we did not evaluate the role of rod pathway activity in driving the pruning of AII AC synapses onto widefield amacrine cell partners. As demonstrated in earlier studies, presynaptic activity can regulate connectivity with one partner and not others. For example, silencing thalamocortical axons prevents selective pruning of synapses onto a subset of sensory-motor neurons, but not others (Mendelsohn et al. 2015). Furthermore, circuit activity is often critical for proper synaptic pruning in inhibitory circuits (Reviewed Lichtman & Colman 2000; Huberman et al. 2008; Hashimoto & Kano 2013; Gamlin et al. 2018). Thus, it is possible that loss of rod pathway activity prevents pruning of the transient synapses onto widefield amacrine cell partners. To test this hypothesis, we propose reconstructing the AII AC synapse distribution using serial blockface EM in mice which lack inhibitory synaptic transmission (VIAAT KO) (Wojcik et al. 2006).

REFERENCES:

Agostinone, J. et al., 2018. Insulin signalling promotes dendrite and synapse regeneration and restores circuit function after axonal injury. *Brain*, 141(7), pp.1963–1980. Available at: https://academic.oup.com/brain/article/141/7/1963/5039589.

Akrouh, A. & Kerschensteiner, D., 2013. Intersecting circuits generate precisely patterned retinal waves. *Neuron*, 79(2), pp.322–334. Available at: http://dx.doi.org/10.1016/j.neuron.2013.05.012.

Almasieh, M. et al., 2012. The molecular basis of retinal ganglion cell death in glaucoma. *Progress in Retinal and Eye Research*, 31(2), pp.152–181. Available at: http://dx.doi.org/10.1016/j.preteyeres.2011.11.002.

Ango, F. et al., 2004. Ankyrin-based subcellular gradient of neurofascin, an immunoglobulin family protein, directs GABAergic innervation at purkinje axon initial segment. *Cell*, 119(2), pp.257–272. Available at: http://linkinghub.elsevier.com/retrieve/pii/S009286740400947X.

Ango, F. et al., 2008. Bergmann Glia and the Recognition Molecule CHL1 Organize GABAergic Axons and Direct Innervation of Purkinje Cell Dendrites A. Ghosh, ed. *PLoS Biology*, 6(4), p.e103. Available at: http://dx.plos.org/10.1371/journal.pbio.0060103.

Asari, H. & Meister, M., 2012. Divergence of visual channels in the inner retina. *Nature Neuroscience*, 15(11), pp.1581–1589. Available at: http://dx.doi.org/10.1038/nn.3241.

Ashrafi, S. et al., 2014. Neuronal Ig/Caspr recognition promotes the formation of axoaxonic synapses in mouse spinal cord. *Neuron*, 81(1), pp.120–129. Available at: http://linkinghub.elsevier.com/retrieve/pii/S0896627313010337.

Badea, T.C. & Nathans, J., 2011. Morphologies of mouse retinal ganglion cells expressing transcription factors Brn3a, Brn3b, and Brn3c: analysis of wild type and mutant cells using genetically-directed sparse labeling. *Vision research*, 51(2), pp.269–79. Available at: http://www.pubmedcentral.nih.gov/articlerender.fcgi?artid=3038626&tool=pmcentrez&rendertype=abstract [Accessed July 17, 2014].

Baden, T. et al., 2013. Spikes and ribbon synapses in early vision. *Trends in Neurosciences*, 36(8), pp.480–488.

Baden, T. et al., 2016. The functional diversity of retinal ganglion cells in the mouse. *Nature*, 529(7586), pp.345–350. Available at: http://dx.doi.org/10.1038/nature16468.

Basu, S. et al., 2010. Purification of Specific Cell Population by Fluorescence Activated Cell Sorting (FACS). *Journal of Visualized Experiments*, (41), pp.3–6. Available at: http://www.jove.com/index/Details.stp?ID=1546.

Baylor, D.A., Fuortes, M.G. & O'Bryan, P.M., 1971. Receptive fields of cones in the retina of the turtle. *The Journal of physiology*, 214(2), pp.265–94. Available at: http://www.ncbi.nlm.nih.gov/pubmed/5579638.

Baylor, D.A., Lamb, T.D. & Yau, K.W., 1979. Responses of retinal rods to single photons. *The Journal of physiology*, 288(1979), pp.613–34. Available at: http://www.ncbi.nlm.nih.gov/pubmed/112243.

Ben-Ari, Y., 2002. Excitatory actions of gaba during development: the nature of the nurture. *Nat Rev Neurosci*, 3(9), pp.728–739. Available at: http://www.ncbi.nlm.nih.gov/pubmed/12209121.

Betley, J.N. et al., 2009. Stringent specificity in the construction of a GABAergic presynaptic inhibitory circuit. *Cell*, 139(1), pp.161–174. Available at: http://linkinghub.elsevier.com/retrieve/pii/S0092867409010484.

Bleckert, A. et al., 2014. Visual space is represented by nonmatching topographies of distinct

mouse retinal ganglion cell types. *Current biology : CB*, 24(3), pp.310–5. Available at: http://www.ncbi.nlm.nih.gov/pubmed/24440397 [Accessed July 11, 2014].

Bleckert, A. & Wong, R.O.L., 2011. Identifying roles for neurotransmission in circuit assembly: Insights gained from multiple model systems and experimental approaches. *BioEssays*, 33(1), pp.61–72.

Bode, A. & Lynch, J.W., 2014. The impact of human hyperekplexia mutations on glycine receptor structure and function. *Molecular Brain*, 7(1), pp.1–12.

Borowska, J., Trenholm, S. & Awatramani, G.B., 2011. An Intrinsic Neural Oscillator in the Degenerating Mouse Retina. *Journal of Neuroscience*, 31(13), pp.5000–5012. Available at: http://www.jneurosci.org/cgi/doi/10.1523/JNEUROSCI.5800-10.2011.

Brasch, J. et al., 2018. Homophilic and Heterophilic Interactions of Type II Cadherins Identify Specificity Groups Underlying Cell-Adhesive Behavior. *Cell Reports*, 23(6), pp.1840–1852.

Brooks, J.M. et al., 2013. A molecular mechanism regulating the timing of corticogeniculate innervation. *Cell Reports*, 5(3), pp.573–581. Available at: http://dx.doi.org/10.1016/j.celrep.2013.09.041.

Brown, N.L. et al., 2001. Math5 is required for retinal ganglion cell and optic nerve formation. *Development*, 2508(128), pp.2497–2508.

Brüggen, B. et al., 2015. Type 2 wide-field amacrine cells in TH:: GFP mice show a homogenous synapse distribution and contact small ganglion cells. *European Journal of Neuroscience*, 41(6), pp.734–747.

Cafaro, J. & Rieke, F., 2010. Noise correlations improve response fidelity and stimulus encoding. *Nature*, 468(7326), pp.964–7. Available at: http://www.ncbi.nlm.nih.gov/pubmed/21131948.

Cafaro, J. & Rieke, F., 2013. Regulation of spatial selectivity by crossover inhibition. *The Journal of neuroscience : the official journal of the Society for Neuroscience*, 33(15), pp.6310–20. Available at: http://www.pubmedcentral.nih.gov/articlerender.fcgi?artid=3687519&tool=pmcentrez&rendertype=abstract [Accessed July 17, 2014].

Carter-Dawson, L.D., LaVail, M.M. & Sidman, R.L., 1978. Differential effect of the rd mutation on rods and cones in the mouse retina. *Investigative ophthalmology & visual science*, 17(6), pp.489–98. Available at: http://www.ncbi.nlm.nih.gov/pubmed/659071.

Casini, G. et al., 1998. Postnatal development of parvalbumin immunoreactive amacrine cells in the rabbit retina. *Brain research. Developmental brain research*, 111(1), pp.107–117.

Cellerino, A. et al., 1998. Brain-derived neurotrophic factor modulates the development of the dopaminergic network in the rodent retina. *Journal of Neuroscience*, 18(9), pp.3351–3362. Available at: http://epublications.uef.fi/pub/urn_isbn_951-27-0083-2/urn_isbn_951-27-0083-2.pdf.

Cembrowski, M.S. et al., 2012. The Mechanisms of Repetitive Spike Generation in an Axonless Retinal Interneuron. *Cell Reports*, 1(2), pp.155–166. Available at: http://dx.doi.org/10.1016/j.celrep.2011.12.006.

Cepko, C.L. et al., 1996. Cell fate determination in the vertebrate retina. *Proceedings of the National Academy of Sciences*, 93(2), pp.589–595. Available at: http://www.pnas.org/cgi/doi/10.1073/pnas.93.2.589.

Chao, D.L., Ma, L. & Shen, K., 2009. Transient cell-cell interactions in neural circuit formation. *Nature Reviews Neuroscience*, 10(4), pp.262–271.

Choi, H. et al., 2014. Intrinsic bursting of AII amacrine cells underlies oscillations in the rd1 mouse retina. *Journal of Neurophysiology*, 112(6), pp.1491–1504. Available at: http://jn.physiology.org/cgi/doi/10.1152/jn.00437.2014.

Chun, M.-H. et al., 1993. Electron microscopic analysis of the rod pathway of the rat retina. *Journal of Comparative Neurology*, 332(4), pp.421–432. Available at: http://doi.wiley.com/10.1002/cne.903320404 [Accessed November 16, 2018].

Cohen, E. & Sterling, P., 1990. Convergence and divergence of cones onto bipolar cells in the central area of cat retina. *Philosophical transactions of the Royal Society of London. Series B, Biological sciences*, 330(1258), pp.323–328.

Crocker-Buque, A. et al., 2015. Experience-Dependent, Layer-Specific Development of Divergent Thalamocortical Connectivity. *Cerebral Cortex*, 25(8), pp.2255–2266.

D'Orazi, F.D., Suzuki, S.C. & Wong, R.O., 2014. Neuronal remodeling in retinal circuit assembly, disassembly, and reassembly. *Trends in Neurosciences*, 37(10), pp.594–603. Available at: http://linkinghub.elsevier.com/retrieve/pii/S0166223614001258.

Deans, M.R. et al., 2011. Control of neuronal morphology by the atypical cadherin fat3. *Neuron*, 71(5), pp.820–832. Available at: http://dx.doi.org/10.1016/j.neuron.2011.06.026.

Demb, J.B. & Singer, J.H., 2012. Intrinsic properties and functional circuitry of the AII amacrine cell. *Visual Neuroscience*, 29, pp.51–60.

Dong, C.-J. & Hare, W. a, 2003. Temporal modulation of scotopic visual signals by A17 amacrine cells in mammalian retina in vivo. *Journal of neurophysiology*, 89(4), pp.2159–2166.

Drinnenberg, A. et al., 2018. How Diverse Retinal Functions Arise from Feedback at the First Visual Synapse. *Neuron*, 99(1), p.117–134.e11.

Duan, X. et al., 2018. Cadherin Combinations Recruit Dendrites of Distinct Retinal Neurons to a Shared Interneuronal Scaffold. *Neuron*, 99(6), p.1145–1154.e6. Available at: https://linkinghub.elsevier.com/retrieve/pii/S0896627318307220.

Dunn, F. a. & Wong, R.O.L., 2012. Diverse Strategies Engaged in Establishing Stereotypic Wiring Patterns among Neurons Sharing a Common Input at the Visual System's First Synapse. *Journal of Neuroscience*, 32(30), pp.10306–10317.

Dunn, F. a. & Wong, R.O.L., 2014. Wiring patterns in the mouse retina: collecting evidence across the connectome, physiology and light microscopy. *The Journal of Physiology*, 592(22), pp.4809–4823. Available at: http://doi.wiley.com/10.1113/jphysiol.2014.277228.

Dunn, F.A. & Rieke, F., 2008. Single-Photon Absorptions Evoke Synaptic Depression in the Retina to Extend the Operational Range of Rod Vision. *Neuron*, 57(6), pp.894–904.

Dutertre, S., Becker, C.-M. & Betz, H., 2012. Inhibitory Glycine Receptors: An Update. *Journal of Biological Chemistry*, 287(48), pp.40216–40223. Available at: http://www.jbc.org/cgi/doi/10.1074/jbc.R112.408229.

Elias, E. et al., 2018. Glutamate Activity Regulates and Dendritic Development of J-RGCs. *Frontiers in Cellular Neuroscience*, 12(August), pp.1–14. Available at: https://www.frontiersin.org/article/10.3389/fncel.2018.00249/full.

Engert, F. & Bonhoeffer, T., 1999. Dendritic spine changes associated with hippocampal long-term synaptic plasticity. *Nature*, 399(6731), pp.66–70. Available at: http://www.ncbi.nlm.nih.gov/htbin-post/Entrez/query?uid=9481071 OWN - NLM STAT-MEDLINE&form=6&db=m&Dopt=l.

Euler, T. et al., 2014. Retinal bipolar cells: elementary building blocks of vision. *Nature Reviews Neuroscience*, 15(8), pp.507–519. Available at: http://www.nature.com/doifinder/10.1038/nrn3783.

Famiglietti, E. V. & Kolb, H., 1975. A bistratified amacrine cell and synaptic circuitry in the inner plexiform layer of the retina. *Brain Research*, 84, pp.293–300.

Farah, M.H. & Easter, S.S., 2005. Cell birth and death in the mouse retinal ganglion cell layer. *Journal of Comparative Neurology*, 489(1), pp.120–134.

Firl, A. et al., 2015. Elucidating the Role of AII Amacrine Cells in Glutamatergic Retinal Waves. *Journal of Neuroscience*, 35(4), pp.1675–1686. Available at: http://www.jneurosci.org/cgi/doi/10.1523/JNEUROSCI.3291-14.2015.

Fisher, L., 1979. Development of Synaptic Arrays in the Inner Plexiform Layer of Neonatal Mouse Retina. *The Journal of comparative neurology*, 187(2), pp.359–72.

Ford, K.J. & Feller, M.B., 2012. Assembly and disassembly of a retinal cholinergic network. *Visual Neuroscience*, 29(1), pp.61–71.

Franke, K. et al., 2017. Inhibition decorrelates visual feature representations in the inner retina. *Nature*, 542(7642), pp.439–444. Available at: http://dx.doi.org/10.1038/nature21394.

Galindo-Romero, C. et al., 2011. Axotomy-induced retinal ganglion cell death in adult mice: Quantitative and topographic time course analyses. *Experimental Eye Research*, 92(5), pp.377–387. Available at: http://dx.doi.org/10.1016/j.exer.2011.02.008.

Gamlin, C.R. et al., 2018. Assembly and maintenance of GABAergic and Glycinergic circuits in the mammalian nervous system. *Neural Development*, 13(1), p.12. Available at: https://neuraldevelopment.biomedcentral.com/articles/10.1186/s13064-018-0109-6.

Ghosh, A. et al., 1990. Requirement for subplate neurons in the formation of thalamocortical connections. *Nature*, 347(6289), pp.179–181. Available at: http://www.nature.com/articles/nature01179.

Godinho, L. et al., 2005. Targeting of amacrine cell neurites to appropriate synaptic laminae in the developing zebrafish retina. *Development (Cambridge, England)*, 132(22), pp.5069–5079.

Godinho, L., 2005. Targeting of amacrine cell neurites to appropriate synaptic laminae in the developing zebrafish retina. *Development*, 132(22), pp.5069–5079. Available at: http://dev.biologists.org/cgi/doi/10.1242/dev.02075.

Golub, J.S. et al., 2012. Hair cell replacement in adult mouse utricles after targeted ablation of hair cells with diphtheria toxin. *The Journal of neuroscience : the official journal of the Society for Neuroscience*, 32(43), pp.15093–105. Available at: http://www.pubmedcentral.nih.gov/articlerender.fcgi?artid=3544304&tool=pmcentrez&rendertype=abstract [Accessed December 29, 2013].

Graf, E.R. et al., 2004. Neurexins induce differentiation of GABA and glutamate postsynaptic specializations via neuroligins. *Cell*, 119(7), pp.1013–1026.

Graydon, C.W. et al., 2018. Synaptic Transfer between Rod and Cone Pathways Mediated by AII Amacrine Cells in the Mouse Retina. *Current Biology*, 28(17), p.2739–2751.e3. Available at: https://doi.org/10.1016/j.cub.2018.06.063.

Günhan-Agar, E., Kahn, D. & Chalupa, L.M., 2000. Segregation of on and off bipolar cell axonal arbors in the absence of retinal ganglion cells. *The Journal of neuroscience : the official journal of the Society for Neuroscience*, 20(1), pp.306–14. Available at: http://www.ncbi.nlm.nih.gov/pubmed/10627608.

Gunhan, E. et al., 2002. Depletion of cholinergic amacrine cells by a novel immunotoxin does not perturb the formation of segregated on and off cone bipolar cell projections. *The Journal of neuroscience : the official journal of the Society for Neuroscience*, 22(6), pp.2265–73. Available at: http://www.ncbi.nlm.nih.gov/pubmed/11896166.

Hartong, D.T., Berson, E.L. & Dryja, T.P., 2006. Retinitis pigmentosa. *Lancet*, 368(9549), pp.1795–1809.

Hashimoto, K. & Kano, M., 2013. Synapse elimination in the developing cerebellum. *Cellular and Molecular Life Sciences*, 70(24), pp.4667–4680.

Heffner, C.D., Lumsden, A.G. & O'Leary, D.D., 1990. Target control of collateral extension and directional axon growth in the mammalian brain. *Science (New York, N.Y.)*, 247(4939),

pp.217–20. Available at: http://www.ncbi.nlm.nih.gov/pubmed/2294603.
Helmstaedter, M. et al., 2013. Connectomic reconstruction of the inner plexiform layer in the mouse retina. *Nature*, 500(7461), pp.168–74. Available at: http://www.ncbi.nlm.nih.gov/pubmed/23925239.
Hertz, J. et al., 2013. A tunable synthetic hydrogel system for culture of retinal ganglion cells and amacrine cells. *Acta Biomaterialia*, 9(8), pp.7622–7629. Available at: http://dx.doi.org/10.1016/j.actbio.2013.04.048.
Hinds, J.W. & Hinds, P.L., 1974. Early ganglion cell differentiation in the mouse retina: An electron microscopic analysis utilizing serial sections. *Developmental Biology*, 37(2), pp.381–416.
Hoffpauir, B.K., 2006. Synaptogenesis of the Calyx of Held: Rapid Onset of Function and One-to-One Morphological Innervation. *Journal of Neuroscience*, 26(20), pp.5511–5523. Available at: http://www.jneurosci.org/cgi/doi/10.1523/JNEUROSCI.5525-05.2006.
Honjo, M. et al., 2000. Differential expression of cadherin adhesion receptors in neural retina of the postnatal mouse. *Investigative Ophthalmology and Visual Science*, 41(2), pp.546–551.
Honjo, T., Nishizuka, Y. & Hayaishi, O., 1968. Diphtheria toxin-dependent adenosine diphosphate ribosylation of aminoacyl transferase II and inhibition of protein synthesis. *The Journal of biological chemistry*, 243(12), pp.3553–5. Available at: http://www.ncbi.nlm.nih.gov/pubmed/4297784 [Accessed November 27, 2018].
Hoon, M. et al., 2014. Functional architecture of the retina: Development and disease. *Progress in retinal and eye research*. Available at: http://www.ncbi.nlm.nih.gov/pubmed/24984227 [Accessed July 15, 2014].
Hoon, M. et al., 2011. Neuroligin-4 is localized to glycinergic postsynapses and regulates inhibition in the retina. *Proceedings of the National Academy of Sciences*, 108(7), pp.3053–3058. Available at: http://www.pnas.org/cgi/doi/10.1073/pnas.1006946108.
Hoon, M. et al., 2015. Neurotransmission plays contrasting roles in the maturation of inhibitory synapses on axons and dendrites of retinal bipolar cells. *Proceedings of the National Academy of Sciences*, p.201510483. Available at: http://www.pnas.org/lookup/doi/10.1073/pnas.1510483112.
Hoon, M., Sinha, R. & Okawa, H., 2017. Using fluorescent markers to estimate synaptic connectivity in situ. In *Methods in Molecular Biology*. Humana Press, New York, NY, pp. 293–320. Available at: http://link.springer.com/10.1007/978-1-4939-6688-2_20 [Accessed November 27, 2018].
Huang, C.C. et al., 2013. Convergence of pontine and proprioceptive streams onto multimodal cerebellar granule cells. *eLife*, 2013(2), pp.1–17.
Hubel, D.H., Wiesel, T.N. & LeVay, S., 1977. Plasticity of Ocular Dominance Columns in Monkey Striate Cortex. *Philosophical Transactions of the Royal Society B: Biological Sciences*, 278(961), pp.377–409. Available at: http://rstb.royalsocietypublishing.org/cgi/doi/10.1098/rstb.1977.0050.
Huberman, A.D., Feller, M.B. & Chapman, B., 2008. Mechanisms underlying development of visual maps and receptive fields. *Annual review of neuroscience*, 31, pp.479–509.
Jeanne, J.M. & Wilson, R.I., 2015. Convergence, Divergence, and Reconvergence in a Feedforward Network Improves Neural Speed and Accuracy. *Neuron*, 88(5), pp.1014–1026. Available at: http://dx.doi.org/10.1016/j.neuron.2015.10.018.
Jeon, C.J., Strettoi, E. & Masland, R.H., 1998. The major cell populations of the mouse retina. *The Journal of neuroscience : the official journal of the Society for Neuroscience*, 18(21), pp.8936–46. Available at: http://www.ncbi.nlm.nih.gov/pubmed/9786999.
Johnson, J. et al., 2003. Vesicular Neurotransmitter Transporter Expression in Developing

Postnatal Rodent Retina: GABA and Glycine Precede Glutamate. *J. Neurosci.*, 23(2), pp.518–529. Available at: http://www.jneurosci.org/cgi/content/abstract/23/2/518%5Cnhttp://www.jneurosci.org/cgi/content/full/23/2/518.

Kakizawa, S. et al., 2000. Critical period for activity-dependent synapse elimination in developing cerebellum. *The Journal of Neuroscience*, 20(13), pp.4954–61. Available at: http://www.ncbi.nlm.nih.gov/pubmed/10864953.

Katz, LC; Shatz, C., 1996. Synaptic Activity and the Construction of Cortical Circuits Author (s): L . C . Katz and C . J . Shatz Published by : American Association for the Advancement of Science Stable URL : http://www.jstor.org/stable/2891573. *Science*, 274(5290), pp.1133–1138.

Kay, J; Roeser, T; Mumm, J; Godinho, L; Mrejeru, A; Wong, R. O.L., and Baier, H., 2004. Transient requirement for ganglion cells during assembly of retinal synaptic layers. *Development*.

Kay, J.N. et al., 2001. Retinal ganglion cell genesis requires lakritz, a Zebrafish atonal Homolog. *Neuron*, 30(3), pp.725–36. Available at: http://www.ncbi.nlm.nih.gov/pubmed/11430806.

Kazama, H. & Wilson, R.I., 2009. Origins of correlated activity in an olfactory circuit. *Nature Neuroscience*, 12(9), pp.1136–1144. Available at: http://dx.doi.org/10.1038/nn.2376.

Keeley, P.W. et al., 2014. Independent genomic control of neuronal number across retinal cell types. *Developmental Cell*, 30(1), pp.103–109. Available at: http://dx.doi.org/10.1016/j.devcel.2014.05.003.

Kerschensteiner, D. et al., 2009. Neurotransmission selectively regulates synapse formation in parallel circuits in vivo. *Nature*, 460(7258), pp.1016–20. Available at: http://www.pubmedcentral.nih.gov/articlerender.fcgi?artid=2746695&tool=pmcentrez&rendertype=abstract [Accessed October 12, 2014].

Kerschensteiner, D., 2014. Spontaneous Network Activity and Synaptic Development. *The Neuroscientist*, 20(3), pp.272–290. Available at: http://journals.sagepub.com/doi/10.1177/1073858413510044.

Kim, I.-J. et al., 2010. Laminar Restriction of Retinal Ganglion Cell Dendrites and Axons: Subtype-Specific Developmental Patterns Revealed with Transgenic Markers. *Journal of Neuroscience*, 30(4), pp.1452–1462. Available at: http://www.jneurosci.org/cgi/doi/10.1523/JNEUROSCI.4779-09.2010.

Kirsch, J. & Betz, H., 1998. Glycine-receptor activation is required for receptor clustering in spinal neurons. *Nature*, 392(6677), pp.717–720.

Kljavin, I.J. et al., 1994. Cell adhesion molecules regulating neurite growth from amacrine and rod photoreceptor cells. *The Journal of neuroscience : the official journal of the Society for Neuroscience*, 14(8), pp.5035–49. Available at: http://www.ncbi.nlm.nih.gov/pubmed/8046466.

Kunzevitzky, N.J. et al., 2013. Amacrine cell subtypes differ in their intrinsic neurite growth capacity. *Investigative ophthalmology & visual science*, 54(12), pp.7603–13. Available at: http://www.pubmedcentral.nih.gov/articlerender.fcgi?artid=3832218&tool=pmcentrez&rendertype=abstract [Accessed December 30, 2014].

Lichtman, J.W. & Colman, H., 2000. Synapse elimination and indelible memory. *Neuron*, 25(2), pp.269–278.

Maletic-Savatic, M., 1999. Rapid Dendritic Morphogenesis in CA1 Hippocampal Dendrites Induced by Synaptic Activity. *Science*, 283(5409), pp.1923–1927. Available at: http://www.ncbi.nlm.nih.gov/pubmed/10082466%0Ahttp://www.sciencemag.org/cgi/doi/10.1126/science.283.5409.1923.

Manookin, M.B. et al., 2008. Disinhibition Combines with Excitation to Extend the Operating Range of the OFF Visual Pathway in Daylight. *Journal of Neuroscience*, 28(16), pp.4136–4150. Available at: http://www.jneurosci.org/cgi/doi/10.1523/JNEUROSCI.4274-07.2008.

Marc, R.E. et al., 2003. Neural remodeling in retinal degeneration. *Progress in Retinal and Eye Research*, 22(5), pp.607–655.

Marc, R.E. et al., 2014. The AII amacrine cell connectome: a dense network hub. *Frontiers in neural circuits*, 8(September), p.104. Available at: http://www.pubmedcentral.nih.gov/articlerender.fcgi?artid=4154443&tool=pmcentrez&rendertype=abstract [Accessed October 10, 2014].

Margolis, D.J. et al., 2014. Network oscillations drive correlated spiking of on and off ganglion cells in the rd1 mouse model of retinal degeneration. *PLoS ONE*, 9(1), pp.1–12.

Margolis, D.J. & Detwiler, P.B., 2011. Cellular Origin of Spontaneous Ganglion Cell Spike Activity in Animal Models of Retinitis Pigmentosa. *Journal of Ophthalmology*, 2011, pp.1–6. Available at: http://www.hindawi.com/journals/joph/2011/507037/.

Masland, R.H., 2012. The Neuronal Organization of the Retina. *Neuron*, 76(2), pp.266–280. Available at: http://dx.doi.org/10.1016/j.neuron.2012.10.002.

Massey, S.C. & Mills, S.L., 1999. Antibody to calretinin stains AII amacrine cells in the rabbit retina: Double-label and confocal analyses. *Journal of Comparative Neurology*, 411(1), pp.3–18.

Matsumoto, N. et al., 2016. Synapse-dependent and independent mechanisms of thalamocortical axon branching are regulated by neuronal activity. *Developmental Neurobiology*, 76(3), pp.323–336.

Matsuoka, R.L., Chivatakarn, O., et al., 2011. Class 5 transmembrane semaphorins control selective mammalian retinal lamination and function. *Neuron*, 71(3), pp.460–473. Available at: http://linkinghub.elsevier.com/retrieve/pii/S0896627311005137.

Matsuoka, R.L., Nguyen-Ba-Charvet, K.T., et al., 2011. Transmembrane semaphorin signalling controls laminar stratification in the mammalian retina. *Nature*, 470(7333), pp.259–263. Available at: http://www.nature.com/doifinder/10.1038/nature09675.

Mendelsohn, A.I. et al., 2015. Activity Regulates the Incidence of Heteronymous Sensory-Motor Connections. *Neuron*, 87(1), pp.111–123. Available at: http://dx.doi.org/10.1016/j.neuron.2015.05.045.

Moleirinho, S. et al., 2013. The expanding family of FERM proteins. *Biochemical Journal*, 452(2), pp.183–193. Available at: http://biochemj.org/lookup/doi/10.1042/BJ20121642.

Mombaerts, P., 2006. Axonal Wiring in the Mouse Olfactory System. *Annual Review of Cell and Developmental Biology*, 22(1), pp.713–737. Available at: http://www.annualreviews.org/doi/abs/10.1146/annurev.cellbio.21.012804.093915.

Morgan, J.L. et al., 2006. Axons and dendrites originate from neuroepithelial-like processes of retinal bipolar cells. *Nature neuroscience*, 9(1), pp.85–92.

Morgan, J.L. et al., 2011. Development of cell type-specific connectivity patterns of converging excitatory axons in the retina. *Neuron*, 71(6), pp.1014–21. Available at: http://www.pubmedcentral.nih.gov/articlerender.fcgi?artid=3184549&tool=pmcentrez&rendertype=abstract [Accessed October 18, 2014].

Morgan, J.L., Schubert, T. & Wong, R.O.L., 2008. Developmental patterning of glutamatergic synapses onto retinal ganglion cells. *Neural development*, 3(March), p.8.

Mosca, T.J. & Luo, L., 2014. Synaptic organization of the Drosophila antennal lobe and its regulation by the Teneurins. *eLife*, 3, p.e03726.

Nelson, R. & Kolb, H., 1985. A17: a broad-field amacrine cell in the rod system of the cat retina. *Journal of neurophysiology*, 54(3), pp.592–614. Available at:

http://www.ncbi.nlm.nih.gov/pubmed/4045539.
Nichols, A.J. & Olson, E.C., 2010. Reelin promotes neuronal orientation and dendritogenesis during preplate splitting. *Cerebral Cortex*, 20(9), pp.2213–2223.
O'Leary, D.D.M. & Terashima, T., 1988. Cortical axons branch to multiple subcortical targets by interstitial axon budding: Implications for target recognition and "waiting periods." *Neuron*, 1(10), pp.901–910.
Okada, M. et al., 2000. Functional correlation of GABA(A) receptor alpha subunits expression with the properties of IPSCs in the developing thalamus. *The Journal of neuroscience : the official journal of the Society for Neuroscience*, 20(6), pp.2202–2208.
Okawa, H. et al., 2014. Interplay of cell-autonomous and nonautonomous mechanisms tailors synaptic connectivity of converging axons in vivo. *Neuron*, 82(1), pp.125–37. Available at: http://www.ncbi.nlm.nih.gov/pubmed/24698272 [Accessed December 5, 2014].
Ozdinler, P.H. & Erzurumlu, R.S., 2002. Slit2, a branching-arborization factor for sensory axons in the Mammalian CNS. *The Journal of neuroscience : the official journal of the Society for Neuroscience*, 22(11), pp.4540–9. Available at: http://www.ncbi.nlm.nih.gov/pubmed/12040061.
Pang, J.-J. et al., 2015. Elevated intraocular pressure decreases response sensitivity of inner retinal neurons in experimental glaucoma mice. *Proceedings of the National Academy of Sciences*, 112(8), p.201419921. Available at: http://www.pnas.org/lookup/doi/10.1073/pnas.1419921112.
Pang, J.-J., Gao, F. & Wu, S.M., 2003. Light-evoked excitatory and inhibitory synaptic inputs to ON and OFF alpha ganglion cells in the mouse retina. *The Journal of neuroscience : the official journal of the Society for Neuroscience*, 23(14), pp.6063–73. Available at: http://www.ncbi.nlm.nih.gov/pubmed/12853425.
Patrizio, A. et al., 2017. Alpha subunit-dependent glycine receptor clustering and regulation of synaptic receptor numbers. *Scientific Reports*, 7(1), pp.1–11. Available at: http://dx.doi.org/10.1038/s41598-017-11264-3.
Pelkey, K. a. et al., 2006. Compartmentalized Ca2+ Channel Regulation at Divergent Mossy-Fiber Release Sites Underlies Target Cell-Dependent Plasticity. *Neuron*, 52, pp.497–510.
Peters, A. & Feldman, M.L., 1976. The projection of the lateral geniculate nucleus to area 17 of the rat cerebral cortex. I. General description. *Journal of Neurocytology*, 5(1), pp.63–84. Available at: http://link.springer.com/10.1007/BF01176183 [Accessed November 19, 2018].
Philbrook, A. et al., 2018. Neurexin directs partner-specific synaptic connectivity in C. elegans. *eLife*, 7, pp.1–30. Available at: https://elifesciences.org/articles/35692.
Pittler, S.J. & Baehr, W., 1991. Identification of a nonsense mutation in the rod photoreceptor cGMP phosphodiesterase beta-subunit gene of the rd mouse. *Proceedings of the National Academy of Sciences*, 88(19), pp.8322–8326. Available at: http://www.pnas.org/cgi/doi/10.1073/pnas.88.19.8322.
Politi, L.E. et al., 2001. Insulin-like growth factor-I is a potential trophic factor for amacrine cells. *Journal of Neurochemistry*, 76(4), pp.1199–1211.
Raviola, E. & Dacheux, R.F., 1987. Excitatory dyad synapse in rabbit retina. *Proceedings of the National Academy of Sciences of the United States of America*, 84(20), pp.7324–7328.
Rees, C.L., Moradi, K. & Ascoli, G.A., 2017. Weighing the Evidence in Peters' Rule: Does Neuronal Morphology Predict Connectivity? *Trends in Neurosciences*, 40(2), pp.63–71. Available at: http://dx.doi.org/10.1016/j.tins.2016.11.007.
Rice, D.S. et al., 2001. The Reelin Pathway modulates the structure and function of retinal synaptic circuitry. *Neuron*, 31(6), pp.929–941.

Rice, D.S. & Curran, T.O.M., 2000. Disabled-1 Is Expressed in Type AII Amacrine Cells in the Mouse Retina. , 338(March), pp.327–338.

Del Río, J.A. et al., 1997. A role for Cajal-retzius cells and reelin in the development of hippocampal connections. *Nature*, 385(6611), pp.70–74.

Rivera, C. et al., 1999. The K+/Cl- co-transporter KCC2 renders GABA hyperpolarizing during neuronal maturation. *Nature*, 397(6716), pp.251–255.

Sagdullaev, B.T., McCall, M.A. & Lukasiewicz, P.D., 2006. Presynaptic Inhibition Modulates Spillover, Creating Distinct Dynamic Response Ranges of Sensory Output. *Neuron*, 50(6), pp.923–935.

Sanes, J.R. & Lichtman, J.W., 1999. Development of the vertebrate neuromuscular junction. *Annual review of neuroscience*, 22, pp.389–442.

Sanes, J.R. & Yamagata, M., 2009. Many paths to synaptic specificity. *Annual review of cell and developmental biology*, 25, pp.161–195.

Scher, J. et al., 2003. AII amacrine cells express the MT1melatonin receptor in human and macaque retina. *Experimental Eye Research*, 77(3), pp.375–382.

Schiavo, G.G. et al., 1992. Tetanus and botulinum-B neurotoxins block neurotransmitter release by proteolytic cleavage of synaptobrevin. *Nature*, 359(6398), pp.832–835. Available at: http://www.nature.com/doifinder/10.1038/359832a0.

Schubert, T. et al., 2008. Development of presynaptic inhibition onto retinal bipolar cell axon terminals is subclass-specific. *Journal of neurophysiology*, 100(1), pp.304–316.

Seabrook, T.A. et al., 2013. Retinal Input Regulates the Timing of Corticogeniculate Innervation. *Journal of Neuroscience*, 33(24), pp.10085–10097. Available at: http://www.jneurosci.org/cgi/doi/10.1523/JNEUROSCI.5271-12.2013.

Shapely, E.-C., 1984. Visual Adaptation and Retinal Gain Controls. *Engineering Sciences*. Available at: http://www.ncbi.nlm.nih.gov/pubmed/11430806.

Shekhar, K. et al., 2016. Comprehensive Classification of Retinal Bipolar Neurons by Single-Cell Transcriptomics. *Cell*, 166(5), p.1308–1323.e30. Available at: http://dx.doi.org/10.1016/j.cell.2016.07.054.

Sieghart, W. et al., 1999. Structure and subunit composition of GABAA receptors. *Neurochemistry International*, 34(5), pp.379–385. Available at: http://linkinghub.elsevier.com/retrieve/pii/S0197018699000455.

Simon, D.K., Roskies, A.L. & O'Leary, D.D.M., 1992. Plasticity in the development of topographic order in the mammalian retinocollicular projection. *Developmental Biology*, 162(2), pp.384–393.

Soto, F. et al., 2012. Spontaneous Activity Promotes Synapse Formation in a Cell-Type-Dependent Manner in the Developing Retina. *Journal of Neuroscience*, 32(16), pp.5426–5439. Available at: http://www.jneurosci.org/cgi/doi/10.1523/JNEUROSCI.0194-12.2012.

Stacy, R.C. & Wong, R.O.L., 2003. Developmental relationship between cholinergic amacrine cell processes and ganglion cell dendrites of the mouse retina. *The Journal of Comparative Neurology*, 456(2), pp.154–166.

Stein, R.B., 1967. The Information Capacity of Nerve Cells Using a Frequency Code. *Biophysical Journal*, 7(6), pp.797–826. Available at: http://dx.doi.org/10.1016/S0006-3495(67)86623-2.

Strettoi, E. et al., 2002. Morphological and Functional Abnormalities in the Inner Retina of the rd/rd Mouse. *The Journal of neuroscience*, 22(13), pp.5492–5504. Available at: http://www.jneurosci.org/content/22/13/5492.short.

Strettoi, E., Raviola, E. & Dacheux, R.F., 1992. Synaptic connections of the narrow-field, bistratified rod amacrine cell (AII) in the rabbit retina. *Journal of Comparative Neurology*,

325, pp.152–168.
Supèr, H., Soriano, E. & Uylings, H.B.M., 1998. The functions of the preplate in development and evolution of the neocortex and hippocampus. *Brain Research Reviews*, 27(1), pp.40–64.
Tai, C. et al., 2014. Impaired excitability of somatostatin- and parvalbumin-expressing cortical interneurons in a mouse model of Dravet syndrome. *Proceedings of the National Academy of Sciences*, 111(30), pp.E3139–E3148. Available at: http://www.pnas.org/cgi/doi/10.1073/pnas.1411131111.
Takahashi, T. et al., 1992. Functional Correlation of Fetal and Adult Forms of Glycine Receptors with Developmental Changes in Inhibitory Synaptic Receptor Channels. *Neuron*, 9, pp.1155–1161.
Takeichi, M., 1995. Morphogenetic roles of classic cadherins. *Current Opinion in Cell Biology*, 7(5), pp.619–627.
Taylor, W.R. et al., 2000. Dendritic computation of direction selectivity by retinal ganglion cells. *Science (New York, N.Y.)*, 289(5488), pp.2347–50. Available at: http://www.sciencemag.org/cgi/doi/10.1126/science.289.5488.2347.
Toth, K. et al., 2000. Differential mechanisms of transmission at three types of mossy fiber synapse. *The Journal of neuroscience*, 20(22), pp.8279–89. Available at: http://www.ncbi.nlm.nih.gov/pubmed/11069934.
Trenholm, S. & Awatramani, G.B., 2015. Origins of spontaneous activity in the degenerating retina. *Frontiers in Cellular Neuroscience*, 9(July), pp.1–7. Available at: http://www.frontiersin.org/Cellular_Neuroscience/10.3389/fncel.2015.00277/abstract.
Tsukamoto, Y. & Omi, N., 2017. Classification of Mouse Retinal Bipolar Cells: Type-Specific Connectivity with Special Reference to Rod-Driven AII Amacrine Pathways. *Frontiers in Neuroanatomy*, 11(October), pp.1–25. Available at: http://journal.frontiersin.org/article/10.3389/fnana.2017.00092/full.
Turner, D.L. & Cepko, C.L., 1987. A common progenitor for neurons and glia persists in rat retina late in development. *Nature*, 328(6126), pp.131–136. Available at: http://www.nature.com/doifinder/10.1038/328131a0.
Uesaka, N. et al., 2005. Activity dependence of cortical axon branch formation: a morphological and electrophysiological study using organotypic slice cultures. *The Journal of neuroscience : the official journal of the Society for Neuroscience*, 25(1), pp.1–9. Available at: http://www.jneurosci.org/cgi/doi/10.1523/JNEUROSCI.3855-04.2005.
Vaney, D.I., 1990. Chapter 2 The mosaic of amacrine cells in the mammalian retina. *Progress in Retinal Research*, 9(9), pp.49–100. Available at: http://linkinghub.elsevier.com/retrieve/pii/0278432790900042.
Vaney, D.I., 1985. The morphology and topographic distribution of AII amacrine cells in the cat retina. *Proceedings of the Royal Society of London. Series B, Biological sciences*, 224(1237), pp.475–88. Available at: http://www.ncbi.nlm.nih.gov/pubmed/2862635 [Accessed November 16, 2018].
Visser, J.J. et al., 2015. An extracellular biochemical screen reveals that FLRTs and Unc5s mediate neuronal subtype recognition in the retina. *eLife*, 4(December2015), pp.1–27.
Voinescu, P.E., Kay, J.N. & Sanes, J.R., 2009. Birthdays of retinal amacrine cell subtypes are systematically related to their molecular identity and soma position. *Journal of Comparative Neurology*, 517(5), pp.737–750.
Völgyi, B. et al., 2004. Convergence and segregation of the multiple rod pathways in mammalian retina. *The Journal of neuroscience : the official journal of the Society for Neuroscience*, 24(49), pp.11182–92. Available at: http://www.pubmedcentral.nih.gov/articlerender.fcgi?artid=2834589&tool=pmcentrez&ren

dertype=abstract [Accessed July 21, 2014].
Wang, K.H. et al., 1999. Biochemical Purification of a Mammalian Slit Protein as a Positive Regulator of Sensory Axon Elongation and Branching. *Cell*, 96(6), pp.771–784. Available at: http://linkinghub.elsevier.com/retrieve/pii/S0092867400805887.
Wang, S.W. et al., 2001. Requirement for math5 in the development of retinal ganglion cells. *Genes & development*, 15(1), pp.24–9. Available at: http://www.ncbi.nlm.nih.gov/pubmed/11156601.
Wässle, H., Puller, C., et al., 2009. Cone contacts, mosaics, and territories of bipolar cells in the mouse retina. *The Journal of neuroscience : the official journal of the Society for Neuroscience*, 29(1), pp.106–17. Available at: http://www.ncbi.nlm.nih.gov/pubmed/19129389 [Accessed June 21, 2014].
Wässle, H., Heinze, L., et al., 2009. Glycinergic transmission in the Mammalian retina. *Frontiers in molecular neuroscience*, 2(July), p.6. Available at: http://www.pubmedcentral.nih.gov/articlerender.fcgi?artid=2777502&tool=pmcentrez&rendertype=abstract [Accessed September 15, 2014].
Wässle, H. et al., 1995. The rod pathway of the macaque monkey retina: Identification of AII-amacrine cells with antibodies against calretinin. *Journal of Comparative Neurology*, 361(3), pp.537–551. Available at: http://doi.wiley.com/10.1002/cne.903610315 [Accessed November 16, 2018].
Wässle, H., Grüunert, U. & Röhrenbeck, J., 1993. Immunocytochemical staining of AII-amacrine cells in the rat retina with antibodies against parvalbumin. *Journal of Comparative Neurology*, 332(4), pp.407–420. Available at: http://doi.wiley.com/10.1002/cne.903320403 [Accessed November 16, 2018].
Watanabe, M. & Kano, M., 2011. Climbing fiber synapse elimination in cerebellar Purkinje cells. *European Journal of Neuroscience*, 34(10), pp.1697–1710.
Watt, A.J. et al., 2009. Traveling waves in developing cerebellar cortex mediated by asymmetrical Purkinje cell connectivity. *Nature Neuroscience*, 12(4), pp.463–473.
Wei, W. et al., 2011. Development of asymmetric inhibition underlying direction selectivity in the retina. *Nature*, 469(7330), pp.402–406. Available at: http://dx.doi.org/10.1038/nature09600.
Werblin, F.S., 2010. Six different roles for crossover inhibition in the retina: correcting the nonlinearities of synaptic transmission. *Visual neuroscience*, 27(1–2), pp.1–8.
Wiesel, T.N. & Hubel, D.H., 1963. SINGLE-CELL RESPONSES IN STRIATE CORTEX OF KITTENS DEPRIVED OF VISION IN ONE EYE. *Journal of Neurophysiology*, 26(6), pp.1003–1017. Available at: http://www.physiology.org/doi/10.1152/jn.1963.26.6.1003.
Williams, M.E. et al., 2011. Cadherin-9 regulates synapse-specific differentiation in the developing hippocampus. *Neuron*, 71(4), pp.640–655. Available at: http://dx.doi.org/10.1016/j.neuron.2011.06.019.
Williams, R.R. et al., 2001. Organization of the inner retina following early elimination of the retinal ganglion cell population: effects on cell numbers and stratification patterns. *Visual neuroscience*, 18(2), pp.233–244.
Williamson, L.C., Fitzgerald, S.C. & Neale, E.A., 1992. Differential Effects of Tetanus Toxin on Inhibitory and Excitatory Neurotransmitter Release from Mammalian Spinal Cord Cells in Culture. *Journal of Neurochemistry*, 59(6), pp.2148–2157. Available at: http://doi.wiley.com/10.1111/j.1471-4159.1992.tb10106.x [Accessed November 28, 2018].
Wojcik, S.M. et al., 2006. A Shared Vesicular Carrier Allows Synaptic Corelease of GABA and Glycine. *Neuron*, 50(4), pp.575–587. Available at: http://linkinghub.elsevier.com/retrieve/pii/S0896627306003072.

Wong, R.O.L., 1999. RETINAL WAVES AND VISUAL SYSTEM DEVELOPMENT. *Annual Review of Neuroscience*, 22(1), pp.29–47. Available at: http://www.ncbi.nlm.nih.gov/pubmed/10202531 [Accessed November 19, 2018].

Wong, W.T. et al., 2000. Rapid dendritic remodeling in the developing retina: dependence on neurotransmission and reciprocal regulation by Rac and Rho. *Journal of Neuroscience*, 20(13), pp.5024–36. Available at: http://www.ncbi.nlm.nih.gov/pubmed/10864960.

Wong, W.T. & Wong, R.O.L., 2001. Changing specificity of neurotransmitter regulation of rapid dendritic remodeling during synaptogenesis. *Nature Neuroscience*, 4(4), pp.351–352.

Yamada, A. et al., 2010. Role of pre- and postsynaptic activity in thalamocortical axon branching. *Proceedings of the National Academy of Sciences*, 107(16), pp.7562–7567. Available at: http://www.pnas.org/cgi/doi/10.1073/pnas.0900613107.

Yamagata, M. & Sanes, J.R., 2008a. Dscam and Sidekick proteins direct lamina-specific synaptic connections in vertebrate retina. *Nature*, 451(7177), pp.465–469. Available at: http://www.nature.com/doifinder/10.1038/nature06469.

Yamagata, M. & Sanes, J.R., 2008b. Dscam and Sidekick proteins direct lamina-specific synaptic connections in vertebrate retina. *Nature*, 451(7177), pp.465–469. Available at: http://www.nature.com/doifinder/10.1038/nature06469.

Yamaizumi, M. et al., 1978. One molecule of diphtheria toxin fragment a introduced into a cell can kill the cell. *Cell*, 15(1), pp.245–250.

Yonehara, K. et al., 2016. Congenital Nystagmus Gene FRMD7 Is Necessary for Establishing a Neuronal Circuit Asymmetry for Direction Selectivity. *Neuron*, 89(1), pp.177–193. Available at: http://linkinghub.elsevier.com/retrieve/pii/S0896627315010387.

Yoshimatsu, T. et al., 2014. Transmission from the dominant input shapes the stereotypic ratio of photoreceptor inputs onto horizontal cells. *Nature communications*, 5(May), p.3699. Available at: http://www.ncbi.nlm.nih.gov/pubmed/24832361.

Young, R., 1985. Cell Differentiation in the Retina of the Mouse. *The Anatomical record*, 212(2), pp.199–205.

Zhang, B. et al., 2015. Neuroligins Sculpt Cerebellar Purkinje-Cell Circuits by Differential Control of Distinct Classes of Synapses. *Neuron*, 87(4), pp.781–796.

Zhang, L. et al., 2006. Shift of Intracellular Chloride Concentration in Ganglion and Amacrine Cells of Developing Mouse Retina. , pp.2404–2416.